EFFECTS OF MACROPORES AND ELECTRIC CHARGES ON SOLUTE TRANSPORT IN SOILS(Dissertation_全文)

AUTHOR(S):

Ishiguro, Munehide

EFFECTS OF MACROPORES AND ELECTRIC CHARGES ON SOLUTE TRANSPORT IN SOILS

MUNEHIDE ISHIGURO

EFFECTS OF MACROPORES AND ELECTRIC CHARGES ON SOLUTE TRANSPORT IN SOILS

By

Munehide Ishiguro

1992

Contents

ACKNOWLEDGEMENTS IV

CHAPTER 1 : INTRODUCTION 1

CHAPTER 2 : SOLUTE TRANSPORT IN SOILS

2.1. INTRODUCTION 5

2.2. DIFFUSION

2.2.1. DIFFUSION EQUATION 6

2.2.2. MOLECULAR DIFFUSION 7

2.2.3. ION DIFFUSION 8

2.2.4. DIFFUSION IN SOILS 9

2.3. DISPERSION

2.3.1. HYDRODYNAMIC DISPERSION IN A TUBE 10

2.3.2. DISPERSION IN SOILS 14

2.4. SOLUTE TRANSPORT IN MACROPORES

2.4.1. EXPERIMENTAL CONSIDERATION 17

2.4.2. MODELS FOR PREFERENTIAL FLOW 23

2.5. ION EXCHANGE AND TRANSPORT IN SOILS

2.5.1. ELECTRIC CHARGE OF SOILS 27

2.5.2. ION EXCHANGE EQUILIBRIA 29

2.5.3. TRANSPORT OF EXCHANGING IONS IN SOILS 31

CHAPTER 3 : MACROPORES OF HARD PAN IN PADDY FIELD

3.1. INTRODUCTION 34

3.2. SEASONAL CHANGES IN DISTRIBUTIONS OF MACROPORES OF HARD PAN AND SUBSOIL IN A PADDY FIELD

3.2.1. EXPERIMENTAL 35

3.2.2. RESULTS AND DISCUSSION 36

3.2.3. SUMMARY 41

3.3. MACROPOROSITY OF HARD PANS

3.3.1. MATERIALS AND METHOD 41

3.3.2. RESULTS 42

CHAPTER 4 : EFFECT OF VERTICAL TUBULAR PORES MADE BY RICE ROOTS ON SOLUTE TRANSPORT IN HARD PANS OF PADDY FIELDS

4.1. INTRODUCTION 44

4.2. MATERIALS AND METHODS 45

4.3. THE MODEL

4.3.1. THE COAXIAL CYLINDRICAL MODEL 47

4.3.2. GOVERNING EQUATIONS AND NUMERICAL PROCEDURE 49

4.4. RESULTS AND DISCUSSION 52

4.5. CONCLUSIONS 59

CHAPTER 5 : CATION EXCHANGE PROCESSES IN HARD PANS OF PADDY FIELDS

5.1. INTRODUCTION 61

5.2. MATERIALS AND METHODS 62

5.3. THE MODEL 63

5.4. RESULTS AND DISCUSSION 68

5.5. CONCLUSIONS 74

CHAPTER 6 : EFFECTS OF VARIABLE CHARGE ON ION TRANSPORT IN AN ALLOPHANIC ANDISOL

6.1. INTRODUCTION 76

6.2. MATERIALS AND METHODS 77

6.3. RESULTS AND DISCUSSION 81

6.4. CONCLUSIONS 90

CHAPTER 7 : EFFECT OF DISTRIBUTION RATIO ON BREAKTHROUGH CURVE

7.1. INTRODUCTION 92

7.2. THEORY 93

7.3. NUMERICAL PROCEDURE 96

7.4. MATERIALS AND METHODS 98

7.5. RESULTS AND DISCUSSION

7.5.1. SAMPLE CALCULATIONS 99

7.5.2. THE EXPERIMENTS 104

7.6. CONCLUSIONS 108

CHAPTER 8 : CONCLUDING REMARKS 110

REFERENCES 112

ACKNOWLEDGEMENTS

During the course of this endeavor, many people contributed to its final success. First, I would like to express my heartfelt gratitude to Prof. Dr. Singo Iwata of Ibaraki University, who patiently guided me and rigorously reviewed my work. Without his assistance and encouragement, this study would not have been completed. I am also indebted to Dr. Setsuo Ooi of the National Research Institute of Agricultural Engineering (NRIAE), who greatly influenced me and who provided much-needed advice, and also to Dr. Masami Nanzyo of Tohoku University, who supplied invaluable insight into the chemical processes involved in this venture. I would like to thank Dr. Kazuhide Adachi of NRIAE, who provided needed advice for the field survey, and also to Prof. Dr. Kazutake Kyuma, Prof. Dr. Tsuyoshi Takahashi, Prof. Dr. Takashi Hasegawa, and Prof. Dr. Takashi Matsumura of Kyoto University for their counsel and many valuable suggestions in the writing of this thesis.

I am also grateful to all the people who kindly contributed their constructive technical assistance: Dr. Olivier G. Cogels of the Catholic University of Louvain in Belgium, Dr. Shin-Ichiro Wada of Kyusyu University, the members of the Soil Physics Seminar in Tsukuba, Dr. Kwan-Choul Song of the Institute of Agricultural Sciences in Korea, Dr. Kouichi Yuita, Dr. Shuichi Hasegawa, and Dr. Ichiro Taniyama of the National Institute of Agro-Environmental Sciences, Dr. Takami Komae of NRIAE, and Ms. Yumiko Shiraki of the University of Tsukuba.

I would also like to thank Dr. Haruo Watanabe and Mr. Katsuyuki Arihara of the Chiba-ken Agricultural Experiment Station for their productive assistance involving the sampling of the soils, Mr. Shuji Okushima of NRIAE for his dedication in overseeing the computer operation involved in this study, Mr. Bryan Thoreson of the University of Arizona for his patient guidance concerning the English language aspect of this study, and to Mrs. Yoshiko Kawaguchi of NRIAE for her meticulous work involving certain figures in this thesis.

Finally, I would like to express my sincere thanks to Prof. Dr. Toshisuke Maruyama of Kyoto University for his counsel and many valuable suggestions in the writing of this thesis, and for his continuing advice and encouragement that he has graciously given since my student days at Kyoto University.

CHAPTER 1

INTRODUCTION

Solutes move in diverse ways in the field. Some move rapidly with water, some move slowly, and some cannot move. Furthermore, the soil structure in the field is complicated, and the geometry of water paths in the field differs from place to place. Solute movement in the field is difficult to predict.

Fertilizer movement is one of the most important concerns in the field of agriculture. In the early stage of chemical fertilizer introduction into Japan, researchers were concerned with its effective use. But, recently, farmers are apt to apply too much chemical fertilizer to save labor. Because the fertilizer can also provide nutrients for other organisms, its discharge induces the eutrophication of closed water areas. Many researchers have become concerned with its discharge from the field for the maintenance of water quality. However, effective fertilizer use is one of the biggest themes even now, because the fertilizer is very precious for farmers in developing countries, and elements of fertilizers such as phosphate are limited resources. Moreover, when fertilizer is applied effectively, its discharge decreases. Good fertilizer management can preserve water quality. Pesticide and herbicide movements are another important concern because they are harmful to living things.

In arid or semiarid areas, water management is important not only for effective water use but also for preventing salt accumulation, because crops cannot grow in salt affected lands. Therefore, salt movement is one of the biggest concerns in these areas. Salt accumulation is not the problem only in these areas. Salt accumulates easily in the greenhouse due to large evapotranspiration rate and small water supply. On the other hand, how to remove salt water is the main concern in a newly reclaimed land which is affected by sea water. When pure water is supplied to the field, the soil swells due to high SAR (sodium adsorption ratio). This brings low permeability. Therefore, it is not easy to remove salt water.

Pollution of irrigation water sometimes brings tremendous damage to the environment. Discharge from Ashio copper mine damaged crops. This matter is well known as the first environmental pollution in Japan. Discharge from Kamioka mine polluted rice with Cd and people who ate it became victims of "itaiitai"-disease. Many suffered and died. These pollutants were heavy metals and adsorbed strongly by soils. Behaviour of such heavy metals in soils became a very important concern. Radioactive contamination due to a nuclear power plant accident or some nuclear wastes is another menace. If this happens, cultivation must be abandoned because of the soil pollution.

A better understanding of the movement and interactions of solutes in the soil is essential to the improvement of soil fertility. This will result in improved control of nutrients in the root zone, as well as the prevention of soil salinity and the removal of salt water from the newly

reclaimed land. Such an understanding has also become crucial in environmental management whenever solutes migrate to, and threaten the quality of, groundwater or surface water resources. It is needed for the improvement of the polluted soil, too.

This study is divided into two parts. The first part (chapter 3, chapter 4 and chapter 5) is the study of solute transport through hard pans of paddy fields. The second part (chapter 6 and chapter 7) is the study of solute transport in Allophanic Andisol. Both soils are common in Japan.

The hard pan layer usually exists below the surface layer in the paddy field. Its permeability is low and it restrains vertical percolation. Therefore it significantly affects the movement of water and solutes in the paddy field. To understand the solute transport in the paddy field, an understanding of the solute transport through the hard pan is important. It has the characteristic soil structure. While its soil matrix is very compact due to the pressure exerted by farm machinery, it has many vertical tubular pores made by rice roots. The effect of vertical tubular pores on solute transport was investigated.

Volcanic ash soils occupy about 16% of the total land area of Japan. They have good soil structure; excess water for upland crops is rapidly discharged from them and much useful water for upland crops is retained in them. Therefore upland crops are cultivated in these areas. Allophane is one of the major clay minerals in volcanic ash soils. Allophanic Andisol has a variable charge. It is negatively and positively charged, and the charge density is strongly influenced by the solution

concentration and pH. The effect of variable charge on ion transport was investigated in this study.

Before going to these parts, basic movements and interactions of solutes in soils will be reviewed in chapter 2.

CHAPTER 2

SOLUTE TRANSPORT IN SOILS

2.1. INTRODUCTION

When a solute is introduced into a soil column it spreads out under the combined action of molecular diffusion and the variation of velocity over the pore water in the soil. Therefore, the effluent concentration from the soil column changes with time. The change of the effluent concentration is usually shown as a breakthrough curve (BTC). Examples are shown in Fig.2-1. The ordinate indicates (effluent concentration c)

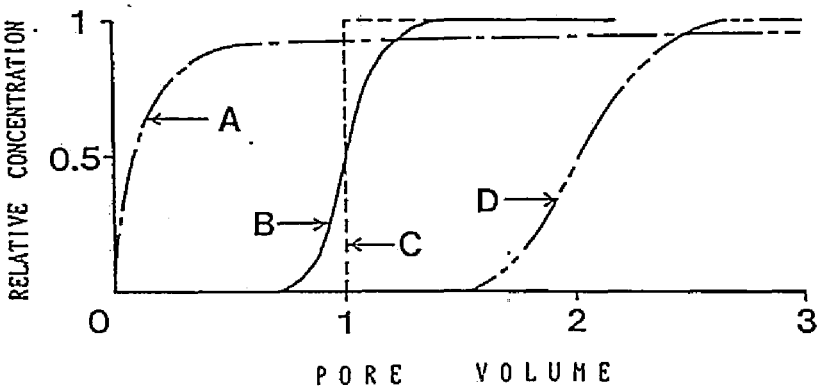

Fig. 2-1 Types of breakthrough curves. Pore volume is the ratio of the volume of effluent to the volume of water in the soil sample.
A: with transmission pores B: longitudinal dispersion
C: piston flow D: with adsorption

/(input concentration co), and the abscissa shows (volume of effluent)/ (volume of water in the soil sample). When the velocity of each solute particle in the flow direction is all same, this is piston type flow. The BTC suddenly changes from 0 to 1 at 1 pore volume (the BTC C). However, because pore water velocity differs in the soil, the solute spreads out under the action of molecular diffusion and the variation of velocity. Then, longitudinal dispersion is observed in the BTC (the BTC B). When the soil has large transmission pores, the solute flows down rapidly through them and diffuses into micropores gradually. The BTC shows early breakthrough and succesive tailing (the BTC A). When the solute is adsorbed on the soil, its discharge is retarded. The BTC shifts to the right (the BTC D). Effects of soil structure and adsorption on solute transport are significant.

Heavy metals, phosphate, and agricultural chemicals are strongly adsorbed in soils and the reactions are not reversible. Adsorption of potassium or ammonium in 2:1 type clay minerals is also irreversible. In this study, those irreversible reactions are not mentioned. Solute transport for non-sorbed solutes and sorbed solutes which reversibly exchange between a solution and a soil by electrostatic force is considered.

2.2. DIFFUSION

2.2.1. DIFFUSION EQUATION

Diffusion processes occur due to the random thermal motion and re-

peated collisions and deflections of molecules in the fluid (often called Brownian motion). When the gradient of the concentration exists, the diffusion flow is observed. The rate of diffusion, I, is given by Fick's first law.

$$I = -D_0 \frac{dc}{dx} \qquad (2.1)$$

where, D_0 is the diffusion coefficient of the solute, c is the concentration, and x is the distance. When the diffusion coefficient is constant, from the law of conservation of mass, we can get the well-known Fick's second law as follows:

$$\frac{\partial c}{\partial t} = D_0 \frac{\partial^2 c}{\partial x^2} \qquad (2.2)$$

where t is the time.

2.2.2. MOLECULAR DIFFUSION

The diffusion coefficient of a molecule is given by the Stokes-Einstein equation as follows:

$$D_0 = \kappa T / 6\pi \mu a \qquad (2.3)$$

where, κ is Boltzmann's constant, T is the absolute temperature, μ is the coefficient of viscosity, and a is the radius of the molecule. Therefore, the diffusion coefficient becomes small as the radius becomes large. In other words, the rate of diffusion differs among the molecules which have different radii.

2.2.3. ION DIFFUSION

When the molecule is an ion, the diffusion coefficient is also expressed by the following equation known as the Einstein relation:

$$D_o = \omega \kappa T / ez \qquad (2.4)$$

where, e is elementary electric charge, z is the valency of the ion, and ω is the electrochemical mobility of the ion defined by the following equation:

$$I = \omega c E \qquad (2.5)$$

where, I is the rate of the ion diffusion, c is the concentration, and E is the intensity of the electric field.

Consider that there are one kind of anion and one kind of cation dissolved in water, and that their radii are different. Then, from the Stokes-Einstein equation, Eq.(2.3), the smaller one advances faster than the larger one. The separation of the anion and the cation produces the diffusion potential, because they have electric charge. The potential makes the speed of smaller one decreased and that of the larger one increased. Finally, both the rates of diffusion become equal. Therefore, the diffusion coefficient of the anion changes when the kind of the companion cation changes, and vice versa. Diffussion coefficients of several solutes in water are shown in Table 2-1. The diffusion coefficient of the ion can be expressed as follows:

$$D_o = \frac{2\omega_+ \omega_-}{z_- \omega_+ + z_+ \omega_-} \frac{\kappa T}{e} \qquad (2.6)$$

where the subscripts, + and - denote the value for the cation and the anion, respectively.

Table 2-1
Diffusion coefficients of electrolytes in water (25℃). $D_o/10^{-5}cm^2s^{-1}$

Electrolyte	Concentration mol dm^{-3}				
	0.001	0.005	0.01	0.05	0.1
$CaCl_2$	1.263	1.213	1.188	1.121	1.110
$SrCl_2$	1.269	1.219	—	—	—
KCl	1.964	1.934	1.917	1.864	1.844
KBr	—	—	—	1.89	1.87
HCl	—	—	—	3.07	3.05

(After Handbook of chemistry, Fundamentals II. Jpn. Soc. Chemistry. 1984 Maruzen p.66)

2.2.4. DIFFUSION IN SOILS

Because the pore passages in the soil are tortuous, the actual path length of diffusion is greater than the apparent straight line distance. Therefore, the diffusion coefficient in the soil, D, is smaller than that in bulk water. The diffusion coefficient in the soil is

$$D = \frac{1}{\tau} D_o \qquad (2.7)$$

where, τ is the tortuosity, and D_o is the diffusion coefficient in bulk water.

Saffman (1959) obtained the diffusion coefficient in a random network of capillaries theoretically as follows;

$$D = \frac{1}{3} D_o \qquad (2.8)$$

Bear (1969) summerized the experimental values of the diffusion

coefficients in saturated granular beds. Approximately, it is given as follows:

$$D = \frac{2}{3} D_0 \qquad (2.8)$$

Ooi (1986) also derived the same value of the diffusion coefficient in granular beds theoretically.

Because the solute only diffuses in pore water, the flux of the solute, I, is

$$I = -\theta D \frac{dc}{dx} \qquad (2.9)$$

where θ is the volume wetness. When the volume wetness and the diffusion coefficient in the soil are constant, Fick's second law is also derived from the law of conservation of mass.

$$\frac{\partial c}{\partial t} = D \frac{\partial^2 c}{\partial x^2} \qquad (2.10)$$

2.3. DISPERSION

2.3.1. HYDRODYNAMIC DISPERSION IN A TUBE

Consider the laminar flow of a solution in a circular tube of radius r. The flow velocity, u(y), at the distance y from the center can be given from Poiseuille's law:

$$u(y) = u_0 (1 - y^2 / r^2) \qquad (2.11)$$

where u_0 is the maximam velocity at the axis (y = 0):

$$u_o = \frac{r^2}{4\mu}\frac{dp}{dx} \qquad (2.12)$$

where, μ is the viscosity, p is the pressure, and x is the longitudinal distance. As shown in Fig.2-2, the velocity, u(y), is a decreasing function of radial distance y.

When the velocity is much faster than the radial diffusion, particles of solutes flow along the stream lines. Then the distribution of the solute in the tube and the distribution of radial mean concentration at time t can be shown in Fig.2-3 (Taylor, 1953). The ordinate of Fig.2-3(b) indicates (effluent concentration c)/(input concentration c_o). In this case, the breakthrough curve (BTC) is given as shown in Fig.2-4 (Nielsen and Biggar, 1962).

On the other hand, when the radial diffusion is not negligible, Taylor (1953) derived theoretically that the solute transport in the tube can be approximated by the following one-dimensional advective dispersive equation:

$$\frac{\partial c}{\partial t} = k\frac{\partial^2 c}{\partial x^2} - u\frac{\partial c}{\partial x} \qquad (2.13)$$

where, k is the dispersion coefficient, and u is the mean velocity. In this case, a particle of the solute in a streamline diffuses radially into another streamline at which the velocity is different; a particle in a streamline of faster velocity moves into a streamline of slower velocity and a particle in a streamline of slower velocity moves into a streamline of faster velocity. After a relatively long time, radial concentrations become all same and the distribution width of concentra-

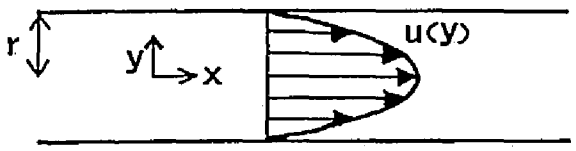

Fig. 2-2 Velocity distribution in a cylindrical tube.

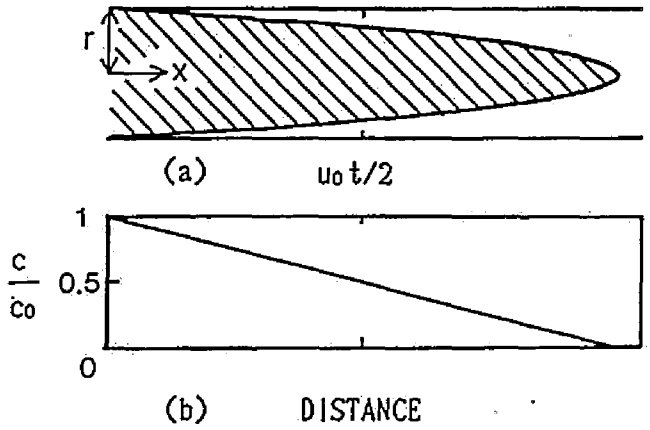

Fig. 2-3 (a) Solute distribution in a tube. (b) Distribution of radial mean concentration. Radial diffusion is negligible.

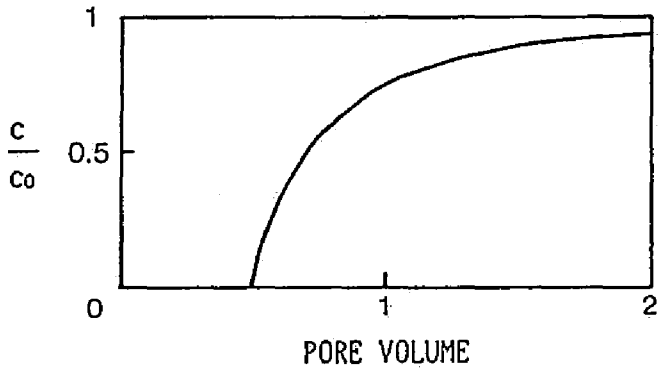

Fig. 2-4 Breakthrough curve for a tube when radial diffusion is negligible. (after Nielsen and Biggar, 1962)

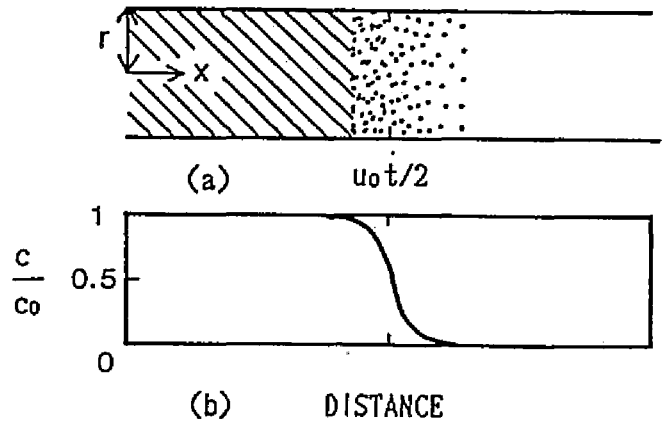

Fig. 2-5 (a) Solute distribution in a tube.
(b) Distribution of radial mean concentration.
Radial diffusion is not negligible.

tion becomes shorter than that in absence of diffusion as shown in Fig.2-5. The dispersion coefficient, k, is

$$k = D_o + \frac{r^2 u^2}{48 D_o} \qquad (2.14)$$

where D_o is the diffusion coefficient in bulk water. If at any time the solute is spread over a length of tube of order L, the time, t_1, necessary for advection to make an appreciable change in concentration is

$$t_1 = \frac{L}{u} \qquad (2.15)$$

The time, t_2, necessary for the radial variation of concentration in the tube to die down to about 1/e of its initial value is

$$t_2 = \frac{r^2}{3.8^2 D_o} \qquad (2.16)$$

Eq.(2.13) and Eq.(2.14) can be applicable when t_1 becomes larger than

t_2.

$$\frac{L}{u} \gg \frac{r^2}{3.8^2 D_0} \qquad (2.17)$$

BTC's in this condition can be shown as in Fig.2-8.

2.3.2. DISPERSION IN SOILS

Solute transport in saturated soils can also be approximated by the one-dimensional advective dispersive equation (2.13).

A porous medium can be assumed to meet the tubular net model as shown in Fig.2-6. If the incoming solute is mixed perfectly (instantaneously) in the connected parts, the dispersion coefficient is approximated to be proportional to the mean velocity (Bolt, 1982; Ooi and Iwata, 1988):

$$k = lu \qquad (2.18)$$

where l is the constant. This type of dispersion is called mechanical dispersion (Bear, 1969).

Bear (1969) summarized many experimental values of the dispersion coefficient in saturated granular beds and roughly divided them into the following 5 zones. The mean velocity increases as the zone number increases.

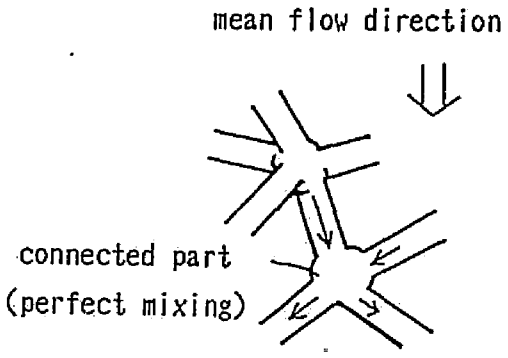

Fig. 2-6 Tubular net model

Zone I: $k = D = \frac{2}{3} D_o$ (2.19)

This is a zone where molecular diffusion predominates.

Zone II: In this zone, the effect of molecular diffusion is of the same order of magnitude as that of mechanical dispersion and the sum of both should be considered.

Zone III: $k = \alpha d u^m \qquad \alpha \fallingdotseq 0.5; \quad 1 < m < 1.2$ (2.20)

where d is the characteristic medium length. Here the main spreading is caused by mechanical dispersion combined with radial molecular diffusion. Radial molecular diffusion tends to reduce the longitudinal spreading; the mechanism is the same as that in a tube as described before.

Zone IV: $k = \beta d u \qquad \beta \fallingdotseq 1.8$ (2.21)

This is a region of mechanical dispersion dominance.

Zone V: This is again a zone of pure mechanical dispersion, but the effects of inertia and turbulence may no longer be neglected. Their role is equivalent to the role of radial molecular diffusion in zone III.

However, the pore structure of soils differs from that of granular beds because they have aggregates or many micropores. Passioura (1971) assumed that viscous flow occurs only in the large pores and that the movement of solute within aggregates occurs only by diffusion as shown in Fig.2-7. Under these assumptions, he derived the dispersion coefficient in a saturated aggregated media as follows:

$$k = \frac{\theta_m}{\theta} D_m + au + \frac{\theta_{im}}{\theta} \frac{a^2 u^2}{15 D_{im}} \qquad (2.22)$$

where, θ is the porosity, θ_m is the macroporosity, θ_{im} is the porosity of the aggregates, D_m is the molecular diffusion coefficient in the macropores, D_{im} is the molecular diffusion coefficient in the aggregates, a is the aggregate radius, and u is the mean pore water velocity. Bolt (1982), Parker and Valocchi (1986), and van Genuchten and Dalton (1986) also obtained similar equations via quite different analyses.

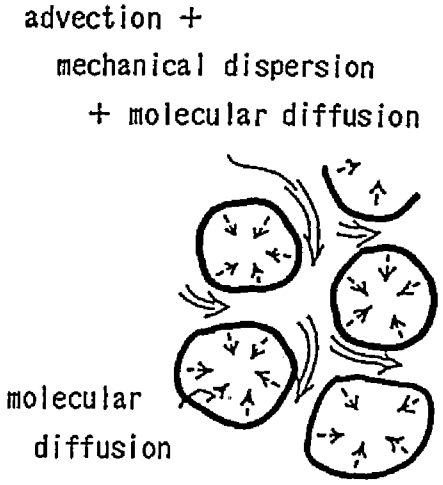

Fig. 2-7 Solute movement in aggregated medium.

Brenner (1962), and Rose and Passioura (1971) showed that a BTC approximated by one-dimensional advective dispersive equation (2.13) can be determined only by the following Péclet number, P:

$$P = uL/k \qquad (2.23)$$

where L is the soil column length. Therefore, the experimental dispersion coefficient can be easily obtained from the BTC because the mean pore water velocity, the soil column length, and the Péclet number are known. BTC's and those Péclet numbers are shown in Fig.2-8.

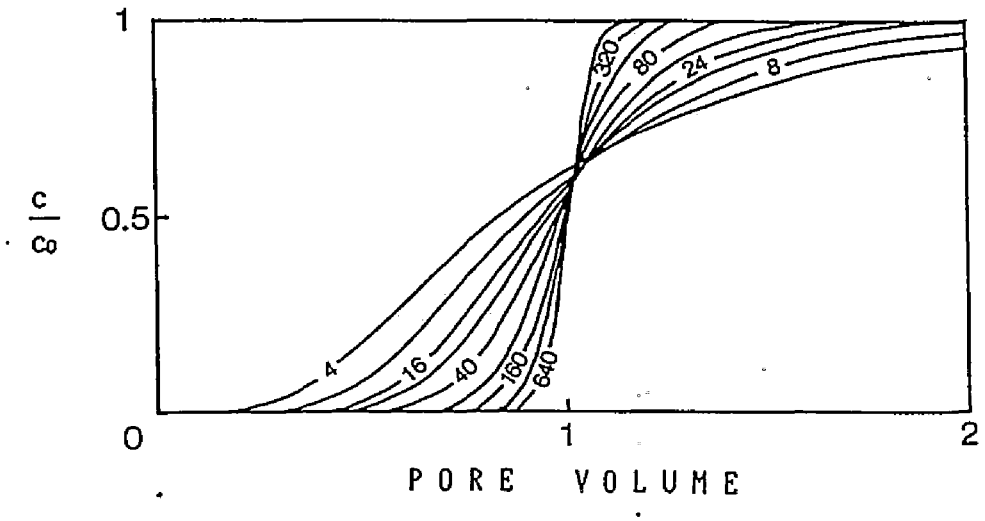

Fig. 2-8 Breakthrough curves derived from one-dimensional advective dispersive equation. The numbers on the curves denote the Péclet numbers. (after Rose and Passioura, 1971)

2.4. SOLUTE TRANSPORT IN MACROPORES

2.4.1. EXPERIMENTAL CONSIDERATION

In undisturbed naturally structured soils with macropores, incoming water and solutes flow down rapidly, and only partial displacement of resident water and solutes by incoming water and solutes occurs. Recognition of such behavior, variously described as "channeling,""short-circuiting,""bypassing,""preferential flow," or "partial displacement" is not new (Schumacher, 1864; Lawes et al., 1882), as pointed out by Thomas et al. (1978) (White 1985b).

In Japan, the effect of cracks on drainage in paddy fields is of

great concern. White vinyl water paint was used to observe water pathways in paddy fields (Yamazaki et al., 1962; Yamazaki et al., 1964; Yamazaki et al., 1966; Maruyama and Morikawa, 1966; Tabuchi et al., 1966a; Tabuchi et al., 1966b; Tabuchi et al., 1966d; Tabuchi et al., 1966e; Nagahama et al., 1968; Fujioka and Maruyama, 1971; Inoue et al., 1988). Recently, the effect of macropores on fertilizer and other pollutants movement raises great concern. Much research is performed to determine these effects. Fluorescein, methylene blue, white vinyl water paint, and uranine have been used as tracers to observe and evaluate water pathways (Ritchie et al., 1972; Kissel et al., 1973; Bouma and Dekker, 1978; Omoti and Wild, 1979; Sakuma et al., 1979; Hatano et al., 1983; Seyfried and Rao, 1987; Miyazaki, 1988). Tokunaga et al. (1984) developed the heavy liquid infiltration method for x-ray radiography. Macropore structures became very clear with this method.

Many experimental evidences of preferential flow in macropores have been reported. Biggar and Nielsen (1962) compared the BTC for three

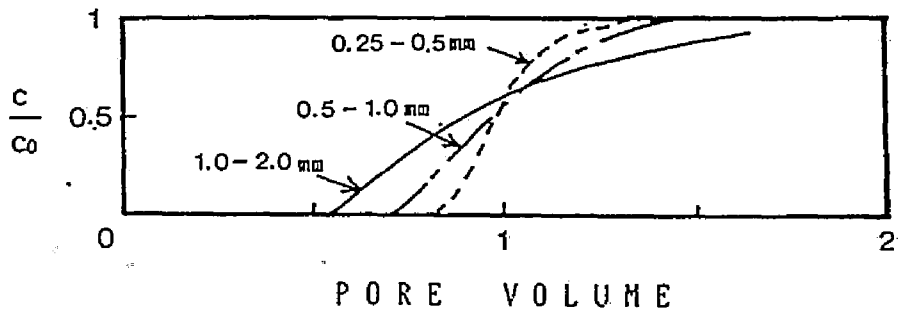

Fig. 2-9 Chloride breakthrough curves from three aggregate size fractions of Aiken clay loam for an average flow velocity of $5.6X10^{-4}$ cm/s at saturation. (after Biggar and Nielsen, 1962)

sizes of aggregates. The curves lost their skewed sigmoid shape and became more convex as the aggregate size increased (Fig.2-9). They concluded that as the aggregate size increased mixing in the column became less complete and the effluent concentration was dominated by flow through the large pores.

Soil structures of undisturbed soils and disturbed soils differ greatly. Elrick and French (1966), Kissel et al. (1973), and McMahon and Thomas (1974) found that, near saturation, solutes moved more rapidly in undisturbed soil than in disturbed soil due to preferential flow in the large connected pores of undisturbed soil. Kissel et al. (1973) reported that BTC on a pore volume basis for a short column of undisturbed soil showed earlier breakthrough than that for a long one. Kolenbrander (1970) showed that the dispersivity, a = k/u (k is the dispersion coefficient; u is the mean pore water velocity), of field soil was three times larger than that of a disturbed soil column. Thomas et al. (1973), and Tyler and Thomas (1977) reported that, due to macropores, solute loss in a soil under no tillage was greater than that under conventional tillage.

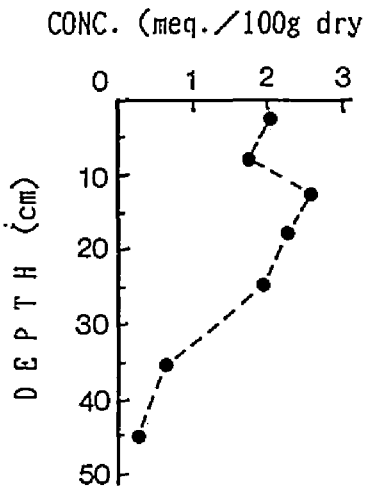

Fig. 2-10 Vertical distribution of incoming chloride in Andisol after application of water. (after Sakuma et al. 1979)

The marked asymmetry of incoming solute distributions and these elution curves in fields have been observed (Blake et al., 1973; Wild and Babiker, 1976; Quisenberry and Phillips, 1976; Sakuma et al., 1979a; Jury et al., 1982). An example of a vertical distribution of Cl^- is shown in Fig.2-10. Rahe et al. (1978) also obtained asymmetric distribution of introduced Escherichia coli populations in the field. Sakuma et al. (1977b) schematically divided the asymmetric BTC into components of direct, middle, and delayed discharges. Van De Pol et al. (1977) reported that the peak of the incoming solute concentration at 63.5 cm depth was reached faster than that at 46.0 cm depth. Shaffer et al. (1979) measured early movement of incoming solute through macropores in the field. Biggar and Nielsen (1976), and Van De Pol et al. (1977) measured solute distributions within a soil profile during the leaching of the solute applied to the field soil. They estimated that pore water velocities were logarithmically normally distributed in the field.

BTC's for soils with large macropores were obtained (Anderson and Bouma, 1977a; Bouma and Anderson, 1977; Kanchanasut et al., 1978; Bouma and Wosten, 1979; Tyler and Thomas, 1981; White et al., 1984; White, 1985a; Smith et al., 1985; Hatano et al., 1985; Seyfried and Rao, 1987; Dyson and White, 1989). They showed early breakthrough and succesive tailing such as the BTC A in Fig.2-1.

Lateral flow rate from macropores to micropores greatly affects solute transport. Smith et al. (1985), and White (1985a) reported that the effluent concentration of introduced E. coli from soil columns with large macropores increased just after the effluent discharged and did

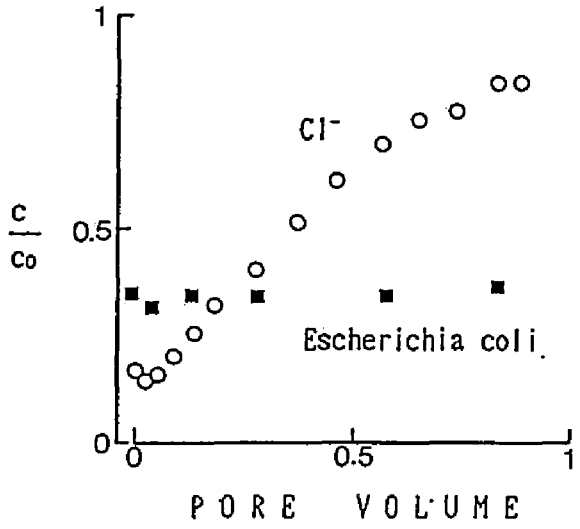

Fig. 2-11 Breakthrough curves for Escherichia coli and Cl^-. The undisturbed Maury silt loam core was irrigated at 20 mm/h. Initial volumetric water content was 0.31. (after Smith et al., 1985)

not change significantly with effluent volume (Fig.2-11). E. coli could only flow downward through large pores and could not diffuse into the micropores. They concluded that this caused the difference between the E. coli BTC and other solute BTC. White et al. (1984) demonstrated that Cl^- showed earlier breakthrough than tritiated water because of slower diffusion of Cl^- into micropores. Bouma and Anderson (1977) applied solution intermittently to soil columns with artificially made vertically continuous cylindrical pores and compared the BTC's for soil constructed of 40% sand and 60% silty clay loam with those of 80% sand and 20% silty loam. The former showed earlier breakthrough due to slower absorption of the solution into micropores.

Because solution flows through large macropores only under near saturated conditions, the effect of macropores on solute transport differs with soil water potential. Quisenberry and Phillips (1976) reported that incoming solute moved rapidly as initial water content increased in the field. Bouma and Dekker (1978) applied methylene blue tracer into dry, clay soils with macrostructures and measured amounts of stains on the walls of large vertical pores. The result showed that solute flowed down faster as application rate increased even at the same applied quantity. Elrick and French (1966) reported that BTC's for undisturbed soils at moisture contents near saturation, showed earlier breakthrough than those for disturbed soils, however, only little difference was observed

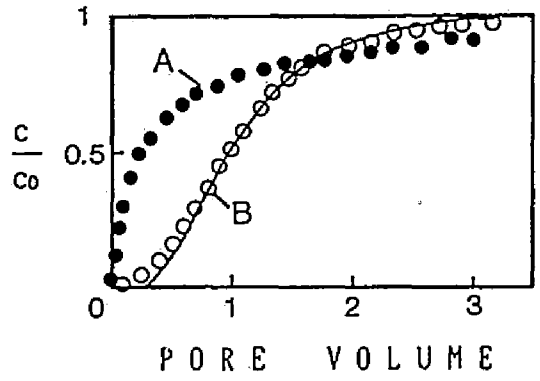

Fig. 2-12 The effect of soil water tension on the tritiated water breakthrough curves for undisturbed clay loam. The solid line represents the best fit of the one-dimensional advective dispersive model in B. (after Seyfried and Rao, 1987)

	A	B	
soil-water tension	0.0	10.2	cm H_2O
soil-water content	0.57	0.53	ml cm^{-3}
Darcy flux	$7.3X10^{-3}$	$3.3X10^{-4}$	cm s^{-1}

between them at the lower moisture conditions. Seyfried and Rao (1987) found that BTC's under saturated or near saturated conditions showed early breakthrough and succesive tailing, however, BTC's under soil water tensions greater than 10.2 cm of water were approximately symmetric in shape and accurately described by the one-dimensional advective dispersive equation (Fig.2-12).

2.4.2. MODELS FOR PREFERENTIAL FLOW

Because the one-dimensional advective dispersive equation could not describe the BTC which shows early breakthrough and tailing, new models for preferential flow were proposed. Bouma (1981) explained solute transport in a soil with macropores using bundles of vertical cylindri-

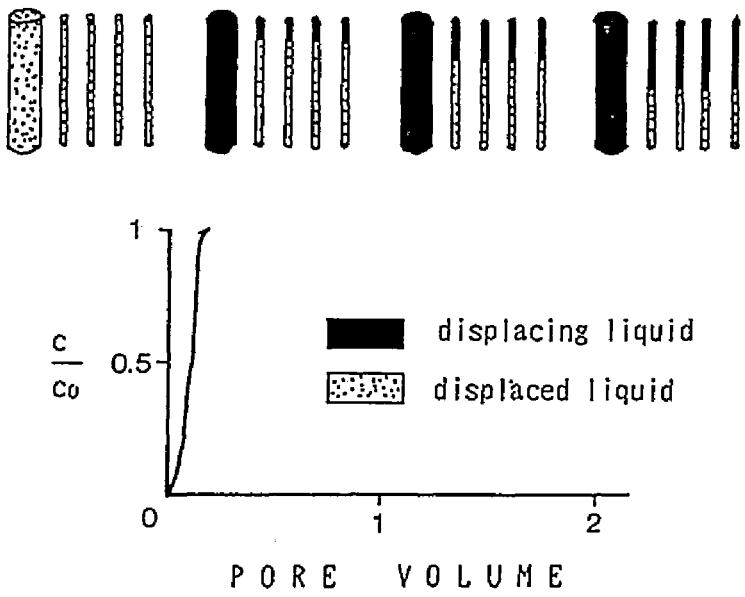

Fig. 2-13 Schematic representation of a breakthrough curve for a soil with a large macropore. (after Bouma, 1981)

cal tubes (Fig.2-13). The model consisted of one larger and many smaller tubes. Because preferential flow occured in the larger tube and flow in the smaller tubes was tiny, the BTC showed early breakthrough and the effluent concentration became almost the same as the input concentration immediately. However, when diffusion between macropores and micropores is not negligible, this model is not accurate.

Deans (1963) divided the liquid phase into mobile and immobile regions and assumed that diffusional transfer between the two liquid regions were proportional to the concentration difference between the mobile and immobile liquids. He neglected longitudinal dispersion in mobile regions. Coats and Smith (1964) expanded Deans' (1963) model to include longitudinal dispersion. This model uses the following equations:

$$\theta_m \frac{\partial c_m}{\partial t} + \theta_{im} \frac{\partial c_{im}}{\partial t} = \theta_m k \frac{\partial^2 c_m}{\partial x^2} - u_m \theta_m \frac{\partial c_m}{\partial x} \qquad (2.24)$$

$$\theta_{im} \frac{\partial c_{im}}{\partial t} = \alpha (c_m - c_{im}) \qquad (2.25)$$

where, θ_m and θ_{im} are the fractions of the soil filled with mobile and stagnant water, respectively, c_m and c_{im} are the concentrations in both the mobile and stagnant regions, k is the dispersion coefficient in the mobile region, u_m is the mean pore water velocity in the mobile liquid, and α is a mass transfer coefficient. Van Genuchten and Wierenga (1976) developed this model into sorption processes in both the dynamic and stagnant regions and assumed that the process was instantaneous and the adsorption isotherm was linear. This type of model is convenient for

soils with structures that are difficult to describe, because information about the soil structure is not needed. However, the mass transfer coefficient, α, was used as a fittng parameter and the physical meaning became vague. Rao et al. (1980a) applied this model to porous ceramic spheres of known radius and indicated that the α value is dependent upon the sphere radius, time of diffusion, volumetric water contents inside and outside the sphere, and the molecular diffusion coefficient. Rao et al. (1980b) measured values of all input parameters of the model in independent experiments. The calculated BTC agreed with the measured BTC. They also identified that large radius spheres, large pore water velocities, and short column lengths led to tailing or asymmetry in BTC's under saturated conditions.

While the above mentioned model used a fitting parameter or an empirical parameter α, models which described the rate of solute transfer between the two pore water regions by Fick's second law of diffusion were presented. Scotter (1978) developed two models of solution flow in soil. Solution flows down vertical cylindrical channels in one and planar cracks in the other. He approximated the soil structure as a regular hexagon with a vertical cylindrical pore in its centre and as a medium with a vertical planar slit, respectively. In both models, there is simultaneous molecular diffusion of the solute into the soil. Rao et al. (1980b), and Rasmuson and Neretnieks (1980) derived the solutions of solute transport in a spherical aggregates model. The governing equations were as follows (van Genuchten and Dalton, 1986):

$$\theta_m \frac{\partial c_m}{\partial t} + \theta_{im} \frac{\partial c_{im}}{\partial t} = \theta_m k \frac{\partial^2 c_m}{\partial x^2} - u_m \theta_m \frac{\partial c_m}{\partial x} \qquad (2.26)$$

$$c_{im}(x,t) = \frac{3}{R^3} \int_0^R r^2 c_a(x,r,t) dr \qquad (2.27)$$

$$\frac{\partial c_a}{\partial t} = \frac{D}{r^2} \frac{\partial}{\partial r} \left(r^2 \frac{\partial c_a}{\partial r} \right) \qquad (0 \leqq r \leqq R) \qquad (2.28)$$

where, c_{im} is the mean concentration of a sphere, c_a is the local concentration of spherical aggregate, R is the radius of the sphere, r is the radial coordinate, and D is the molecular diffusion coefficient in the aggregate. Grisak and Pickens (1980), and Tang et al. (1981) obtained the solutions of the model with a single vertical planar void. Sudicky and Frind (1982) developed the solutions for the case of transport in a system of discrete multiple-parallel fractures. Van Genuchten et al. (1984) gave the solution for the coaxial cylindrical model. Although these models are physically reasonable, they are adoptable only when the soil structure is similar to the model.

Because soil structures are usually heterogeneous in a field, their hydraulic properties vary from point to point and the transport of solute also differs from profile to profile. It is very difficult to measure all the field data which represent in exact detail the solute transport. Dagan and Bresler (1979), and Bresler and Dagan (1981) treated the solute concentration on field scale as a random variable and described the solute transport with mathematical techniques. Jury (1982) proposed a transfer function model in which the probability density function of the solute travel time was used. The concentration $c_L(W)$ at

the depth, L, and at the cumulative water input, W, was expressed as follows (Jury et al., 1986):

$$c_L(W) = \int_0^W f(W-W' \mid W')c_{IN}(W')dW' \qquad (2.29)$$

where, $f(W-W' \mid W')$ is the probability density function; that is, the probability that a solute injected at the cumulative water input, W', will reach the depth, L, after the cumulative water input, W. $c_{IN}(W')$ is the injected solute concentration at the cumulative water input, W'. Jury (1982) adopted a lognormal distribution to the probability function, because some measured data showed lognormal distribution of velocities in fields. This model is not concerned with the mechanism of solute transport in a field. The probability density function which resulted in the best agreement between the measured and calculated concentration curves was taken.

The definition of macroporosity is not unity as Beven and Germann (1982) summarized. There are many types of macropores such as pores formed by the soil fauna, pores formed by plant roots, cracks and fissures, and natural soil pipes. Even a uniformly packed soil column has relatively large pores and small pores. The dominant factor affecting solute transport must be considered in modelling.

2.5. ION EXCHANGE AND TRANSPORT IN SOILS

2.5.1. ELECTRIC CHARGE OF SOILS

Clay minerals in soils have electric charge. The two types of charge

are: permanent charge and variable charge.

Permanent charge is produced by isomorphous substitution for 2:1 type clay minerals. When Si^{4+} in a tetrahedral layer are substituted by Al^{3+}, or when Al^{3+} in an octahedral layer are replaced by Mg^{2+} or Fe^{2+}, the clay is charged negatively. Permanent charge density in 1:1 type clay minerals is very small.

Variable charge exists on the edge of crystalline clay minerals and on the surface of allophane and imogolite. Oxygens and hydroxyls with unsatisfied valences are linked with silicon or alminum. The charges on these oxygens and hydroxyls depend on the pH of the soil solution. Part of the hydroxyls linked with silicon produce negative charge by ionization:

$$Si]\text{-}OH \rightleftarrows Si]\text{-}O^- + H^+ \qquad (2.30)$$

where Si]- represents that Si is a part of the clay mineral. When H^+ concentration increases (pH decreases), H^+ is apt to be adsorbed by $Si]\text{-}O^-$. Because the reaction advances to the left side, negative charge decreases. On the other hand, part of the hydroxyls linked with aluminum produce positive charge by addition of H^+:

$$Al]<^{OH}_{OH_2} + H^+ \rightleftarrows Al]<^{OH_2}_{OH_2^+} \qquad (2.31)$$

When H^+ concentration increases (pH decreases), H^+ is apt to be adsorbed by hydroxyls. Because the reaction proceeds to the right side, positive charge increases. After all, positive charge increases and negative charge decreases as the pH decreases (Iimura, 1966). Variable

charge is sensitive to the soil solution condition. Amount of the ion adsorption increases as the ion concentration increases (Wada and Okamura, 1980; Okamura and Wada, 1983). The temperature of the solution also affects the amount of adsorption (Wada and Harada, 1971).

Humic substances, aluminum and iron oxide, oxyhydroxide, and hydroxide minerals also have variable charges. They are dependent on solution pH, too.

Humic substances include large amounts of carboxyls. Part of the carboxyls produce negative charge by ionization:

$$-COOH \rightleftarrows -COO^- + H^+ \qquad (2.32)$$

Aluminum and iron oxide, oxyhydroxide, and hydroxide are positively charged by addition of H^+:

$$Al]\text{-}OH + H^+ \rightleftarrows Al]\text{-}OH_2^+ \qquad (2.33)$$

$$Fe]\text{-}OH + H^+ \rightleftarrows Fe]\text{-}OH_2^+ \qquad (2.34)$$

Si]-OH produces positive charge when pH decreases, and Al]-OH and Fe]-OH produce negative charge when pH increases. However, such pH conditions are rare in soils in Japan.

2.5.2. ION EXCHANGE EQUILIBRIA

Because ions are adsorbed by electrostatic force, local equilibrium between the composition of the exchange complex and that of the soil solution is reached instantaneously. The relationship between them is usually expressed by a normalized exchange isotherm (Fig.2-14). Consider that there are two kinds of counterions, A and B. The exchange isotherm

in Fig.2-14 is graphed in terms of ion A. The abscissa of the exchange isotherm indicates the ratio of the A concentration to the total counterion concentration in the soil solution. The ordinate shows the ratio of the amount of exchangeable A to the amount of the total exchangeable counterions in the exchange phase. If ion A is preferred more than ion B in the soil, the exchange isotherm becomes convex upwards. On the other hand, if ion B is preferred over ion A in the soil, the exchange isotherm becomes concave upwards. If there is no ion exchange selectivity between them, the exchange isotherm becomes linear.

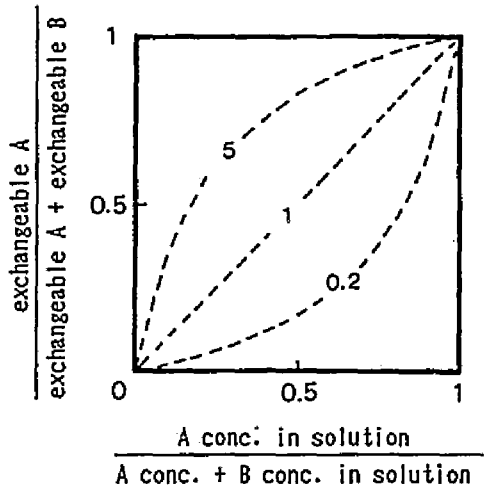

Fig. 2-14 Normalized exchange isotherms. Competing two ions A and B are existing in the exchange phase and the soil solution. Numbers on curves denote the selectivity coefficient, K.

Assume that ion A and ion B are homovalent. The equilibrium relationship between the composition of the exchange complex and that of the soil solution can be expressed by the following equation:

$$\frac{q_A}{q_B} = K\frac{a_A}{a_B} \qquad (2.35)$$

where, q is the amount of adsorbed ion per unit weight of the dry soil, a is the ion activity in the soil solution. The subscripts, A and B,

denote the values for ion A and ion B, respectively. K is the Kerr selectivity coefficient. To simplify the equation, we assume that the activities are equal to the concentrations, c.

$$\frac{q_A}{q_B} = K\frac{c_A}{c_B} \qquad (2.36)$$

Then, when K is larger than unity, the exchange isotherm is convex upwards. When K is smaller than unity, the exchange isotherm becomes concave upwards. When K is unity, the exchange isotherm is linear.

Experimental evidence shows that the relative preference of clays for the monovalent cations increases as the radius of the cation increases as follows:

$$\mathrm{Li(60pm)} < \mathrm{Na(90pm)} < \mathrm{K(133pm)} < \mathrm{Rb(148pm)} < \mathrm{Cs(169pm)} \qquad (2.37)$$

The radius of the hydrated cation decreases as the radius of the cation increases. The reason for the preference is assumed to be that the electric force between negative charges on the clay surface and the cation becomes stronger as the radius of hydrated cation decreases (Wada, 1981). On the other hand, significant preference is less pronounced among the divalent cations.

2.5.3. TRANSPORT OF EXCHANGEABLE IONS IN SOILS

Consider that the solution of the sorbed cation M^+ and non-sorbed anion N^- are introduced into a soil whose cation exchange capacity is q $mol_c\ kg^{-1}$. The volume wetness, θ, of the soil during infiltration and the incoming solute concentration, c, are set to be constant. The infil-

tration front of each ion in the soil profile is assumed to keep the initial shape. When the solution is applied V cm^3 cm^{-2}, the infiltration distance, x^-, of anion N^- is

$$x^- = V/\theta \tag{2.38}$$

On the other hand, the infiltration distance, x^+, of cation M^+ is obtained from the material balance equation (Bolt, 1978).

$$cV = x^+ (\theta c + \rho q) \tag{2.39}$$

where ρ is the bulk density of the soil. Then,

$$x^+ = \frac{V}{\theta (D_g + 1)} = \frac{x^-}{(D_g + 1)} \tag{2.40}$$

where, D_g is the distribution ratio, defined as (Bolt et al., 1978):

$$D_g = \frac{\rho q}{\theta c} \tag{2.41}$$

This number signifies the relative storage for the ion, that is the excess amount adsorbed compared to the amount in solution, both quantities being specified in mol_c per 1 kg of soil. The infiltration distance of the sorbed cation is shorter than that of the non-sorbed anion due to cation exchange. The infiltration distance of sorbed cation becomes short as the distribution ratio increases. That is, the distance becomes short as the cation exchange capacity increases and the incoming solute concentration decreases.

The infiltration front of the sorbed cation is influenced by longitudinal dispersion and the exchange isotherm. The shape becomes diffuse

due to longitudinal dispersion. The effect of the exchange isotherm on the shape of the front is well-known (DeVault, 1943; Lai and Jurinak, 1972; Bolt, 1978; Cho, 1985; Schulin et al., 1986; Mitsuno, 1988; Toride and Nakano, 1991). When the exchange isotherm is concave upwards, the shape of the front becomes more diffuse (unfavorable exchange). When the exchange isotherm is convex upwards (favorable exchange), it becomes sharp. Influence of the exchange isotherm on the shape is shown in Fig.2-15.

In a field or an undisturbed soil sample which has macropores, sorbed ion movement is greatly complicated due to preferential flow.

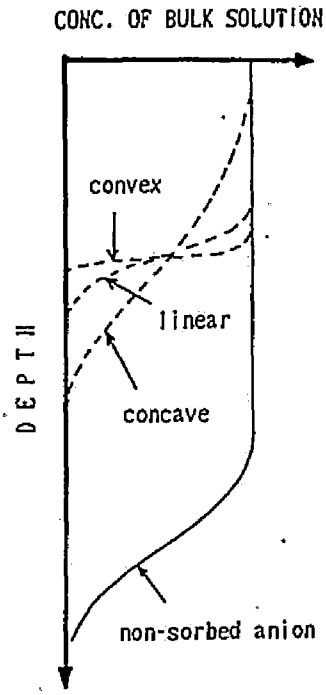

Fig. 2-15 Effect of the shape of the exchange isotherm on the concentration distribution in the soil profile.

CHAPTER 3

MACROPORES OF HARD PAN IN PADDY FIELD

3.1. INTRODUCTION

Macropores influence water and solute movement in soils. Because paddy soils are usually under flooded condition, the effect of macropores on water and solute transport is especially significant. Many studies on the effect of cracks on drainage in paddy fields are available (Kanou et al., 1961; Yamazaki et al., 1962; Yamazaki et al., 1964; Yamazaki et al., 1966; Maruyama, 1966a; Maruyama, 1966b; Maruyama and Morikawa, 1966; Tabuchi, 1966; Tabuchi et al., 1966a; Tabuchi et al., 1966b; Tabuchi et al., 1966c; Tabuchi et al., 1966d; Tabuchi et al., 1966e; Nagahama et al., 1968; Fujioka and Maruyama, 1971; Maruyama and Kimata, 1973). As the permeability of the hard pan layer is very low during irrigation period, observation of the soil structure of the layer is especially important for a good understanding of water and solute movement in the paddy field. However, detailed observations of their seasonal changes are not available.

In section 2 of this chapter, seasonal changes in distributions of macropores of a hard pan and a subsoil layer are studied. During non-irrigation period, many cracks are seen in these layers. However, after

ponding and puddling, cracks disappear. Then, vertical tubular pores made by rice roots (Masujima, 1970; Tokunaga et al., 1985; Narioka, 1990) become the predominant macropores. These macroporosities of hard pans of several soil groups in paddy fields are reported in section 3 of this chapter. Non-sorbing solute transport and sorbing solute transport in the hard pans are studied in chapter 4 and in chapter 5, respectively.

In section 2 of this chapter, the macropores denote the pores which were stained by a dilute solution of white vinyl water paint. On the other hand, the macropores denote the vertical tubular pores made by rice roots in section 3 of this chapter. The latter definition of the macropores is used in chapter 4 and chapter 5.

3.2. SEASONAL CHANGES IN DISTRIBUTIONS OF MACROPORES OF HARD PAN AND SUBSOIL IN A PADDY FIELD

3.2.1. EXPERIMENTAL

All experiments were conducted on the 1 ha paddy field in the National Research Institute of Agricultural Engineering in Tsukuba city. The well-drained area near the drainage canal and the ill-drained area near the inlet for irrigation water were selected for the experiments. The soil was Andisol, soil texture was clay loam, organic matter content was 19 %, and density of solids was 2.31 g/cm^3. Puddling depth was about 10 cm.

In order to observe macropores such as cracks and root holes, a di-

lute solution of white vinyl water paint in water (about 5% by volume) was used. After digging hollows, 50 X 50 cm and 13 cm deep, the dilute solution was poured into the hollows during several days. Each plot was dug several centimeters deep, leaving the new bottom surface horizontal. Stained macropores and newly penetrated rice roots were sketched on transparent sheets. This was repeated for several depth. At the same time, vertical distributions of soil hardness in the soil profiles were measured by Yamanaka's soil hardness meter. The soil was also sampled from the hard pan with a 100 cm^3 steel cylinder, and volume wetness and bulk density were measured by the oven dry method. The volume fractions of three component phases of the hard pan were calculated with the data of volume wetness, dry bulk density, and density of solids.

These measurements were performed just before puddling (mid-April), just after mid-summer drainage (early in August), and just before harvest (late in September) in 1986. Only well-drained site was measured just after mid-summer drainage.

Percolation rates at the well-drained site and the ill-drained site were measured under flooded condition before mid-summer drainage by using a rapid-response percolation meter.

3.2.2. RESULTS AND DISCUSSION

Distributions of newly extended rice roots in horizontal sections of the well-drained site just after mid-summer drainage are shown in Fig.3-1. Many rice roots which penetrated into the hard pan and the subsoil were observed as Kawata et al. (1980) indicated. The diameter

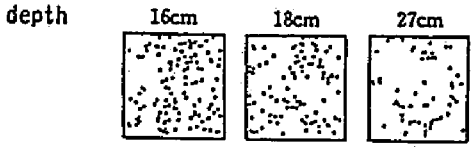

root density	0.127cm^{-2}	0.103cm^{-2}	0.076cm^{-2}
percent of the area occupied by roots	0.06%	0.05%	0.03%

Fig. 3-1 Distributions of rice roots in horizontal sections of well-drained site just after mid-summer drainage. The length of each side of the regular square is 30 cm.

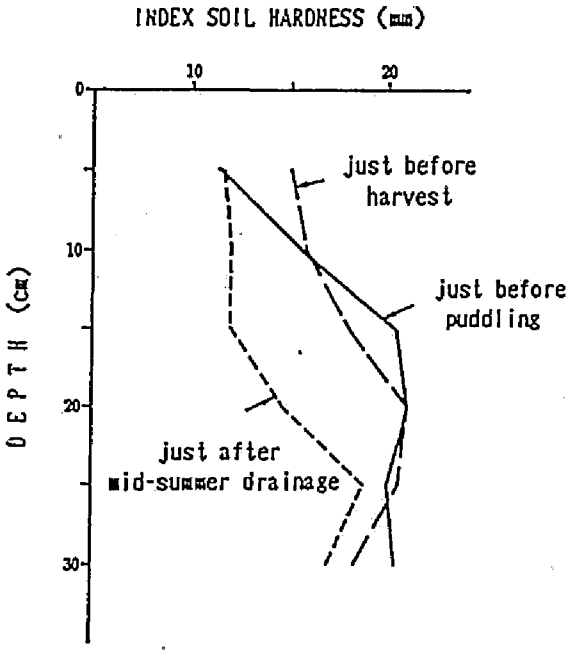

Fig. 3-2 Seasonal change of vertical distributions of soil hardness with Yamanaka's soil hardness meter. Each value is the average of 5 data.

of the roots ranged from 0.5 mm to 1.0 mm. Numbers of roots per unit area and rates of the areas which were occupied by roots are also shown in Fig.3-1. It is assumed that vertical tubular pores will be formed

after the decay of these roots.

Vertical distributions of soil hardness at the well-drained site are shown in Fig.3-2. The soil hardness is evaluated by the index length which indicates the contracted length of the spring of Yamanaka's soil hardness meter. While the index lengths of the hard pan and the subsoil were more than 20 mm just before puddling, they decreased approximately to 15 mm just after mid-summer drainage. Takijima et al. (1969) reported that the penetration of roots was inhibited when the index length became larger than 15 mm and no roots could penetrate when it became more than 23 mm in alluvial soils. Therefore, the data in Fig.3-2 indicates that rice roots could penetrate easily into the hard pan and the subsoil after flooding.

The soil's component phases of the hard pan are shown in Fig.3-3. Significant seasonal differences were not observed. However, small differences were seen between the ill-drained site and the well-drained site. The solid phase of the well-drained site was larger than that of the ill-drained site, and the liquid phase of the well-drained site was

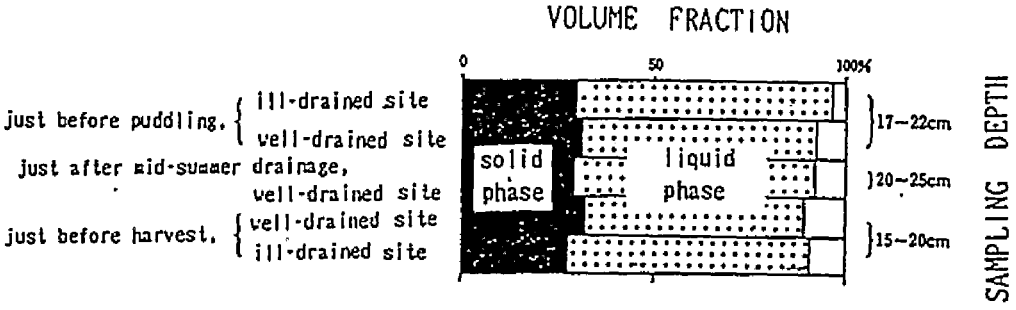

Fig. 3-3 The soil's component phases. Each value is the average of 3 data.

smaller than that of the ill-drained site. There were also small differences at the well-drained site between the data just after mid-summer drainage, and the data just before puddling and those just before harvest. The solid phase ratio just after mid-summer drainage was smaller than that just before puddling and that just before harvest, and the liquid phase just after mid-summer drainage was larger than that just before puddling and that just before harvest. These results may be caused to the difference in drainage conditions. Though each data was the average in triplicate, more measurements are necessary to derive a firm conclusion.

Distributions of stained macropores are shown in Fig.3-4. The number of stained macropores just after mid-summer drainage was much less than others. Kodama and Hishinuma (1959), and Adachi (1988) reported that soil particles dispersed by puddling clog macropores in upper parts of hard pans. This phenomenon is thought to be a cause of the decrease of the stained macropores. On the other hand, after a soil sample of the hard pan which initially had fine cracks was saturated by percolation for about one month, no cracks were observed with the unaided eyes. This result indicates that the swelling of the soil matrix of the hard pan was also a cause of the disappearance of the stained macropores. Another possible cause of the disappearance of the stained macropores was the penetration of rice roots into tubular pores as Kawata et al. (1980) pointed out.

Difference of stained macropore distributions between the well-drained site and the ill-drained site can be observed clearly in

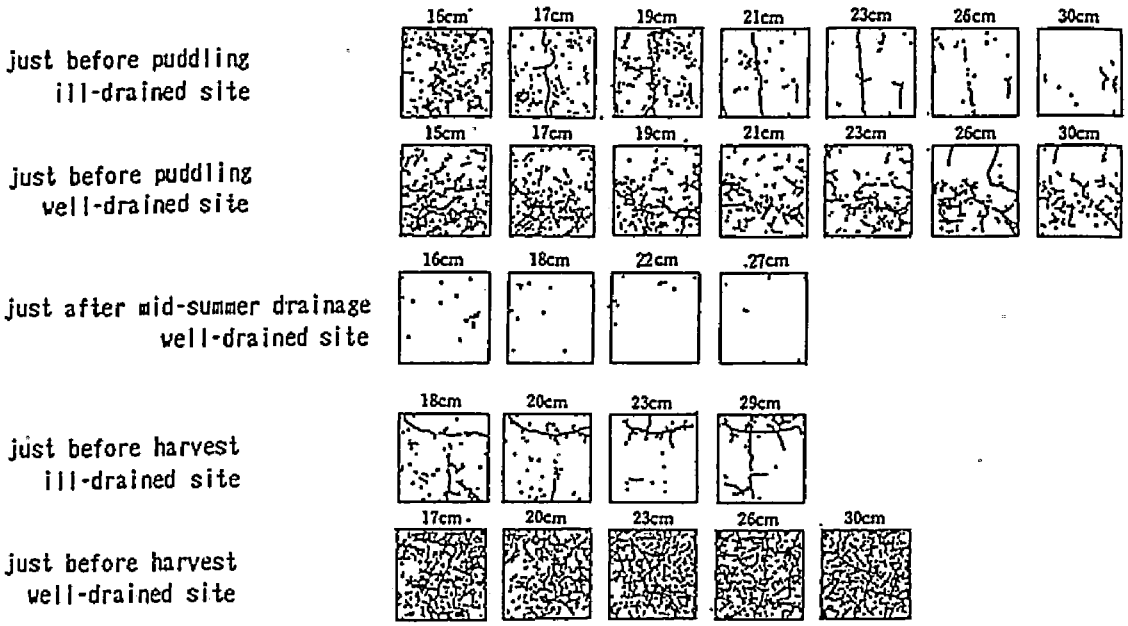

Fig. 3-4 Distributions of stained macropores. The numbers denote the depth. The length of each side of the regular square is 30 cm.

Fig.3-4. The amount of stained macropores at the well-drained site was larger than that at the ill-drained site. The percolation rate at the well-drained site was about 18.5 mm/d, while that at the ill-drained site was about 3.1 mm/d before mid-summer drainage. As the soil located below more than 30 cm from the surface at the ill-drained site was clayey, this soil lowered the permeability of the ill-drained site. Because only small amount of stained macropores were observed just after mid-summer drainage, it is thought that better drainage resulted in the more increase of macropores. The widths of these cracks were about 0.2 mm, the diameters of tubular pores were less than 0.2 mm.

3.2.3. SUMMARY

The experiments were conducted on the hard pan and the subsoil in the paddy field of Andisol and the following results were obtained:

1. Distributions of macropores changed seasonally with farm management. The stained macropores decreased after puddling under flooded condition due to clogging by dispersed soil particles, swelling of soil matrixes, and penetration of rice roots into tubular pores.
2. Differences in distributions of macropores between the well-drained site and the ill-drained site were observed. Good subsurface drainage led to an increase of macropores.
3. Penetration of rice roots was observed. Vertical tubular pores would be formed after the decay of these roots.
4. The hard pan and the subsoil became soft enough for rice roots to penetrate into them under flooded condition.
5. Little seasonal difference and little spatial difference of the soil's component phases were observed.

3.3. MACROPOROSITY OF HARD PANS

3.3.1. MATERIALS AND METHOD

Undisturbed soil samples of hard pans taken from five different paddy soils, 4 cm long and 10 cm in diameter, were used in the breakthrough experiments. More details of the experiment will be discussed in the next chapter. The soil samples were collected during or after the harvest season of the rice. Soil column data used for the breakthrough ex-

periments are shown in Table 4-1 in the next chapter.

After the end of the breakthrough experiments, the relationship between water content and suction in desorption was determined by means of a tension membrane assembly. Macroporosities of the vertical tubular pores made by rice roots were determined by using the differential water capacity curves which were obtained from the data.

3.3.2. RESULTS

During preparation of the experiment, fine cracks were observed in the soil samples excluding the sand sample. But, at the end of the experiments no cracks were visible with the naked eyes. In this experiment, most of the macropores seemed to be vertical tubular pores made by rice roots. Therefore, the word "macropore" is used to indicate a vertical tubular pore.

Differential water capacity curves of the samples are shown in Fig.3-5. Tubular pores made by vertical roots and lateral roots commonly exist in hard pans, the former being larger than the latter (Tokunaga et al., 1985; Narioka, 1990). Therefore, two peaks would be observed at low suction in the differential water capacity curve. Then, the volume of the vertical tubular pores (the macropores) was assumed to correspond to the area in the rise appearing in the range of lowest suction in the differential water capacity curve of the sample, as shown in Fig.3-5 by shading. Small amounts observed at low suction in the curves were ignored as measurement errors. In the case of the gray lowland soil to which chemical fertilizer was applied, the measurement failed at a

suction of 27.65 cm of H_2O. Therefore, the final effluent volume minus the effluent volume at a suction of 15.9 cm was assumed to be the volume of the macropores, because the curve increased from a suction of 15.9 cm. The obvious peak corresponding to the macropores in the sand curve was not observed. Because the hard pan of the sand did not become soft even under saturated condition and a crack did not occur in it, a root could not penetrate into it. Therefore, macropores were not found in sand. The measured macroporosities are shown in Table 4-1. The values ranged from 0.83% to 2.04%. The influence of these few macropores on solute transport will be discussed in the next chapter.

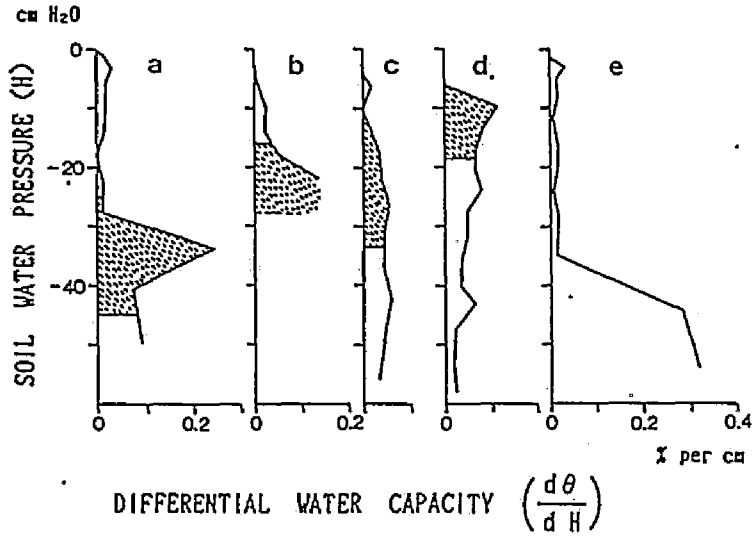

Fig. 3-5 The differential water capacity curves and the ranges of vertical tubular pores (shaded areas). θ denotes the volume wetness and H indicates the soil water pressure. a. Gray lowland soil, compost applied ; b. Gray lowland soil, chemical fertilizer applied ; c. Andisol ; d. Gley soil ; e. Sand.

CHAPTER 4

EFFECT OF VERTICAL TUBULAR PORES MADE BY RICE ROOTS ON SOLUTE TRANSPORT IN HARD PANS OF PADDY FIELDS

4.1. INTRODUCTION

As permeability of a hard pan layer is very low during irrigation period, the existence of the layer has a significant effect on water and solute transport in the paddy field. Therefore, clarifying the mechanism of solute transport in the layer is important for effective fertilizer use and preservation of water quality.

Solutes move through a soil under the action of advection and molecular diffusion. Consequently, the solute movement is defined mainly by the water flow in the soil, and the water flow is governed by the pore geometry. Many field and laboratory studies have indicated that preferential solute transport through large soil voids occurs, and many models adaptable for preferential solute transport have been presented as mentioned in section 4 of chapter 2. However, since the pore geometry in natural soils is too complex to describe as a model, most of those models use some fitting parameters to predict the solute transport.

In this chapter, a coaxial cylindrical model in which only one pa-

rameter is used was adopted to simulate non-sorbed Br^- transport through the hard pans of paddy fields. Calculated values were close to the measured values. The results proved that vertical tubular pores made by rice roots, whose radii were less than 1mm, had a significant effect on solute transport as transmission pores in the hard pans.

4.2. MATERIALS AND METHODS

Undisturbed soil samples of hard pans taken from five different paddy soils, 4cm long and 10cm in diameter, which were described in section 3 of chapter 3, were used in the breakthrough experiments (Fig.4-1).

The experimental procedure was as follows:

1. An undisturbed soil sample was saturated with water.
2. A 0.1 $mol_c\ L^{-1}$ $CaCl_2$ solution was supplied sufficiently to the sample to adsorb Ca^{2+}.
3. Pure water was supplied to discharge Ca^{2+} and Cl^- from the bulk solution.

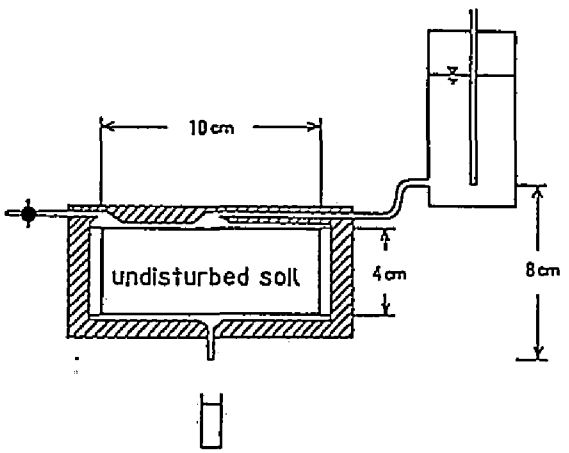

Fig. 4-1 Schematic cross-section of apparatus used for collecting samples of effluent from soil column.

Table 4-1
Soil column data used for the breakthrough experiments

	hydraulic conductivity cm/s (measured)	porosity % (measured)	vertical macro-porosity* % (measured)	mean velocity in vertical macropores* cm/s (from Eq.(4.4))	soil texture
Gray lowland soil compost applied	1.1×10^{-5}	49.8	2.04	1.1×10^{-3}	LiC
Gray lowland soil chemical fertilizer applied	7.9×10^{-5}	50.2	1.94	8.1×10^{-3}	LiC
Andisol	1.8×10^{-4}	71.3	0.83	4.4×10^{-2}	CL
Gley soil	4.8×10^{-4}	53.6	0.99	9.7×10^{-2}	LiC
Sand	5.2×10^{-4}	50.4	—	—	S

* All or most of the vertical macropores consisted of the vertical tubular pores made by rice roots.

4. After a 0.1 mol$_c$ L^{-1} $SrBr_2$ solution was supplied, measuring of the concentration of the output solution was begun.

Non-sorbed Br^- transport is discussed in this chapter. Adsorbed cations of Sr^{2+} and Ca^{2+} will be discussed in the next chapter.

Soil column data used for the breakthrough experiments is shown in Table 4-1. Because the soil samples were treated as materials in this experiment, the water flow conditions were different from those in the fields.

4.3. THE MODEL

4.3.1. THE COAXIAL CYLINDRICAL MODEL

A coaxial cylindrical model was proposed to describe solute transport through a hard pan having vertical tubular pores made by rice roots. The model assumes that the soil is composed of a bundle of cylindrical soil matrixes with a constant radius R and that each soil matrix has a cylindrical macropore with a constant r in its center (Fig.4-2).

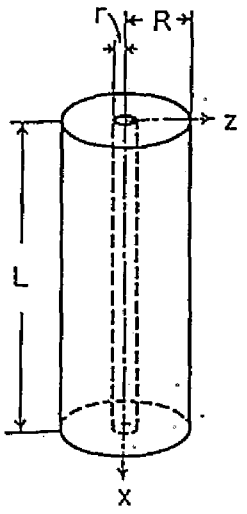

Fig. 4-2 Schematic picture of a coaxial cylindrical model.

Consider the soil sample to consist of n cylinders. As all the sectional areas of the cylinders are assumed to be equal to the sectional area of the soil sample, we get

$$n\pi R^2 = \pi l^2 \qquad (4.1)$$

where l is the radius of the soil sample (=5cm). That is, R is in fact an equivalent radius such that the volume defined by n times the volume of the fictitious cylinder is equal to the total volume of the sample. As the volume of all the cylindrical macropores with a radius r is assumed to be equal to the volume of the macropores in the soil sample, we obtain

$$n\pi r^2 L = v \qquad (4.2)$$

where L is the length of the soil sample (=4cm) and v is the volume of the macropores in the soil sample. We can get R from Eq.(4.1) and Eq.(4.2):

$$R = (\pi L/v)^{0.5} lr \qquad (4.3)$$

Assuming that the water discharge rate through soil matrix would be relatively negligible, we can obtain the mean velocity, u, in the macropore:

$$u = \frac{\pi R^2}{\pi r^2} Q = \frac{\pi l^2 L}{v} Q \qquad (4.4)$$

where Q is the measured water flux. As a result of the above assumption, a solute moves only by molecular diffusion into the soil matrix. The molecular diffusion coefficient of Br^-, D, in the soil matrix is (Bear, 1969; Ooi, 1986; Jpn.Soc.Chemistry, 1984)

$$D = \frac{2}{3} Do = 8.0X10^{-6} cm^2/s \qquad (4.5)$$

where Do is the molecular diffusion coefficient of Br^- in free water.

Since, according to Eq.(4.3), the radius of the cylinder R is a

function of the radius of the macropore r, all the parameters used become known if r is given. In calculation, the r which results in the best agreement between the measured and the calculated breakthrough curves (BTC's) for Br^- is taken as the value of r.

4.3.2. GOVERNING EQUATIONS AND NUMERICAL PROCEDURE

We assume that 1) a solute under consideration moves with the mean velocity u in a macropore without ion exchange and 2) no cross-sectional concentration gradient is present in it[1]. The general equation for solute transport in the macropore is then

$$\pi r^2 \frac{\partial C}{\partial t} = 2\pi r \theta D \left. \frac{\partial C}{\partial z} \right|_{z=r+} - \pi r^2 u \frac{\partial C}{\partial x} \qquad (4.6)$$

where C is the concentration, t is the time, θ is the porosity in the soil matrix, z is the radial distance, and x is the vertical distance.

Since the solute is assumed to move only by molecular diffusion in the soil matrix, the general equation for solute transport without ion exchange in the soil matrix is given by

$$\frac{\partial C}{\partial t} = D \frac{\partial^2 C}{\partial x^2} + \frac{D}{z} \frac{\partial}{\partial z} \left(z \frac{\partial C}{\partial z} \right) \qquad (4.7)$$

The initial and boundary conditions are as follows:

$$C(x,z,0) = 0 \quad 0 < x \leqq L,\ 0 \leqq z \leqq R,\ t = 0$$

---

[1] These assumptions are adequate because the cases presented here satisfy Eq.(2.17) in chapter 2.

$$C(0,z,t) = Co = \text{const.} \qquad 0 \leqq z \leqq R,\ t \geqq 0$$

$$\frac{\partial C(x,R,t)}{\partial z} = 0 \qquad 0 < x \leqq L,\ t \geqq 0$$

$$\frac{\partial C(L,z,t)}{\partial x} = 0 \qquad 0 \leqq z \leqq R,\ t \geqq 0$$

The discretization scheme of the coaxial cylindrical model is shown in Fig.4-3. The macropore was not divided radially. The soil matrix was divided into 5 sections radially. The cylinder was divided into 10 sections vertically. The nodes of concentrations were put at the center of each section.

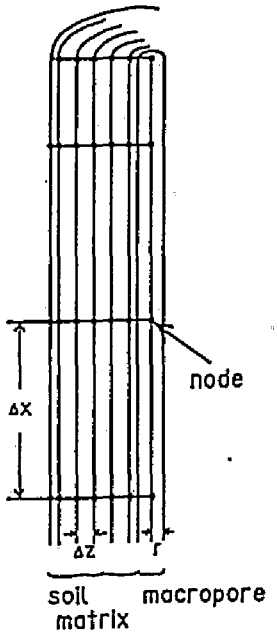

Fig. 4-3 Discretization scheme of the coaxial cylindrical model.

The discretization equation related to the concentration C(x,0,t) in the macropore is given by the integration of the general equation (4.6) over the control volume which contains the point (x,0) from t-Δt to t (see Fig.4-4(b)).

$$\iint_w \pi r^2 \frac{\partial C}{\partial t}\, dxdt$$

$$= \iint_w 2\pi r \theta D \frac{\partial C}{\partial z}\bigg|_{z=r+} dxdt$$

$$- \iint_w \pi r^2 u \frac{\partial C}{\partial x}\, dxdt \qquad (4.8)$$

$$w = \{ (x,t) : x-\Delta x/2 \leqq x \leqq x+\Delta x/2,\ t-\Delta t \leqq t \leqq t \}$$

In order to approximate Eq.(4.8), we use the upwind scheme for the ad-

vective term by setting $u\Delta t=\Delta x$, and the fully implicit scheme for the diffusive term. We obtain

$$\alpha \cdot C(x,0,t) = \beta \cdot C(x, r+\Delta z/2, t) + \gamma \cdot C(x-\Delta x, 0, t-\Delta t) \qquad (4.9)$$

$$\alpha = \beta + \gamma$$

$$\beta = \frac{2\theta D r \Delta x}{\Delta z}$$

$$\gamma = \frac{r^2 u}{2}$$

where Δx is the increment in x, Δz is the increment in z, Δt is the increment in time, and θ is the porosity in the soil matrix.

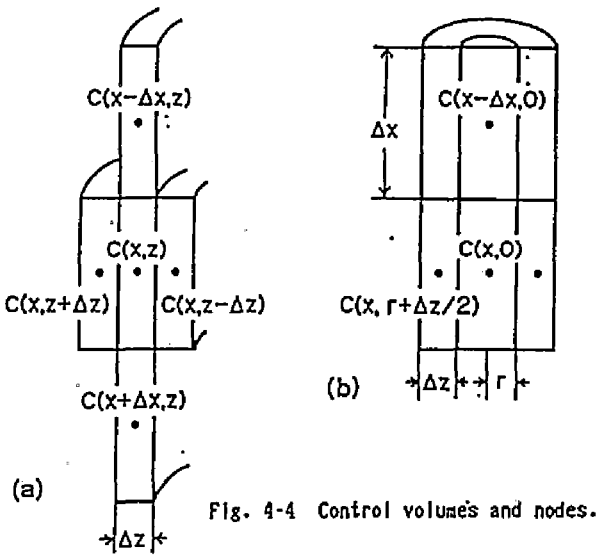

Fig. 4-4 Control volumes and nodes.

The discretization equation related to the concentration $C(x,z,t)$ in the soil matrix is given by the integration of the general equation (4.7) multiplied by z over the control volume which contains the position (x,z) from $t-\Delta t$ to t (see Fig.4-4(a)). We can get an approximation equation using the fully implicit scheme.

$$\alpha \cdot C(x,z,t) = \beta \cdot C(x+\Delta x, z, t) + \gamma \cdot C(x-\Delta x, z, t) + \delta \cdot C(x, z+\Delta z, t) + \varepsilon \cdot C(x, z-\Delta z, t) + \zeta \cdot C(x, z, t-\Delta t) \qquad (4.10)$$

$$\alpha = \beta + \gamma + \delta + \varepsilon + \zeta$$

$$\beta = \gamma = \frac{Dz\Delta z}{\Delta x}$$

($\beta = 0$ at $x=L-\Delta x/2$)

$$(\gamma = \frac{2Dz\Delta z}{\Delta x},\ C(x-\Delta x,z,t) = C(0,z,t)$$

$$= C_o \text{ at } x=\frac{\Delta x}{2})$$

$$\delta = \frac{D(z+\Delta z/2)\Delta x}{\Delta z}$$

($\delta = 0$ at $z=R-\Delta z/2$)

$$\varepsilon = \frac{D(z-\Delta z/2)\Delta x}{\Delta z}$$

$$(\varepsilon = \frac{2Dr\Delta x}{\Delta z},\ C(x,z-\Delta z,t) = C(x,0,t)$$

$$\text{at } z=r+\Delta z/2)$$

$$\zeta = \frac{z\Delta z\Delta x}{\Delta t}$$

Unknown concentrations are obtained by solving the simultaneous algebraic Eqs.(4.9) and Eqs.(4.10) (Patankar, 1980).

4.4. RESULTS AND DISCUSSION

The measured BTC's for Br^- are shown in Fig.4-5. When a nonreactive solute flows through a uniform porous medium, the BTC is approximately

predicted by solving the one-dimensional advective dispersive equation (De Smedt and Wierenga, 1984). The measured curves for the gray lowland soil to which compost was applied and for the sand were each estimated approximately by the analytical solution of the equation by Lapidus and Amundson (1952) as shown in Fig.4-5. As specific obvious macropores were not recognized in the differential water capacity curve of the sand, the sand is assumed to be a uniform porous medium. The agreement between its

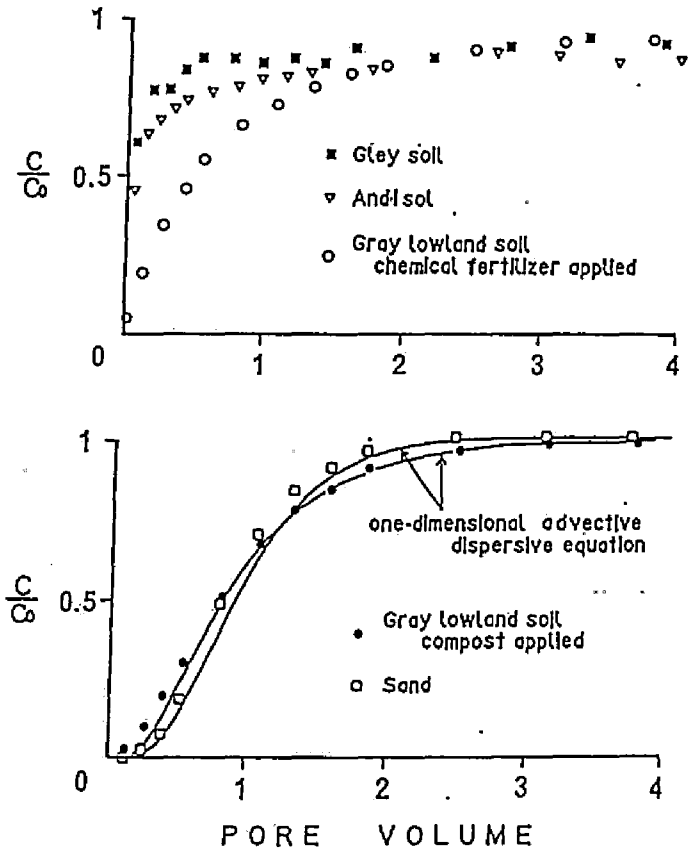

Fig. 4-5 Comparison of measured breakthrough curves (data points) and analytical solutions (solid lines) for Br^- displacement.

measured and analytical values also suggests that it is a uniform porous medium. On the contrary, the BTC's for the other three soils could not be approximated by the equation. These curves, which are similar to that of a soil with large voids, are very steep at their initial stage and tail away afterwards. This result suggests that a preferential flow through vertical tubular pores made by rice roots would occur in each soil.

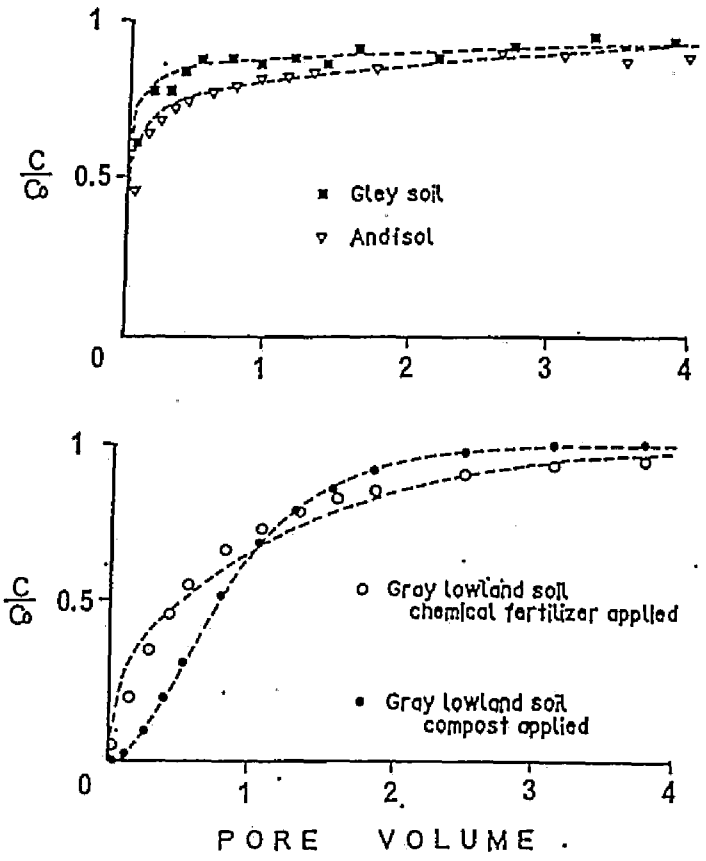

Fig. 4-6 Comparison of measured (data points) and calculated (----- the coaxial cylindrical model) breakthrough curves for Br^- displacement.

Table 4-2
Numerical results of the coaxial cylindrical model

	radius of macropore[a] r mm	radius of soil mantle R mm	density of macropore[a] cm^{-2}
Gray lowland soil compost applied	0.55	3.85	2.1
Gray lowland soil chemical fertilizer applied	0.45	3.23	3.1
Andisol	0.40	4.40	1.6
Gley soil	0.33	3.32	2.9

[a] "Macropore" indicates the vertical tubular pore made by a rice root.

To evaluate quantitatively the effect of the vertical tubular pores on solute transport, a numerical calculation based on the coaxial cylindrical model was performed. As shown in Fig.4-6, the calculated BTC's agreed well respectively with the measured curves. The calculated radii of the macropores, r, and of the cylinders, R, and the calculated densities of the macropores are shown in Table 4-2. The calculated radii of the macropores, r, ranged from 0.33mm to 0.55mm. These values are close to the radius of a main root of rice existing in a tipical hard pans. Tokunaga et al.(1985) measured the density of the macropores and got values from $1cm^{-2}$ to $1.5cm^{-2}$. The calculated densities are larger than that, but approximately close.

The mean velocities in the macropores of each soil differ significantly from each other. The highest velocity is about 100 times larger than the lowest velocity (Table 4-1). The differences in the mean velocities suggest different degrees of disorder in the water passages resulting from obstacles in the macropores. The calculated concentration distributions in the coaxial cylinders in the case of the fastest velocity and of the slowest velocity were compared at the same pore volume (0.3 pore volume) in Fig.4-7. In the case of the fastest velocity, since the elapsed time from 0 to 0.3 pore volume is short (551sec), only a very small amount of Br^- is distributed into the soil matrix by molecular diffusion. On the other hand, in the case of the slowest velocity, since the elapsed time is long (20700sec), the amount of Br^- diffusing into the soil matrix is large. Therefore, the higher the velocity becomes, the steeper is the BTC at the initial stage.

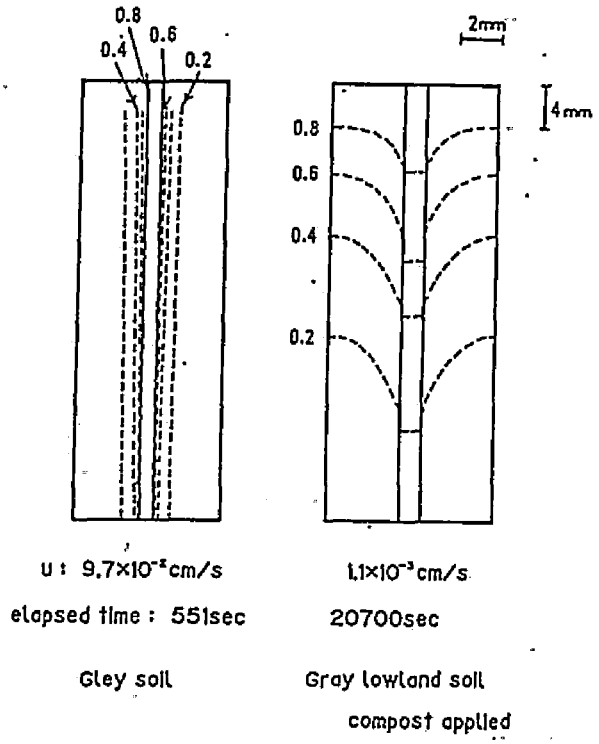

Fig. 4-7 Calculated concentration distributions in the coaxial cylinders in the case of the fastest velocity and of the slowest velocity at 0.3 pore volume. The numbers on the dashed lines represent relative conccentrations.

The main mechanisms of Br^- transport in the cylinder are the advection in the macropore and the radial molecular diffusion into the soil matrix from the macropore. Which mechanism is dominant can be roughly estimated by the following method ; used by Taylor(1953) for the evaluation of hydrodynamic dispersion in a tube as shown in section 3 of chapter 2. The time necessary for advection to make an appreciable change in concentration, t_1, is

Table 4-3

Comparison of the time for advection in the macropore and the time for radial molecular diffusion in the soil matrix

	time for advection t_1	time for radial diffusion t_2	$\frac{t_1}{t_2}$
Gray lowland soil applied compost	3600 sec	1300 sec	2.8
Gray lowland soil applied chemical fertilizer	490	890	0.55
Andisol	91	1700	0.054
Gley soil	41	940	0.044

$$t_1 = \frac{L}{u} \qquad (4.11)$$

The time necessary for the radial variation of concentration in the soil matrix to die down to about 1/e of its initial value, t_2, is

$$t_2 = \frac{R^2 - r^2}{3.8^2 D} \qquad (4.12)$$

These values for each soil sample are shown in Table 4-3. When $t_1 \ll t_2$, the BTC is steep at the initial stage. On the other hand, when $t_1 \gg t_2$, the BTC becomes a skewed sigmoid curve.

4.5. CONCLUSIONS

We make the following conclusions from the breakthrough experiments and from the model simulations for the undisturbed hard pans of the paddy fields:

1. The coaxial cylindrical model in which only one parameter is used was adopted to simulate non-sorbed Br^- transport through the hard pans of the paddy fields. All the calculated values were close to the measured values.
2. Vertical tubular pores made by rice roots, whose radii were less than 1mm, significantly affected solute transport through the hard pans of the paddy fields. That is, preferential flow occured in them. When the mean velocity in the pores was faster, solute discharged rapidly before diffusing well into the soil matrix. On the other hand, when the mean velocity in the pores was slower, solute

discharged slowly while sufficiently diffusing into the soil matrix.

CHAPTER 5

CATION EXCHANGE PROCESSES IN HARD PANS OF PADDY FIELDS

5.1. INTRODUCTION

Cations like NH_4^+ and K^+ are important nutrients for rice. On the other hand, the discharge of such nutrients sometimes causes eutrophication of a closed water area. Therefore, to clarify how cations move in paddy field soils is important for effective fertilizer use and preservation of water quality.

Commonly, clay minerals and organic matter in soils have negative charges and adsorb cations existing in the soils by electrostatic force. The cation exchange reactions occurring in the soils are reversible (excluding transition elements) and the reaction times are much smaller than the time necessary for the moving of the cations. Therefore, when one kind of cation flows into a soil and is exchanged for another previously adsorbed cation, the adsorbed amounts of the competing two kinds of cations and their concentrations in the bulk solution can be assumed to reach an local equilibrium state (as e.g. Lai and Jurinak, 1971; Valocchi et al., 1981; van Eijkeren and Loch, 1984; Selim et al., 1987).

In this chapter, cation exchange processes in the hard pans of paddy fields were studied. Cation transport was simulated assuming a local

equilibrium between the concentrations of the competing two kinds of cations in the bulk solution and the amounts of the adsorbed cations in the soil. The simulation was performed by using the values which were obtained from the calculation of non-sorbed Br^- transport in the previous chapter. The results thus calculated explained the measured values well. In addition, the CEC values of the soils obtained in breakthrough experiments (undisturbed soils) and those by batch experiments (well disturbed soils) were compared. The results showed that cations could exchange well even in the compact hard pans provided that the cations are supplied sufficiently and sufficient time is expended for the experiment.

5.2. MATERIALS AND METHODS

Ca^{2+} and Sr^{2+} breakthrough experiments (BTE's) were performed using the undisturbed hard pans of five different paddy fields. The equipment, the soil samples and the procedure were all the same as those described in the previous chapter.

A batch experiment was performed to measure the amount of adsorbed Ca^{2+} in the well disturbed soils. The method of Wada and Okamura (Wada and Okamura, 1977) was adopted for the batch experiment. The procedure was as follows:

1. The soil sample (about 2g; <2mm) was equilibrated with a 0.1 mol$_c$ L^{-1} $CaCl_2$ solution.
2. The soil sample was equilibrated with a dilute $CaCl_2$ solution with

the same concentration as the output concentration in the BTE just before the 0.1 $mol_c\ L^{-1}$ $SrBr_2$ solution was applied.

3. After the Ca^{2+} was replaced completely by 0.1 $mol_c\ L^{-1}$ $SrBr_2$, the amount of Ca^{2+} released was measured.

On the other hand, the amount of adsorbed Ca^{2+} in the BTE's was obtained from the entire amount of discharged Ca^{2+}.

5.3. THE MODEL

A coaxial cylindrical model including ion exchange was applied to describe Ca^{2+} and Sr^{2+} transport in hard pans having vertical tubular pores made by rice roots. This model is similar to the model without ion exchange described in the previous chapter except for the general equation for the soil matrix. The general equation including ion exchange for solute transport in the soil matrix is

$$\frac{\partial C}{\partial t} + \frac{\partial}{\partial t}\left(\frac{\rho q}{\theta}\right) = D\frac{\partial^2 C}{\partial x^2} + \frac{D}{z}\frac{\partial}{\partial z}\left(z\frac{\partial C}{\partial z}\right) \qquad (5.1)$$

where C is the Sr^{2+} concentration of the bulk solution, t is the time, ρ is the bulk density of the soil, q is the amount of adsorbed Sr^{2+} per unit weight, θ is the porosity, D is the molecular diffusion coefficient (= 8.0×10^{-6} cm^2/s), x is the vertical distance, and z is the radial distance.

In the BTE's, Sr^{2+} moved into the soil matrix and exchanged with

Ca^{2+} which had been adsorbed initially. Since the cations moved slowly, the following equilibrium equation can be assumed.

$$\frac{q}{q_c} = K\frac{a}{a_c} \qquad (5.2)$$

where q is the amount of adsorbed Sr^{2+} per unit weight, q_c is the amount of adsorbed Ca^{2+} per unit weight, a is the Sr^{2+} activity in the bulk solution, a_c is the Ca^{2+} activity in the bulk solution, and K is the Kerr selectivity coefficient. As the selectivity coefficient between Sr^{2+} and Ca^{2+} is about 1 (Bruggenwert and Kamphorst, 1982), it is assumed that there is no ion exchange selectivity between them. Then, one can rearrange Eq.(5.2) such that

$$\frac{q}{q_c} = \frac{C}{C_c} \qquad (5.3)$$

where C is the Sr^{2+} concentration in the bulk solution, C_c is the Ca^{2+} concentration in the bulk solution. The adsorbed amount of all cations q_A is

$$q_A = q + q_c \qquad (5.4)$$

Considering the electroneutrality of the bulk solution, we get

$$C_B = C + C_c \qquad (5.5)$$

where C_B is the Br^- concentration in the bulk solution. From Eq.(5.3), Eq.(5.4) and Eq.(5.5), we get

$$q = \frac{C}{C_B} q_A \qquad (5.6)$$

C_B is calculated by the coaxial cylindrical model as described in the previous chapter and q_A is given by measuring the entire amount of dis-

charged Ca^{2+} in the BTE's. Substituting Eq.(5.6) into the general equation (5.1), we obtain

$$\frac{\partial C}{\partial t} + \frac{\partial}{\partial t}\left(\frac{\rho q_R C}{\theta C_B}\right) = D\frac{\partial^2 C}{\partial x^2} + \frac{D}{z}\frac{\partial}{\partial z}\left(z\frac{\partial C}{\partial z}\right) \qquad (5.7)$$

The discretization equation related to the Sr^{2+} concentration $C(x,z,t)$ in the soil matrix is given by the integration of the general equation (5.7) multiplied by z over the control volume which contains the position (x,z) from $t-\Delta t$ to t. We get an approximation equation by using the fully implicit scheme.

$$\alpha \cdot C(x,z,t) = \beta \cdot C(x+\Delta x,z,t) + \gamma \cdot C(x-\Delta x,z,t) + \delta \cdot C(x,z+\Delta z,t) + \varepsilon \cdot C(x,z-\Delta z,t) + \zeta \cdot C(x,z,t-\Delta t) \qquad (5.8)$$

$$\alpha = \beta + \gamma + \delta + \varepsilon + \frac{z\Delta z\Delta x}{\Delta t}\left(1 + \frac{\rho q_R}{\theta C_B(x,z,t)}\right)$$

$$\beta = \gamma = \frac{Dz\Delta z}{\Delta x}$$

($\beta = 0$ at $x = L - \Delta x/2$)

($\gamma = \frac{2Dz\Delta z}{\Delta x}$, $C(x-\Delta x,z,t) = C(0,z,t) = C_o$ at $x = \frac{\Delta x}{2}$)

$$\delta = \frac{D(z+\Delta z/2)\Delta x}{\Delta z}$$

($\delta = 0$ at $z=R-\Delta z/2$)

$$\varepsilon = \frac{D(z-\Delta z/2)\Delta x}{\Delta z}$$

($\varepsilon = \frac{2Dr\Delta x}{\Delta z}$, $C(x,z-\Delta z,t) = C(x,0,t)$

at $z=r+\Delta z/2$)

$$\zeta = \frac{z\Delta z\Delta x}{\Delta t}\left(1 + \frac{\rho q_A}{\theta C_B(x,z,t-\Delta t)}\right)$$

where Δx is the increment in x, Δz is the increment in z, and Δt is the increment in time. The concentrations C are obtained by solving the simultaneous algebraic equations (4.9) in the previous chapter and (5.8). Then, Ca^{2+} concentration is given from Eq.(5.5). The same measured values and calculated parameters as those in the previous chapter are used in calculation.

On the other hand, the one-dimensional advective dispersive equation including ion exchange can be used to describe Ca^{2+} and Sr^{2+} transport in the hard pan of the sand, since non-sorbed Br^- transport was approximated by the equation without exchange. The general equation is

$$\frac{\partial C}{\partial t} + \frac{\partial}{\partial t}\left(\frac{\rho q}{\theta}\right) = k\frac{\partial^2 C}{\partial x^2} - u\frac{\partial C}{\partial x} \qquad (5.9)$$

where k is the dispersion coefficient and u is the mean pore velocity. The value k ($=1.03\times10^{-3}cm^2/s$) was calculated by using the Péclet number (Rose and Passioura, 1971) which gives the best agreement between

the measured and analytical breakthrough curves (BTC's) for non-sorbed Br^-. The values θ (=0.504) and u ($=2.05\times10^{-3}$cm/s) were measured in the BTE. Substituting Eq.(5.6) into q in Eq.(5.9), we obtain

$$\frac{\partial C}{\partial t} + \frac{\partial}{\partial t}\left(\frac{\rho q_A C}{\theta C_B} \right) = k\frac{\partial^2 C}{\partial x^2} - u\frac{\partial C}{\partial x} \qquad (5.10)$$

The discretization equation for the general equation (5.10) is given by the integration of the general equation (5.10) over a control volume from $t-\Delta t$ to t. We get an approximation equation by using the exponential scheme and the fully implicit scheme (Patankar, 1980).

$$\alpha \cdot C(x,t) = \beta \cdot C(x+\Delta x,t) + \gamma \cdot C(x-\Delta x,t) + \delta \cdot C(x,t-\Delta t) \qquad (5.11)$$

$$\alpha = \beta + \gamma + \delta + \frac{\Delta x}{\Delta t}\left(1 + \frac{\rho q_A}{\theta C_B(x,t)} \right)$$

$$\beta = \frac{u}{\exp(P)-1}$$

($\beta = 0$ at $x=L-\Delta x/2$)

$$\gamma = \frac{u \exp(P)}{\exp(P)-1}$$

($\gamma = u$ at $x=\Delta x/2$)

$$\delta = \frac{\Delta x}{\Delta t}\left(1 + \frac{\rho q_A}{\theta C_B(x,t-\Delta t)} \right)$$

where $P = u\Delta x/k$ and L is the soil column length (= 4cm). The concentrations C are obtained by solving the simultaneous algebraic equations (5.11). The numerical calculation was carried out by setting Δx=0.1cm

and Δt=10.0sec.

5.4. RESULTS AND DISCUSSION

The transport of non-sorbed ions in hard pans having vertical tubular pores made by rice roots has been made clear in the previous chapter. In this chapter, the transport of exchangeable cations in the hard pans was studied.

The cation movements were simulated by using only the measured values and parameters which were given in the calculation of non-sorbed Br^- in the previous chapter. The calculated BTC's for Ca^{2+} and Sr^{2+} agreed with the measured ones as shown in Fig.5-1.

The behavior of exchangeable cations accompanied by water movement in hard pans having vertical tubular pores made by rice roots can be explained in the same way as was done for non-sorbed Br^- movements in the previous chapter. The distributions of the calculated Sr^{2+} concentrations in the coaxial cylinders for the soil having the fastest velocity in its macropores and for that having the slowest velocity at the same pore volume (0.3 pore volume) are shown in Fig.5-2. In the case of faster velocity, since the elapsed time was short at the same pore volume, the amount of Sr^{2+} moving into the soil matrix was very small. Consequently the exchange and discharge of Ca^{2+} proceeded very gradually. On the other hand, in the case of slower velocity, since the elapsed time was long at the same pore volume, the amount of Sr^{2+} moving into

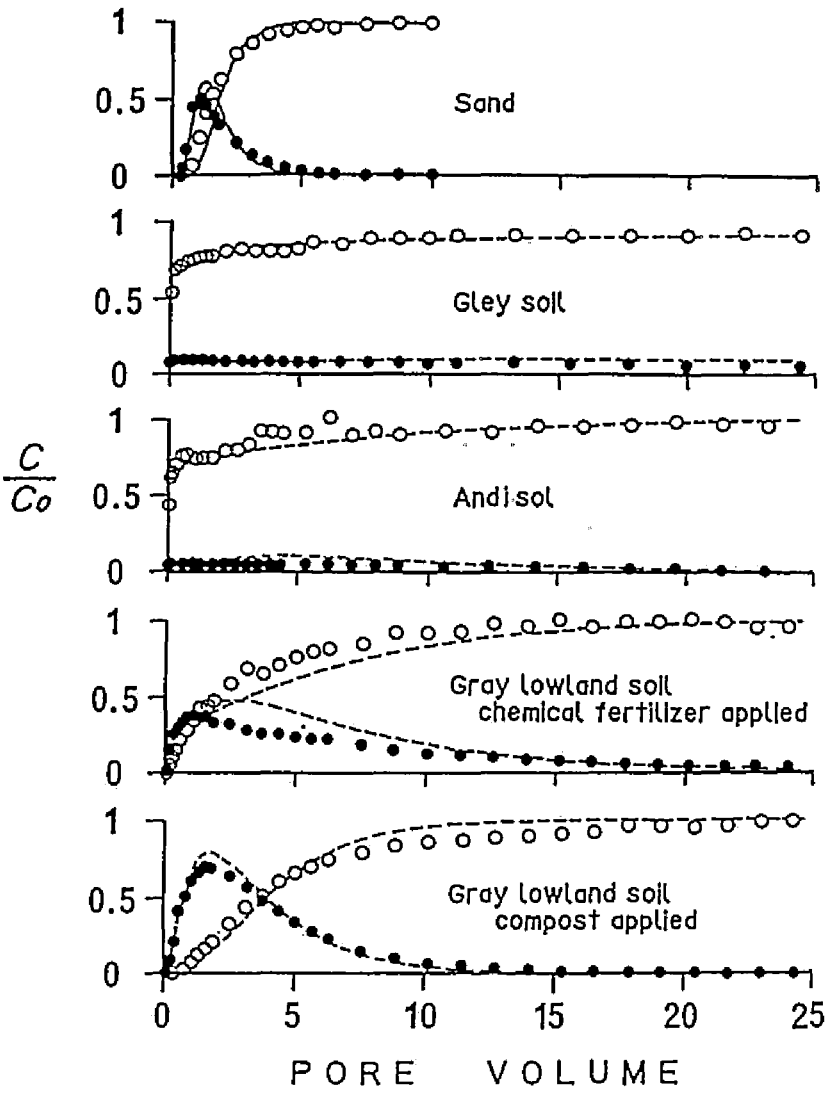

Fig. 5-1 Comparison of measured ($\bigcirc Sr^{2+}$; $\bullet Ca^{2+}$) and calculated (— one-dimensional advective dispersive equation with adsorption, ---- the coaxial cylindrical model) breakthrough curves for cation displacement.

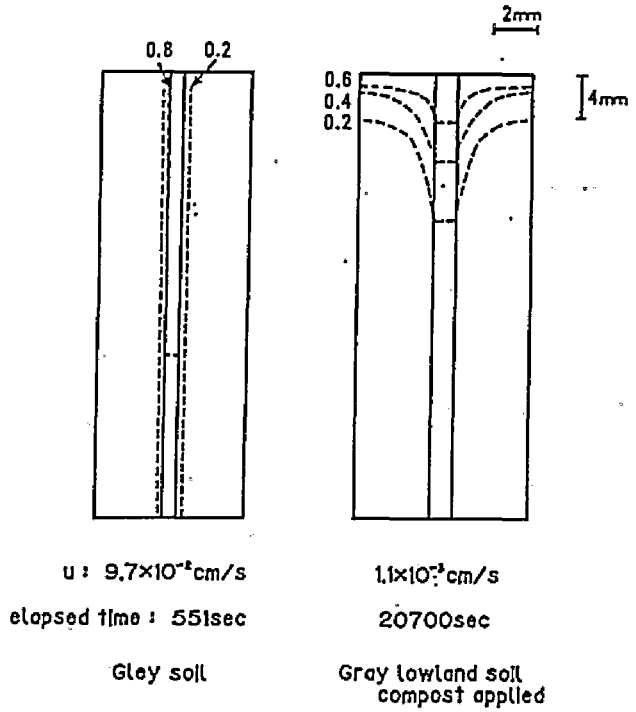

Fig. 5-2 Distributions of calculated Sr^{2+} concentration in the coaxial cylinders in the case of the fastest velocity and of the slowest velocity at 0.3 pore volume. The numbers on the dashed lines represent relative concentrations.

the soil matrix was large. As a result, the amount of Ca^{2+} exchanged and discharged during the initial stage of the BTC's was large. In the case of the sand, since Sr^{2+} flowed uniformly into the pores, it exchanged well with Ca^{2+} and the released Ca^{2+} was discharged sufficiently during the initial stage of the BTC.

The amounts of adsorbed Ca^{2+} obtained by the batch experiments and those obtained by the BTE's are shown in Table 5-1. Since the BTE's for the andisol and the gley soil were stopped before the discharge of Ca^{2+} was completely finished, the amounts of adsorbed Ca^{2+} after stopping the

Table 5-1

Amounts of adsorbed Ca^{2+} obtained by batch experiments and breakthrough experiments

	amount of adsorbed Ca^{2+}			
	breakthrough experiment		batch experiment	$\frac{A}{B}$
	mol$_c$/L	A mol$_c$/kg	B mol$_c$/kg	
Gray lowland soil compost applied	0.188	0.145	0.135	1.07
Gray lowland soil chemical fertilizer applied	0.214	0.150	0.155	0.97
Andisol	0.081[a]	0.117[a]	0.141	0.83
Gley soil	0.313[a]	0.172[a]	0.290	0.59
Sand	0.049	0.031	0.032	0.96

[a] The value was estimated to extend Ca^{2+} breakthrough curve to the latter part which was not measured.

experiments were estimated by extending the measured Ca^{2+} BTC's. Therefore the values for the andisol and the gley soil in Table 5-1 are approximate. Excluding these values, the amounts of adsorbed Ca^{2+} in the respective soils in both the BTE's and the batch experiments are almost same. The results show that cations can exchange completely even in undisturbed compacted soil matrixes as well as in well disturbed soils under the laboratory experimental conditions.

When the CEC of the soil is large, input cations penetrate into the soil slowly due to adsorption. Eliminating the effect of the CEC on cat-

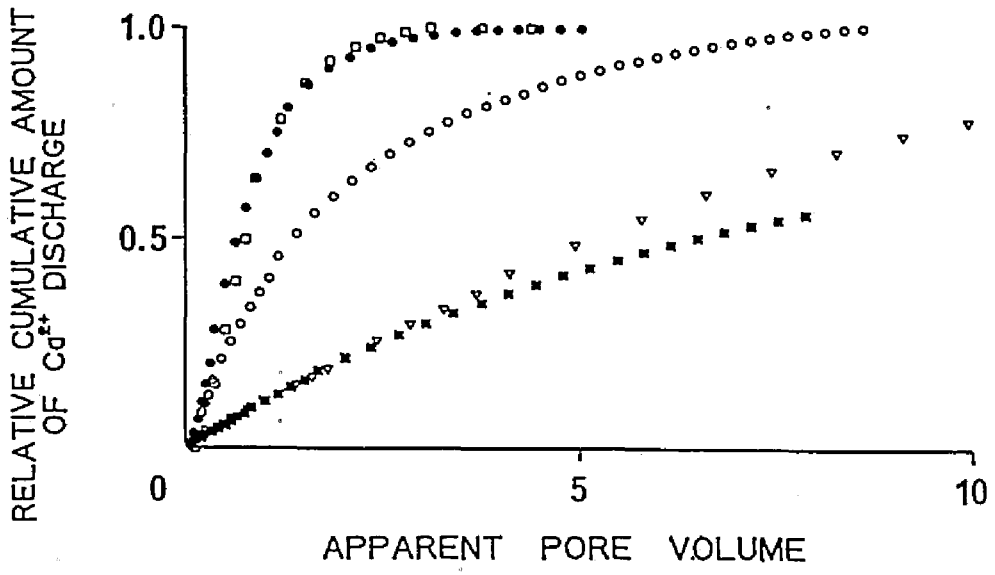

Fig. 5-3 Cumulative amount of Ca^{2+} discharge in breakthrough experiments as a function of apparent pore volume.
□ Sand ■ Gley soil ▽ Andisol
○ Gray lowland soil;chemical fertilizer applied
● Gray lowland soil;compost applied

ion discharge curves, unit of apparent pore volume is used instead of that of pore volume in abscissa. The apparent pore volume is defined as follows (Dufey et al., 1982):

$$1 \text{ apparent pore volume} = V\left(\frac{\rho q_A}{\theta C_o} + 1\right) \quad (L) \qquad (5.12)$$

where, V is the total water volume of a soil sample (L), ρ is the bulk density of the soil (kg L^{-1}), q_A is the total amount of adsorbed Ca^{2+} per unit weight (mol_c kg^{-1}), θ is the volume wetness, and C_o is the input solution concentration (mol_c L^{-1}). Changes in the cumulative amount of Ca^{2+} discharge standardized by the total amount of Ca^{2+} dis-

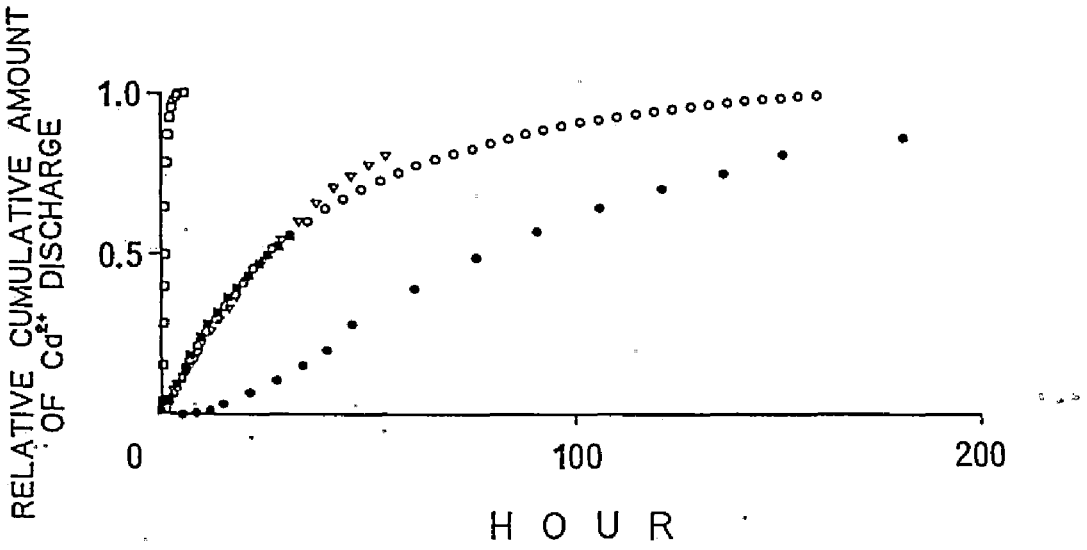

Fig. 5-4 Cumulative amount of Ca^{2+} discharge in breakthrough experiments as a function of time.
□ Sand ■ Gley soil ▽ Andisol
○ Gray lowland soil;chemical fertilizer applied
● Gray lowland soil;compost applied

charge are shown in Fig.5-3. It can be clearly seen in Fig.5-3 that the faster the mean velocity is in the macropore, the higher is the cumulative amount of water discharge necessary to completely discharge Ca^{2+}.

The changes in the curves of the cumulative Ca^{2+} discharge as a function of time are shown in Fig.5-4. In the case of faster velocity in the macropore, because the exchangeable solute was supplied more quickly, the time required to finish Ca^{2+} discharge became shorter. In the case of the sand, since Sr^{2+} flowed uniformly and rapidly into the pores, the curve shows the quickest discharge of Ca^{2+}.

5.5. CONCLUSIONS

Cation transport in the undisturbed hard pans was simulated assuming the local equilibrium between the concentrations of Ca^{2+} and Sr^{2+} in the bulk solution and the amounts adsorbed during the cation exchange process. Cation transport in the hard pans having vertical tubular pores was explained by the coaxial cylindrical model. Cation transport in the sand was approximated by the one-dimensional advective dispersive equation including ion exchange. The simulation was performed using the measured values and parameters which have been given in the calculation of non-sorbed Br^-. The results explained the measured BTC's well.

When the mean velocity in the tubular pores was fast, Sr^{2+} was discharged rapidly before diffusing well into the soil matrix. Consequently, the initially adsorbed Ca^{2+} was discharged gradually. On the other hand, when the mean velocity was slow, Sr^{2+} was discharged slowly, suf-

ficiently diffusing into the soil matrix. As a result, a larger amount of Ca^{2+} was exchanged and discharged during the initial stage of the BTC's. In the case of the sand, since Sr^{2+} flowed uniformly through the uniform porous medium, it was exchanged with Ca^{2+} and the released Ca^{2+} was sufficiently discharged during the initial stage of the BTC.

The amounts of adsorbed Ca^{2+} obtained by the batch experiments and the BTE's were compared. The results showed that cations could exchange well even in the compact hard pans provided that the cations are supplied sufficiently and sufficient time is expended for the experiment.

CHAPTER 6

EFFECTS OF VARIABLE CHARGE ON ION TRANSPORT IN AN ALLOPHANIC ANDISOL

6.1. INTRODUCTION

Because the density of variable charge in a soil is influenced by the solution concentration and the pH, ion transport in the soil is also affected by them. However, few studies on the effects of solution pH on breakthrough curves (BTC's) for exchanging ions have been reported (Chan et al., 1978; Chan et al., 1980a; Chan et al., 1980b; Nielsen et al., 1986). Those for an Allophanic Andisol under unsaturated conditions are particularly rare. Chan et al. (1978) indicated that amount of adsorbed cations in an oxidic soil increased as a pH of input solution increased. Chan et al. (1980a) showed that the Cl^- BTC for the oxidic soil was affected by solution pH and ionic strength. Nielsen et al. (1986) also showed the effect of solution pH on Cl^- BTC's for an Oxisol under saturated conditions. The Cl^- BTC shifted to the left as the pH increased, due to the change of the charged sites. They also reported that the influence of the charge in the soil on the BTC became significant as the solution concentration decreased.

Allophanic Andisol has both positive and negative variable charges, which is dependent on solution pH and ionic strength (e.g., Iimura, 1966 ; Okamura and Wada, 1983). Therefore, as Chan et al. (1980a) suggested, ion transport in the soil is strongly affected by solution pH and ionic strength. In this chapter, the effects of solution pH and concentration on ion transport in an Allophanic Andisol under saturated and unsaturated conditions are reported. The cases studied here involved ion exchange in binary anion (Br^--Cl^-) and cation (Sr^{2+}-Ca^{2+}) systems under a constant total concentration condition and a constant pH condition. The charge characteristics such as the AEC, the CEC, and the exchange isotherms were measured under different pH conditions and concentrations. Those results are compared with the BTC's.

6.2. MATERIALS AND METHODS

The soil studied was an Allophanic Andisol (Typic Hydrudand) from a field at the National Institute of Agro-Environmental Sciences in Tsukuba, Japan. The soil sample was collected from the 4B21 horizon. The soil contained 49.5 % of clay and 1.16 % of organic carbon. The clay fraction was dominated by allophane and imogolite. The amorphous material and allophane content determined using the method of Kitagawa (1977) was 41.4 %. The free aluminum oxide and the free iron oxide measured using the method of Mehra and Jackson (1959) were 2.43 % and 4.71 %, respectively. The pH in a 1:2.5 soil/water suspension and that in a 1:2.5 soil/(1 M KCl) suspension were 5.62 and 5.56, respectively. The

detailed measurement methods for the soil is written in the materials No.3, Department of Chemistry, the National Institute of Agricultural Sciences (1984).

BTC's were obtained from both saturated and unsaturated soil columns. A schematic cross-section of the apparatus for unsaturated conditions is shown in Fig. 6-1. An acrylic column of 30-cm length and 6.5-cm inner diameter was used. The column was wrapped in moist gauze to prevent soil water evaporation during the experiment. Soil water potentials in the soil column were adjusted to about -1.96 kPa during the percolation. Namely, the hydraulic gradient was about 1.0. To keep the soil water pressures at -1.96 kPa, the interface between atmosphere and water in the mariotte device was set at about 20 cm below the top of the soil column, and the outlet of the effluent was set at about 20 cm below the bottom of the soil column. The apparatus for saturated conditions had no air vent and the BTC's for saturated conditions were obtained under the hydraulic gradient, 0.5. The interface between atmosphere and water in the mariotte device was placed at the same level as that of the top of the soil column and the outlet of the effluent was set at 15 cm above the bottom of the soil column. The volumetric water contents under unsaturated conditions and those under saturated conditions ranged from 64 % to 72 % and from 72 % to 77 %, respectively.

The cases studied here involved ion exchange in binary anion (Br^--Cl^-) and cation (Sr^{2+}-Ca^{2+}) systems under a constant total concentration condition and a constant pH condition. The miscible-displacement experiments were carried out at different total concentration (0.001 mol。

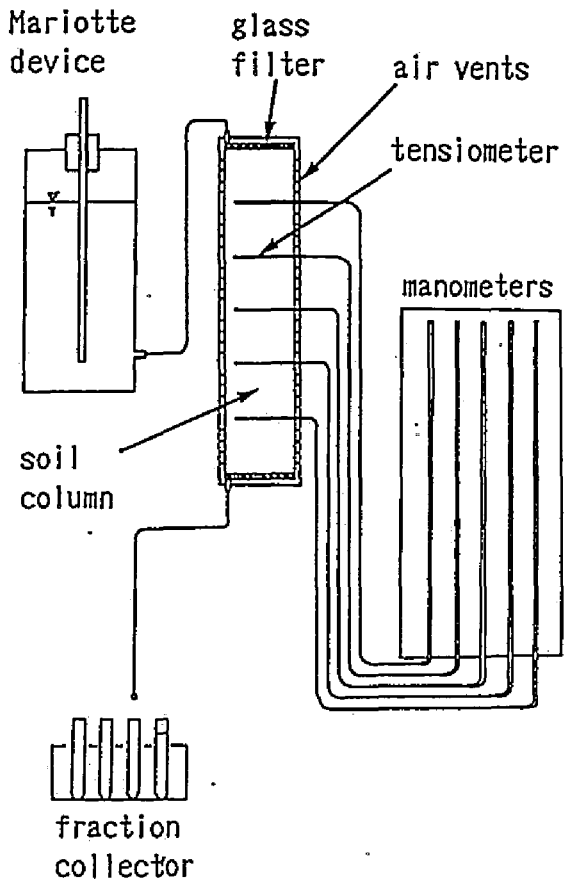

Fig. 6-1 Schematic cross-section of apparatus used to obtain breakthrough curves under unsaturated conditions.

L^{-1}, 0.005 mol_c L^{-1}, 0.01 mol_c L^{-1}, and 0.1 mol_c L^{-1}) and pH (from 4.2 to 7.65). The procedure was as follows :

1. The soil sample was equilibrated with a 1 mol_c L^{-1} $CaCl_2$ solution adjusted with HCl or $Ca(OH)_2$ to a desired pH (about pH 4, 5, 7.5 or pH not adjusted).
2. After setting the volumetric water content of the soil sample about the same as that in the field condition (about 63 %), the

soil was passed through a 2 mm sieve. The sieved soil was packed to a bulk density of 510 kg m^{-3} (the same value as the field condition).

3. After the soil column was saturated by capillary action with a $CaCl_2$ solution at a prescribed concentration (0.001 mol_c L^{-1}, 0.005 mol_c L^{-1}, 0.01 mol_c L^{-1}, or 0.1 mol_c L^{-1}), the $CaCl_2$ solution was percolated. A $CaCl_2$ solution at the prescribed concentration was adjusted at the same pH as the effluent pH. This adjusted solution was percolated sufficiently.
4. A $SrBr_2$ solution at the same concentration as that of the input $CaCl_2$ solution was adjusted at the same pH (from 4.2 to 7.65) as that of the effluent $CaCl_2$ solution. Then, after the $SrBr_2$ solution was supplied into the soil column under constant hydraulic gradient, the measurement of the concentration of the output solution was begun.

To compare the difference between transport of chemically reactive and inert solutes, tritiated water was used in some $SrBr_2$ solutions.

Sr^{2+}-Ca^{2+} exchange isotherms and Br^--Cl^- exchange isotherms were measured using a modified version of the method of Wada and Okamura (1980).

The AEC and the CEC in the BTC were estimated from the entire amount of discharged Cl^- minus the amount of Cl^- initially existed in the bulk solution of the soil column, and the former amount of Ca^{2+} minus the latter amount of Ca^{2+}, respectively. Those values were compared with those from the batch method of Wada and Okamura (1980).

Sr^{2+} and Ca^{2+} were analyzed by atomic absorption spectrophotometry. Br^- for Br^--Cl^- exchange isotherms was measured by radioactivation analysis. Cl^- and the other Br^- were measured by ion chromatography.

6.3. RESULTS AND DISCUSSION

Clay minerals in soils have charges, and consequently, adsorb counterions existing in the soils by electrostatic force. The AEC and the CEC of the Allophanic Andisol were measured, because the movement of the counterions in the soil is influenced by the charge densities. The

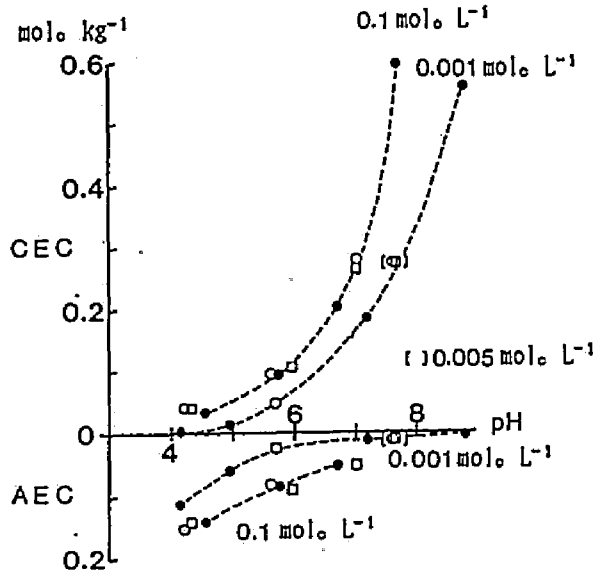

Fig. 6-2 Effects of pH and concentration on the AEC and the CEC.

● batch experiment
○ saturated
□ unsaturated
} breakthrough experiment

effects of the total solution concentration and the pH on the AEC and the CEC are shown in Fig. 6-2. The results are similar to those obtained by Okamura and Wada (1983). Namely, the AEC decreases and the CEC increases as the pH increases, and both of them increase as the total concentration increases. The AEC and the CEC estimated from the BTC's were similar to those measured using the batch method of Wada and Okamura (Fig. 6-2). These results corroborate the results obtained in chapter 5 that the CEC measured in the batch method and those estimated from the BTC for the undisturbed hard pans under the same solution conditions were almost same. These results show that input ions exchanged sufficiently with initially adsorbed ions in the Allophanic Andisol during the movement of the ions.

Because the shape of an exchange isotherm affects the BTC, exchange isotherms for the Allophanic Andisol were determined. The Sr^{2+}-Ca^{2+} exchange isotherms graphed in terms of exchangeable Sr^{2+} as a fraction of total exchangeable cations and Sr^{2+} concentration as a fraction of total cation concentrations are shown in Fig. 6-3. The effect of the pH on the Sr^{2+}-Ca^{2+} exchange isotherm is clear. The exchange isotherm becomes convex upwards at lower pH (4.55 to 5.75) and it becomes linear or slightly concave upwards at the higher pH of about 6.9. These results indicate an exchanger preference for Sr^{2+} over Ca^{2+} as the pH decreases. The effect of the total solution concentration on the Sr^{2+}-Ca^{2+} exchange isotherm is not significant. It seems that there is no difference among the exchange isotherms for different total concentrations having an identical pH. The Br^--Cl^- exchange isotherms graphed in terms of ex-

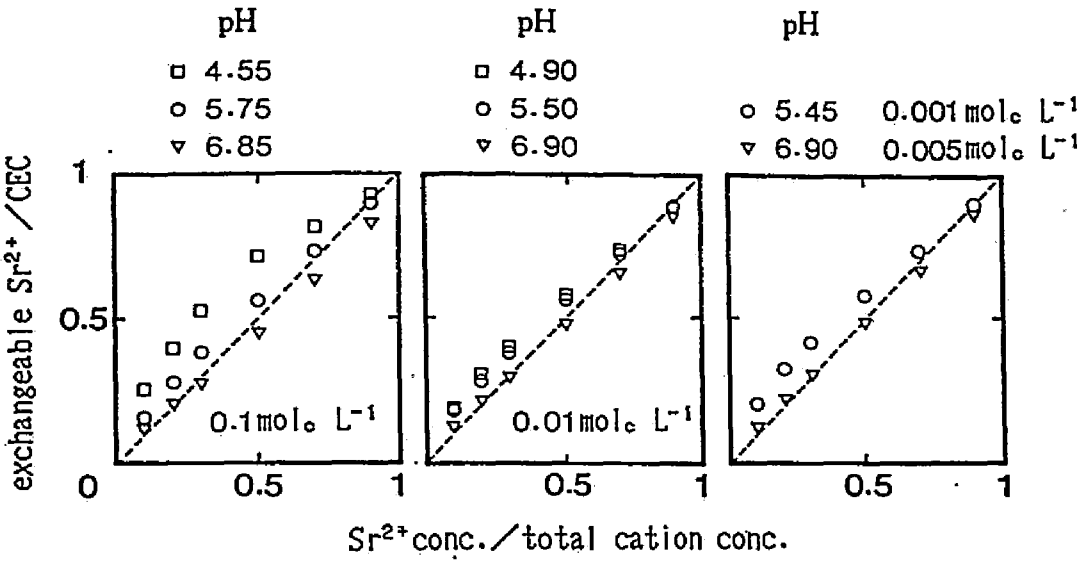

Fig. 6-3 Effects of pH and total concentration on the Sr^{2+}-Ca^{2+} exchange isotherms.

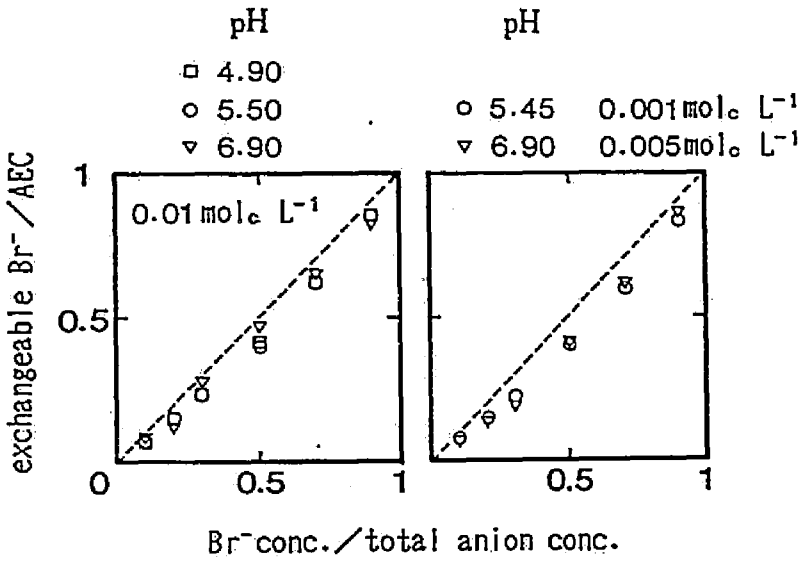

Fig. 6-4 Effects of pH and total concentration on the Br^--Cl^- exchange isotherms.

changeable Br^- as a fraction of total exchangeable anions and Br^- concentration as a fraction of total anion concentrations are shown in Fig. 6-4. The effect of the pH on the Br^--Cl^- exchange isotherm is not great. The results plotted in Fig. 6-4 are concave upwards and they move marginally closer to a linear relationship as the pH increases.

Measured BTC's are shown in Figs. 6-5 and 6-6. The effluent pHs kept almost constant during the miscible-displacement experiments. The pHs in the experiments ranged from 4.2 to 7.65. Those values for each run are denoted in Figs. 6-5 and 6-6 with concentrations.

Observed BTC's under saturated conditions showing the effect of total concentration and solution pH on the displacement process are illustrated in Fig. 6-5. Comparing the Sr^{2+} and Br^- BTC's for the total concentration of 0.01 $mol_c\ L^{-1}$, the Sr^{2+} BTC shifts to the right as the pH increases while Br^- BTC shifts to the left as the pH increases. Meanwhile, the CEC becomes larger as the pH increases while the AEC becomes smaller as the pH increases. The shifts of the BTC's correspond to the change in the AEC and the CEC. When the AEC or the CEC is large, greater amounts of the input solution are required for the counterion to penetrate to a fixed depth. Therefore, Br^- flowed out slowly at lower pH because of large AEC and Sr^{2+} discharged slowly at higher pH because of large CEC. The influence of the total concentration is observed among the BTC's for 0.1 $mol_c\ L^{-1}$ and pH 5.6, 0.01 $mol_c\ L^{-1}$ and pH 5.75, and 0.001 $mol_c\ L^{-1}$ and pH 5.7. The BTC shifts to the right as the total concentration decreases. When the input concentration is lower, greater amounts of the input solution are needed for the counterion to penetrate

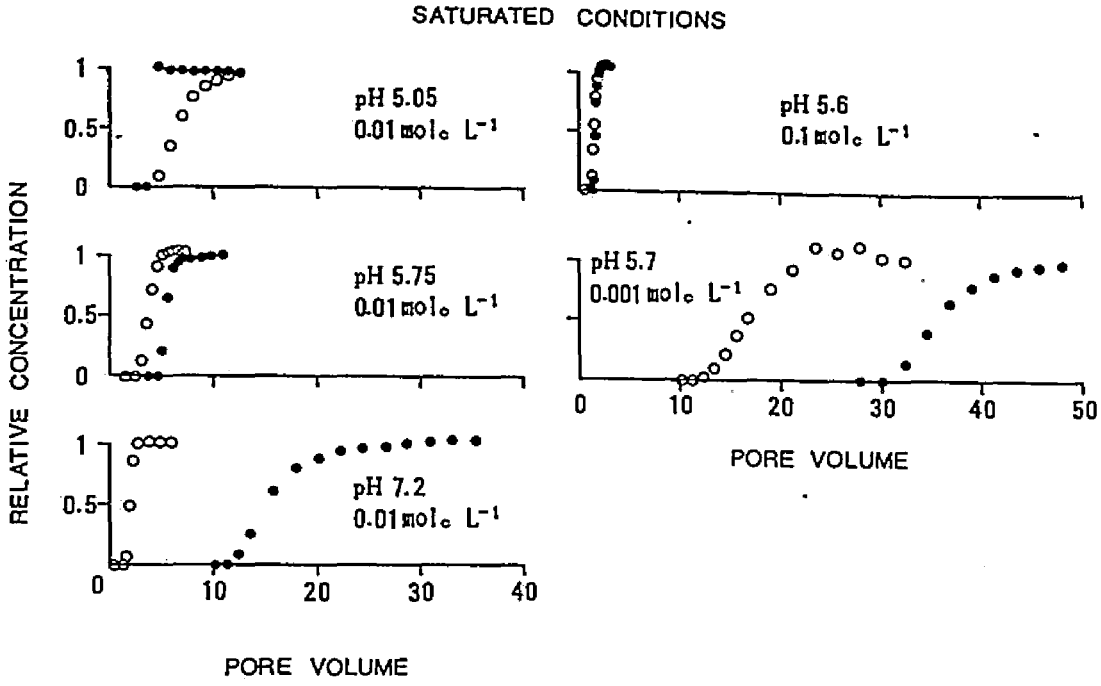

Fig. 6-5 Observed breakthrough curves showing the effects of pH and total concentration on the displacement process indicated by pore volume. (○Br^- ; ●Sr^{2+})

to a fixed depth because the supplied amount of the counterion contained in unit solution volume is smaller. Nielsen et al. (1986) showed similar BTC's for Cl^- using an Oxisol. From our results, we confirmed that the change in the BTC corresponds to the change in the ion exchange capacity and the total concentration.

To eliminate the effects of the AEC and the CEC on the BTC's, apparent pore volumes (Dufey et al., 1982) can be used on the abscissa for those figures. The apparent pore volume is given from data of the BTC as follows:

$$1 \text{ apparent pore volume} = \int_0^{\infty} (1 - C(w)/C_o)dw \quad (m^3) \quad (6.1)$$

where C(w) is the output concentration of Br^- or Sr^{2+} ($mol_c\ L^{-1}$), C_o is the input concentration of Br^- or Sr^{2+} ($mol_c\ L^{-1}$), and w is the volume of effluent (m^3). If there is no selectivity between two competing kinds of counterions in the soil, the BTC for each ion as a function of apparent pore volume becomes same as that for an inert solute (Dufey et al., 1982).

Observed BTC's for Br^- and Sr^{2+} as a function of apparent pore volume are shown in Figs. 6-6-1 to 6-6-3. BTC's for tritiated water were also added in Figs. 6-6-1 to 6-6-3 as an inert case. It is clear from the figures that the effect of the pH on ion transport in the soil is observed even though the effects of the AEC and the CEC are eliminated. The Br^- BTC's under saturated conditions and at 0.01 $mol_c\ L^{-1}$ under unsaturated conditions become diffuser than those for tritiated water as the pH decreases (Figs. 6-6-1(a), 6-6-2, and 6-6-3(a)). The Sr^{2+} BTC's under saturated conditions and at 0.01 $mol_c\ L^{-1}$ and 0.1 $mol_c\ L^{-1}$ under unsaturated conditions become steeper than those for Br^- as the pH decreases (Figs. 6-6-1, 6-6-2, and 6-6-3(a)). These results are explained using the exchange isotherms. Because the Br^--Cl^- exchange isotherm tends to become concave upwards at lower pH, the Br^- BTC becomes diffuse at lower pH. Conversely, because the Sr^{2+}-Ca^{2+} exchange isotherm becomes convex at lower pH, the Sr^{2+} BTC becomes steep as the pH decreases. As is well known, the former is a type of non-favorable exchange and the latter is a type of favorable exchange (e.g., DeVault,

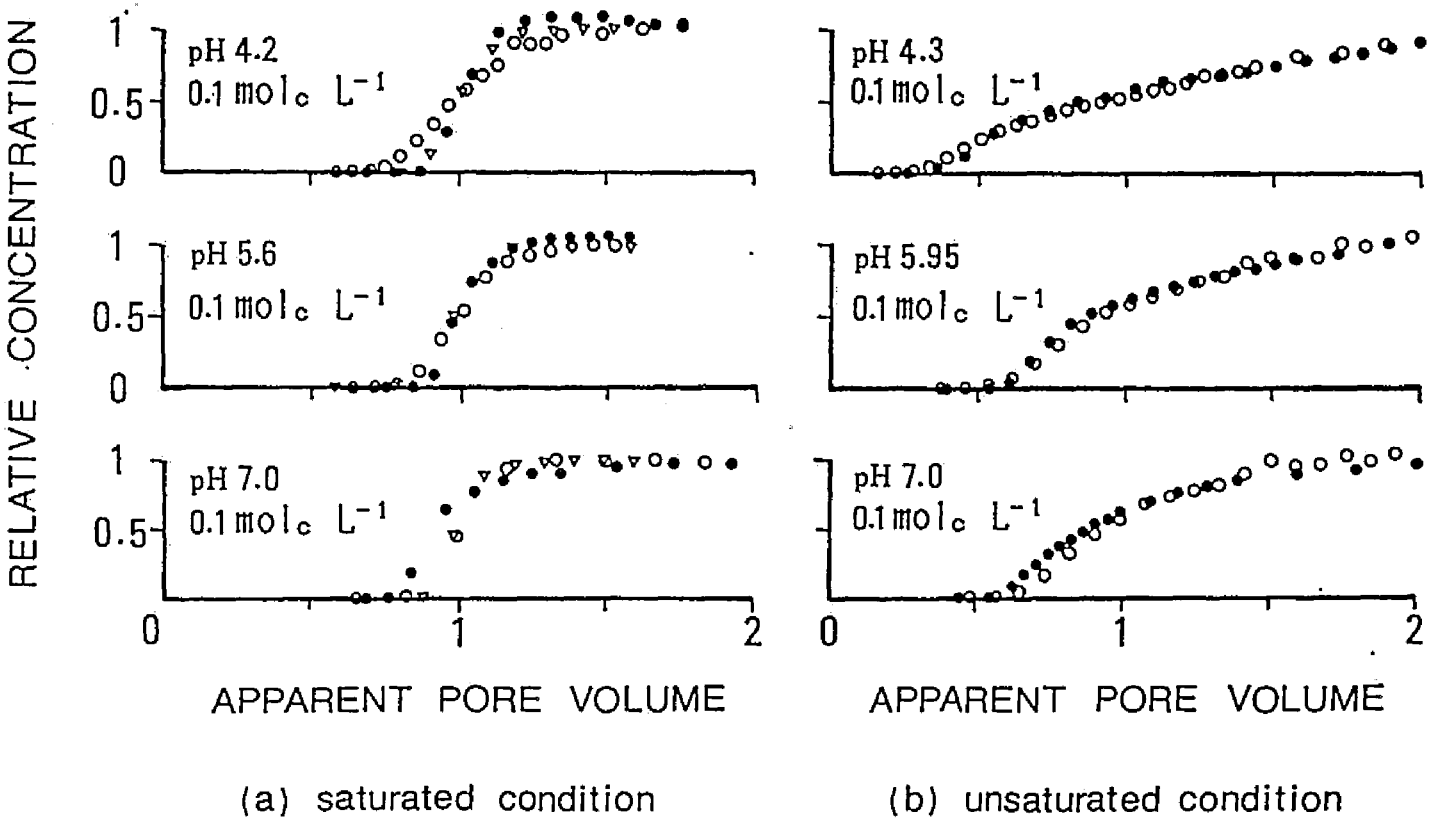

Fig. 6-6-1 Observed breakthrough curves showing the effect of pH on the displacement process indicated by apparent pore volume. (○Br^- ; ●Sr^{2+} ; ▽ tritiated water)

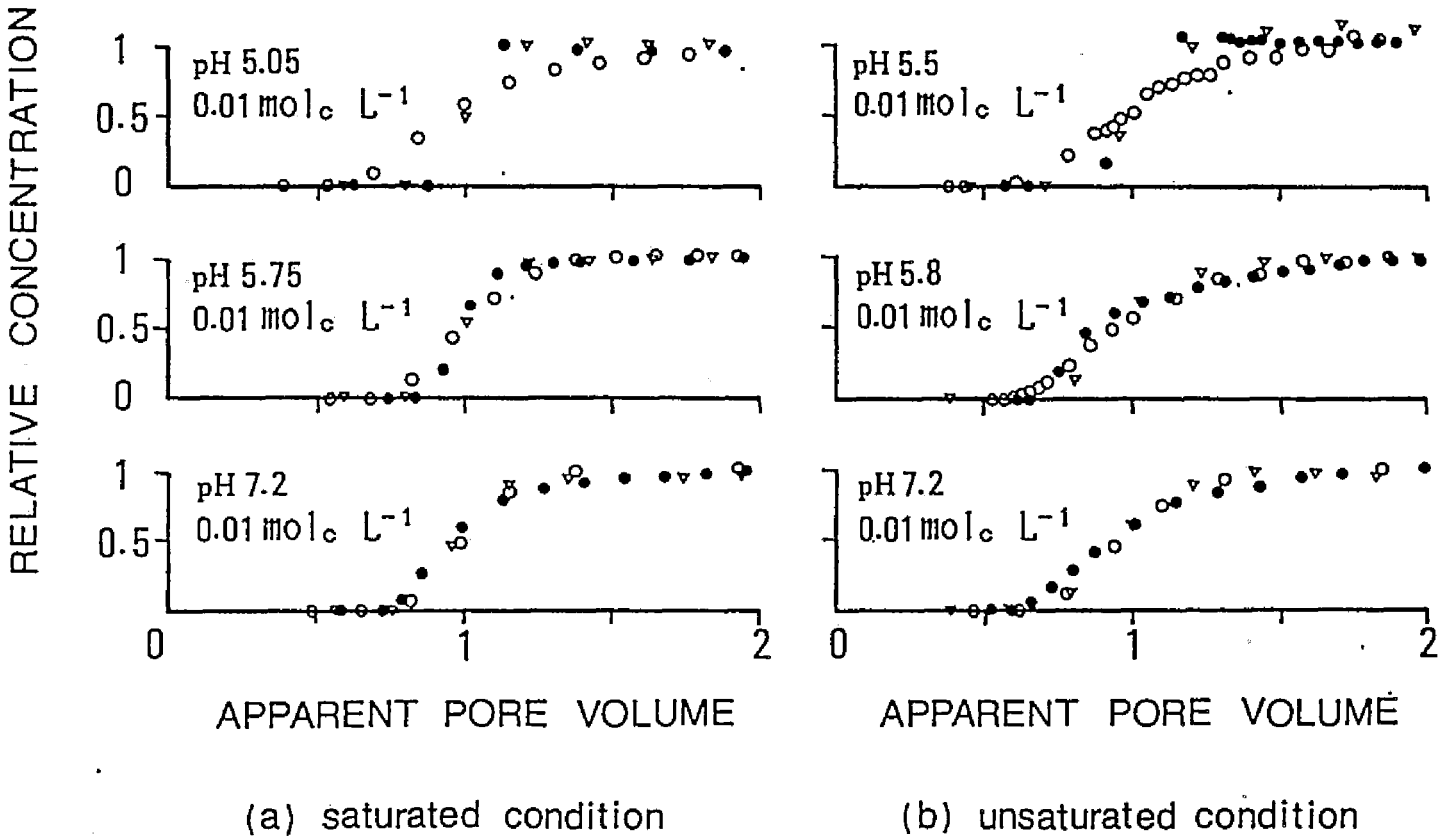

Fig. 6-6-2 Observed breakthrough curves showing the effect of pH on the displacement process indicated by apparent pore volume. (○Br^- ; ●Sr^{2+} ; ▽ tritiated water)

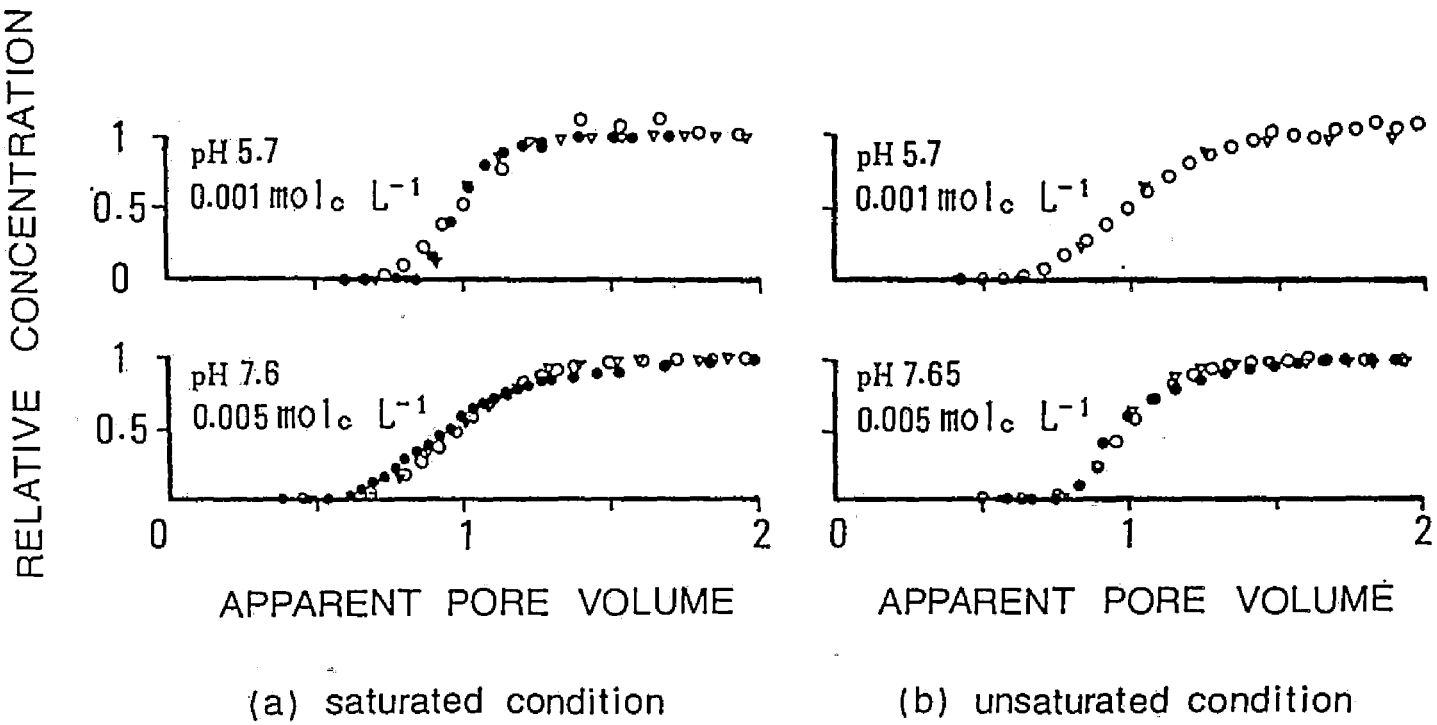

Fig. 6-6-3 Observed breakthrough curves showing the effect of pH on the displacement process indicated by apparent pore volume. ($\circ Br^-$; $\bullet Sr^{2+}$; ∇ tritiated water)

1943; Lai and Jurinak, 1972; Bolt, 1978; Cho, 1985; Schulin et al., 1986 ; Mitsuno, 1988; Toride and Nakano, 1991). The BTC's for tritiated water fall between the Sr^{2+} BTC and the Br^- BTC, or almost in the same position as either of them as shown in Figs. 6-6-1(a), 6-6-2, and 6-6-3. These results are roughly explained with the exchange isotherms for Sr^{2+} and Br^-, because the BTC's for tritiated water are the same as those for an adsorbing ion whose exchange isotherm is linear (Dufey et al., 1982).

Comparisons of the BTC's under saturated conditions with those under unsaturated conditions are also shown in Figs. 6-6-1 to 6-6-3. The BTC's for the total concentration of 0.1 $mol_c\ L^{-1}$ under unsaturated conditions (Fig. 6-6-1(b)) are more diffuse than those under saturated conditions (Fig. 6-6-1(a)). However, based on the relationship between the Sr^{2+} BTC and the Br^- BTC, no notable differences were observed between the BTC's under saturated conditions and those under unsaturated conditions.

6.4. CONCLUSIONS

The effects of the solution concentration and the pH on ion transport in the Allophanic Andisol were studied. The solution concentration and the pH affected the AEC and the CEC of the Allophanic Andisol significantly. The solution pH also affected the ion exchange isotherms. The increase of the AEC or the CEC delayed the movement of the counterions, and changes in the exchange isotherm altered the shape of the BTC. When the input concentration was low, the counterion penetrated more

slowly because the supplied amount of the counterion contained in the unit solution volume was small.

The BTC's under unsaturated conditions were compared with those under saturated conditions at different pH and concentration conditions. Based on the relationship between the Sr^{2+} BTC and the Br^{-} BTC, no notable differences were observed between the BTC's under saturated conditions and those under unsaturated conditions.

The influence of the solution concentration and the pH cannot be ignored when considering ion transport in an Allophanic Andisol.

CHAPTER 7

EFFECT OF DISTRIBUTION RATIO ON BREAKTHROUGH CURVE

7.1. INTRODUCTION

The influences of the total counterion concentration of the input solution, the ion exchange capacity of the soil, and the ion exchange isotherm on ion transport in the Allophanic Andisol were clarified experimentally in the preceding chapter. In this chapter, these effects on breakthrough curves (BTC's) are considered numerically.

Ion exchange reactions are important processes governing the fate of dissolved nutrients and other chemicals in crop fields. Ion exchange reactions delay the ion movement in soils. The mean penetrating velocity, depth, time, and retardation of exchanging ion are given in various studies (Higgins, 1959; Bolt, 1978; Roberts et al., 1980; Mansell et al., 1986). Aris and Amundson (1973) determined the relation between the retention time of an adsorbing solute and that of a nonreactive solute when there was no dispersion and no mass transfer limitation. Schweich and Sardin (1981) applied this relation to ion exchange. Valocchi (1980) noted that, when the exchange isotherm is linear, the breakthrough curve (BTC) for an exchanging ion shifts to the right in proportion to the value of the retardation factor in the figure.

The shapes of BTC's with different mean breakthrough times can be easily compared when the BTC's are normalized by their mean breakthrough times. Dufey et al. (1982) showed that when the adsorption isotherms was linear a normalized BTC for an adsorbed solute was similar to a BTC for a non-sorbed solute, with its shape determined by the Péclet number. As is well known, a BTC becomes flatter with a concave isotherm and becomes steeper with a convex isotherm (e.g., DeVault, 1943; Lai and Jurinak, 1972; Bolt, 1978; Cho, 1985; Schulin et al., 1986; Mitsuno, 1988; Toride and Nakano, 1991). However, the shapes of normalized BTC's have not been determined when the distribution ratio, D_σ, the ratio of the amount of ions adsorbed in the soil to that in the solution in unit volume of the soil, differs among the BTC's.

In this chapter, the influence of D_σ on normalized BTC's with nonlinear isotherms was evaluated numerically and experimentally. The cases studied here involve ion exchange in a binary system at a constant total concentration under steady-state water-flux conditions. The BTC's were calculated and interpreted by using a normalized, one-dimensional advective dispersive equation. The analytical results from these calculations were then compared with experimental data of transport of exchanging cations and exchanging anions in laboratory columns of an Allophanic Andisol.

7.2. THEORY

The case considered here is an exchange in a binary homovalent sys-

tem at a constant total concentration ($mol_c\ m^{-3}$) under a steady-state water-flux condition. An input ion, ion 1, penetrates into a soil and displaces an initially adsorbed ion, ion 2. Instantaneous equilibrium between the adsorbed ions and the ions in the solution is assumed.

We assume distribution of homovalent ions 1 and 2 between solution and adsorbed phases is described as follows:

$$\frac{q_1}{q_2} = K_{1/2}\frac{c_1}{c_2} \qquad (7.1)$$

where, q_1 and q_2 are the amounts in the exchange phase ($mol_c\ kg^{-1}$) of ions 1 and 2, respectively, c_1 and c_2 are the concentrations in the soil solution ($mol_c\ m^{-3}$) of ions 1 and 2, respectively, and $K_{1/2}$ is simply referred to as the selectivity coefficient of ions 1 over 2 (Valocchi et al., 1981; Selim et al., 1987). This selectivity coefficient was first introduced by Rubin and James (1973). We consider that the total ion concentration is time invariant in a binary system; therefore,

$$c_o = c_1 + c_2 \qquad (7.2)$$

where c_o is the total concentration ($mol_c\ m^{-3}$) of ions having the same charge. Assuming the ion exchange capacity is constant under the constant total concentration we get

$$q_o = q_1 + q_2 \qquad (7.3)$$

where q_o is the ion exchange capacity ($mol_c\ kg^{-1}$). From Eqs. (7.1), (7.2), and (7.3), Valocchi et al. (1981) showed that

$$Q_1 = \frac{K_{1/2}C_1}{(K_{1/2}-1)C_1+1} \qquad (7.4)$$

where Q_1 is the relative amount of ion 1 in the exchange phase and C_1 is

the relative concentration of ion 1 in the soil solution. They are represented as

$$Q_1 = q_1 / q_o \qquad (7.5)$$

$$C_1 = c_1 / c_o \qquad (7.6)$$

As Hashimoto et al. (1964) showed, the one-dimensional, advective dispersive equation with ion exchange in a soil is

$$R_f \frac{\partial C_1}{\partial t} = D \frac{\partial^2 C_1}{\partial x^2} - u \frac{\partial C_1}{\partial x} \qquad (7.7)$$

where t is time (s), D is a dispersion coefficient ($m^2\ s^{-1}$), x is distance (m), u is a mean pore water velocity ($m\ s^{-1}$). The variable R_f is a retardation factor (Hashimoto et al., 1964) defined by

$$R_f = 1 + D_g \frac{\partial Q_1}{\partial C_1} \qquad (7.8)$$

where D_g is a distribution ratio (Bolt et al., 1978). D_g is defined by

$$D_g = \frac{\rho q_o}{\theta c_o} \qquad (7.9)$$

where ρ is the bulk density ($kg\ m^{-3}$) and θ is the volume wetness ($m^3\ m^{-3}$). Similar to the method used by Selim and Mansell (1976), Eq. (7.7) can be put into dimensionless form by introducing the following dimensionless variables:

$$X = x / L \qquad (7.10)$$

$$T = \frac{ut}{(D_g + 1)L} \qquad (7.11)$$

where L is the objective length. The dimensionless time, T, equals the ratio of the real time to the mean time required for ion 1 to move

through the distance, $x = L$. Dufey et al. (1982) defined the effluent volume at $T = 1$ as the "apparent pore volume." From these, Eq. (7.7) can be put into the dimensionless form

$$\frac{\partial C_1}{\partial T} = \frac{1}{f P_e}\frac{\partial^2 C_1}{\partial X^2} - \frac{1}{f}\frac{\partial C_1}{\partial X} \qquad (7.12)$$

where P_e, the Péclet number for mass transfer, is uL/D, and

$$f = \frac{R_f}{D_g + 1} = \frac{1}{D_g + 1} + \frac{D_g}{D_g + 1}\frac{\partial Q_1}{\partial C_1} \qquad (7.13)$$

The derivative, $\partial Q_1/\partial C_1$, in Eq. (7.13) is determined by the exchange isotherm. Differentiating Eq. (7.4) by C_1 we obtain (Schulin et al., 1986)

$$\frac{\partial Q_1}{\partial C_1} = \frac{K_{1/2}}{[\ 1 + (K_{1/2} - 1)C_1\ ]^2} \qquad (7.14)$$

The initial condition and boundary condition that we consider in this study are

$C_1 = 0$ at $T = 0$ for $0 < X$, and

$C_1 = 1$ at $X = 0$ for $T > 0$.

7.3. NUMERICAL PROCEDURE

Because an exact analytical solution of Eq. (7.12) is only available when the selectivity coefficient is unity (van Genuchten and Cleary, 1982), Eq. (7.12) was solved numerically. The discretization of Eq. (7.12) is given by the following exponential and fully implicit schemes (Patankar 1980):

$$\alpha \cdot C_1(X,T) = \beta \cdot C_1(X+\Delta X,T) + \gamma \cdot C_1(X-\Delta X,T) + \delta \cdot C_1(X,T-\Delta T) \quad (7.15)$$

where, ΔX is the increment in dimensionless distance, ΔT is the increment in dimensionless time, and

$$\alpha = \beta + \gamma + \delta \quad (7.16)$$

$$\beta = \frac{1}{A\{\exp(B)-1\}} \quad (7.17)$$

$$(\beta = 0 \text{ at } X = 1-\Delta X/2)$$

$$\gamma = \frac{\exp(B)}{A\{\exp(B)-1\}} \quad (7.18)$$

$$(\gamma = 1/A \text{ at } X = \Delta X/2)$$

$$\delta = \frac{\Delta X}{\Delta T} \quad (7.19)$$

where

$$A = \frac{1}{D_g + 1} + \frac{D_g}{D_g + 1} \frac{Q_1(X,T) - Q_1(X,T-\Delta T)}{C_1(X,T) - C_1(X,T-\Delta T)} \quad (7.20)$$

$$B = P_e \Delta X \quad (7.21)$$

When D_g, $K_{1/2}$, P_e, ΔX, and ΔT are specified, the concentrations, C_1, are obtained at temporal and spatial points of interest by solving simultaneous algebraic equations (7.15). The numerical calculations were carried out using a uniform grid with $\Delta X = 1/30$ for $P_e = 50$, or with $\Delta X = 1/90$ for $P_e = 250$, and ΔT in the range of 2.2 to 3.4×10^{-3}.

Sample calculations were performed for $D_g = 0$, 1, 10, 50, $K_{1/2} = 0.5$, 1, 2, and $P_e = 50$. The specific combinations of the parameters used are shown in Table 7-1.

Calculated BTC's were compared with BTC's from experimental data. The distribution ratio, D_e, for these calculations were calculated from Eq. (7.9) by substituting experimental data. The values that gave the best agreement between the measured and calculated BTC for non-sorbed, tritiated water were chosen as P_e for the calculations of the exchanging ion BTC's. Reasonable values for $K_{1/2}$ were chosen for the calculations by curve fitting the measured exchange isotherms with Eq. (7.4).

7.4. MATERIALS AND METHODS

Miscible-displacement experiments were carried out in order to identify the effect of D_e on the normalized BTC. The miscible-displacement experiments for the Allophanic Andisol were carried out in binary cation (Sr^{2+}-Ca^{2+}) and anion (Br^--Cl^-) systems at constant total ion concentration and constant pH, and the Sr^{2+}-Ca^{2+} exchange isotherms and Br^--Cl^- exchange isotherms were measured using a modified version of the method of Wada and Okamura (1980) as described in the preceding chapter. The ion exchange capacities of Br^- and Sr^{2+} for each run of the miscible-displacement experiments were estimated from the measured BTC's. The ion exchange capacity, q_o ($mol_c\ kg^{-1}$), was calculated as

$$q_o = \left(\int_0^W [c_o - c_i(w)]dw - c_o \theta V \right) / (\rho V) \qquad (7.22)$$

where w is the effluent volume (m^3), $c_i(w)$ is the output concentration ($mol_c\ m^{-3}$) of ion I at w, W is the effluent volume (m^3) at that $c_i(w)$ has just increased to c_o, and V is the inner volume of the acrylic col-

umn (m^3). The data for the experiments are presented in Table 7-2.

7.5. RESULTS AND DISCUSSION

7.5.1. SAMPLE CALCULATIONS

Numerical calculations were carried out in order to evaluate the effect of D_g on the normalized BTC. From Eq. (7.12), ion transport can be predicted when f and P_e are known. Because f is obtained from D_g and $\partial Q_1/\partial C_1$ (Eq. (7.13)), and $\partial Q_1/\partial C_1$ is determined from $K_{1/2}$ and C_1 (Eq. (7.14)), Dg, $K_{1/2}$, and P_e must be known to calculate ion transport.

The combinations of D_g, $K_{1/2}$, and P_e for the sample calculations are shown in Table 7-1. As Selim and Mansell (1976) described, the dimensionless, advective dispersive equation for a linear exchange isotherm is equal to that for a nonreactive solute. In this case, Eq. (7.12) becomes

$$\frac{\partial C_1}{\partial T} = \frac{1}{P_e}\frac{\partial^2 C_1}{\partial X^2} - \frac{\partial C_1}{\partial X} \qquad (7.23)$$

Therefore, these BTC's are determined for P_e as Dufey et al. (1982) indicated. Because the general equations for ion transport for a linear exchange isotherm (cases 3A, 3B, and 3C in Table 7-1) were exactly identical to those for a nonreactive solute (case 1 in Table 7-1), seven sample calculations were carried out.

The calculated BTC's are shown in Figs. 7-1 and 7-2. The abscissa denotes the dimensionless time T. Following the convention used by Dufey

Table 7-1

Combinations of parameters for the example calculations.

Case no.	Distribution ratio D_e	Selectivity coefficient $K_{1/2}$	Péclet no. P_e
		nonreactive solute	
1	0	—	50
		concave exchange isotherm	
2A	1	0.5	50
2B	10	0.5	50
2C	50	0.5	50
		linear exchange isotherm	
3A	1	1	50
3B	10	1	50
3C	50	1	50
		convex exchange isotherm	
4A	1	2	50
4B	10	2	50
4C	50	2	50

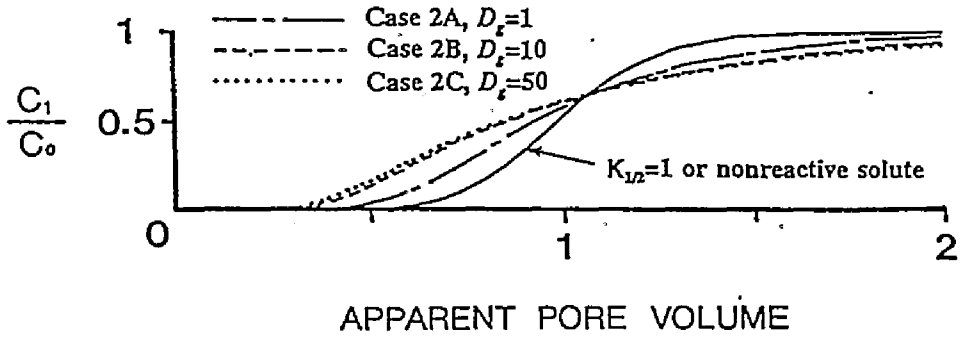

Fig. 7-1 Effect of distribution ratio, D_g, on the breakthrough curves at $K_{1/2}$ = 0.5 and P_e = 50 as a function of apparent pore volume.

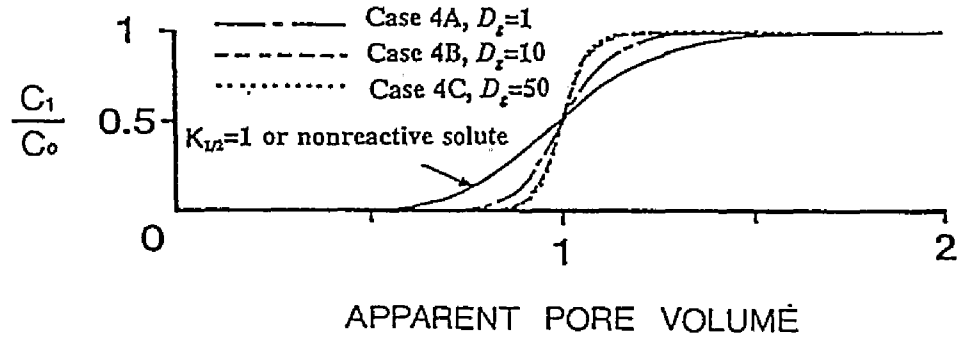

Fig. 7-2 Effect of distribution ratio, D_g, on the breakthrough curves at $K_{1/2}$ = 2 and P_e = 50 as a function of apparent pore volume.

et al. (1982), the apparent pore volume is used as the unit of the dimensionless time T. In Fig. 7-1 because the displaced ion, ion 2, was preferred to the input ion, ion 1, in the cases of concave isotherm (2A, 2B, and 2C; $K_{1/2}$ = 0.5), these BTC's are flatter than the BTC for the linear isotherm case where $K_{1/2}$ = 1. Also seen in Fig. 7-1 as D_g increases from 1 to 10 the BTC at $K_{1/2}$ = 0.5 is flatter. In Fig. 7-2, because ion 1 was preferred to ion 2, in the cases of convex isotherm (4A, 4B, and 4C; $K_{1/2}$ = 2), these BTC's are steeper than the BTC for $K_{1/2}$ =

1. Also, as D_e increases from 1 to 10 the BTC at $K_{1/2} = 2$ is steeper. This result shows that the influence of the nonlinear isotherm on the normalized BTC's increase as D_e increases.

On the other hand, as shown in Fig. 7-1, the BTC for case 2C where $D_e = 50$ almost agrees with that for case 2B where $D_e = 10$, although D_e for case 2C is much larger than D_e for case 2B. The same relation is observed between the BTC's for case 4B and 4C in Fig. 7-2; that is, when D_e is much larger than unity, the normalized BTC's with a similar P_e and $K_{1/2}$ remains almost same, even though the values of D_e differ.

In the sample calculations homovalent exchange was assumed in order to use the simple relationship in Eq. (7.1) for the distribution of two ions between solution and adsorbed phases. However, the obtained results are also valid for a binary heterovalent system because the exchange isotherm determines the BTC.

The results obtained from the sample calculations can be explained by examining the equations themselves. For the case of nonlinear exchange isotherms when D_e is not much greater than unity, the term $1/(D_e+1)$ in Eq. (7.13) decreases and the term $D_e/(D_e+1)$ increases as D_e increases from 0. Also, because $\partial Q_1/\partial C_1$ is multiplied by $D_e/(D_e+1)$, the influence $\partial Q_1/\partial C_1$ exerts on f becomes greater as D_e increases. This is shown in Fig. 7-3. Therefore, the effect of a nonlinear exchange isotherm on the normalized BTC increases as D_e increases, since $\partial Q_1/\partial C_1$ is determined by the exchange isotherm. This is the reason why the BTC at $K_{1/2} = 0.5$ is flatter and the BTC at $K_{1/2} = 2$ is abrupter as D_e increases from 1 to 10.

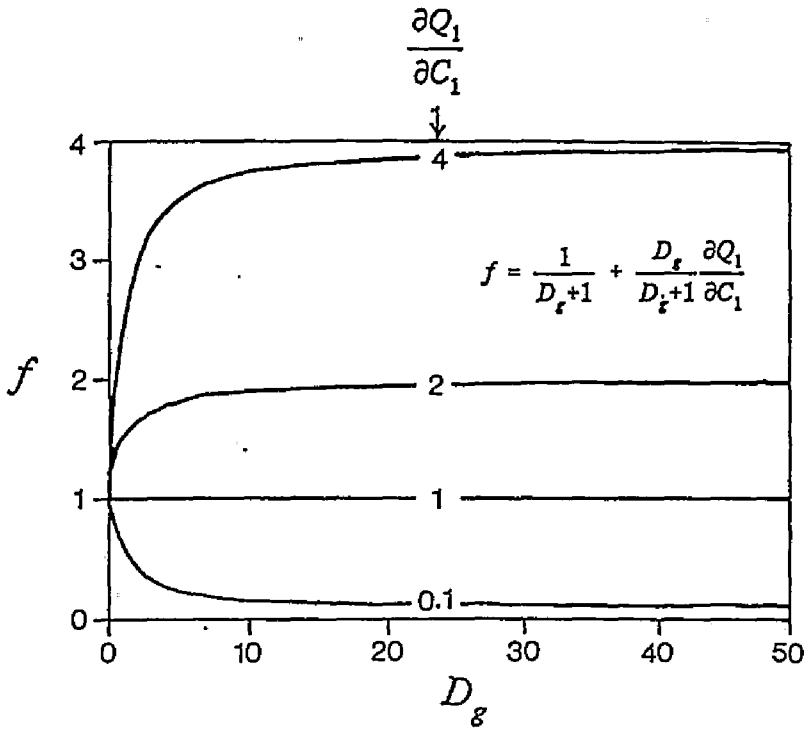

Fig. 7-3 Influence of D_g and $\partial Q_1/\partial C_1$ on f (Eq.(7.13)). The numbers on the curves denote $\partial Q_1/\partial C_1$.

Also for the case of nonlinear exchange isotherms when D_g is much larger than unity, the terms $1/(D_g+1)$ and $D_g/(D_g+1)$ in Eq. (7.13) become approximately 0 and 1, respectively, and f is approximated by $\partial Q_1/\partial C_1$. This last approximation is shown in Fig. 7-3. Because the influence of D_g on f is small, ion transport can be almost determined for P_e and $\partial Q_1/\partial C_1$. Therefore, the influence of D_g on normalized BTC's is negligible. This is the reason why the BTC's for cases 2B and 2C are similar to each other, and why, cases 4B and 4C are similar even though the values of D_g differ substantially.

7.5.2. THE EXPERIMENTS

Miscible-displacement experiments, using the Allophanic Andisol, were carried out in order to identify the effect of D_o on the normalized BTC. The measured and calculated BTC's for Run 1 are shown in Fig. 7-4, and those for Run 2 are shown in Fig. 7-5. The conditions and parameters for these runs are listed in Table 7-2. The measured exchange isotherms and the exchange isotherms used in the calculations for the Sr^{2+}-Ca^{2+} system are shown in Fig. 7-6 and those for the Br^--Cl^- system in Fig. 7-7. Because the exchange isotherms were measured using the batch method, those pH values differed from the pH values of the miscible-displacement experiments for Runs 1 and 2. The measured Sr^{2+}-Ca^{2+} exchange isotherms indicate that the isotherm becomes more convex as the pH decreases (Fig. 7-6) as described in the preceding chapter. However, although Run 1 was carried out for a pH of 4.2, an exchange isotherm with less than a pH of 4.55 was not detected. The two required conditions for the Sr^{2+}-Ca^{2+} exchange isotherm for Run 1 were that the Sr^{2+}-Ca^{2+} isotherm be slightly more convex than the measured isotherm at pH 4.55, and also that the isotherm produce the calculated BTC that would agree with the observed BTC. Under these conditions, a value of 3 for $K_{Sr/Ca}$ for Run 1 was obtained by fitting a curve to the measured data. The other $K_{Sr/Ca}$ and $K_{Br/Cl}$ values for Runs 1 and 2 were obtained by curve fitting the measured exchange isotherms.

The calculated BTC's agree well with those observed as shown in Figs. 7-4 and 7-5. Although $K_{Br/Cl}$ is the same for the Br^- BTC's for

Table 7-2

Soil column data for the Allophanic Andisol and parameters, D_0, $K_{1/2}$, P_e, used for the numerical calculations.

pH	Concentration	Bulk density	Volume wetness	Mean pore water velocity	Ion	ion exchange capacity	D_0	$K_{1/2}$	P_e
	$mol_c\ m^{-3}$	$kg\ m^{-3}$	$m^3\ m^{-3}$	$\mu m\ s^{-1}$		$cmol_c\ kg^{-1}$			
Run 1									
4.2	100	510	0.723	6.85	Sr	4.10	0.29	3.0	250
					Br	15.11	1.07	0.7	250
Run 2									
5.05	10	510	0.734	0.72	Sr	5.13	3.56	1.5	250
					Br	8.63	6.00	0.7	250

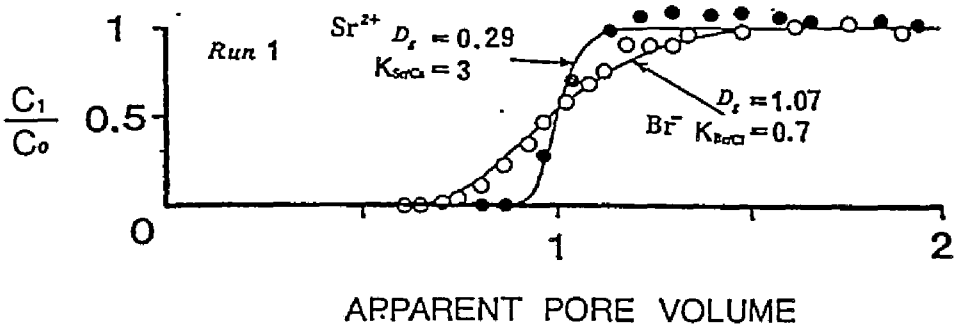

Fig. 7-4 Comparison of measured breakthrough curves (OBr⁻ ; ●Sr²⁺) for Run 1 and calculated breakthrough curves (solid lines).

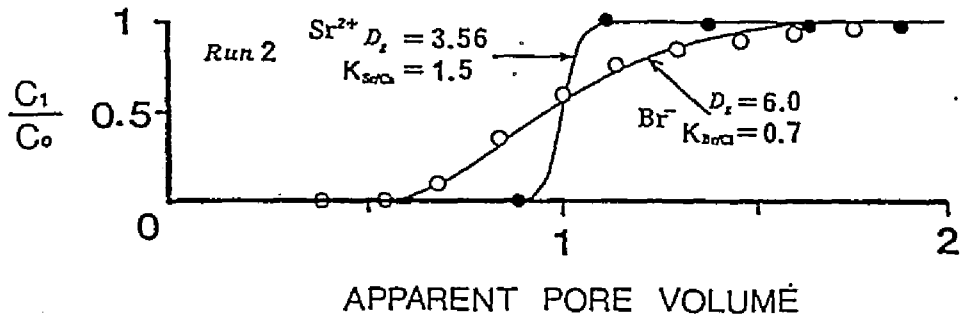

Fig. 7-5 Comparison of measured breakthrough curves (OBr⁻ ; ●Sr²⁺) for Run 2 and calculated breakthrough curves (solid lines).

'Runs 1 and 2, the Br^- BTC for Run 2 is flatter than that for Run 1. The reason is that D_g for Run 2 for Br^- is larger than that for Run 1, so that the influence of the Br^--Cl^- exchange isotherm for Run 2 is greater than that for Run 1. Therefore, the BTC for Run 2 is flatter.

As is well known, a BTC becomes steeper as $K_{1/2}$ increases (e.g., DeVault, 1943; Lai and Jurinak, 1972; Bolt, 1978; Cho, 1985; Schulin et al., 1986; Mitsuno, 1988; Toride and Nakano, 1991). However, although $K_{Sr/Ca}$ for Run 1 is larger than that for Run 2, the Sr^{2+} BTC for Run 1

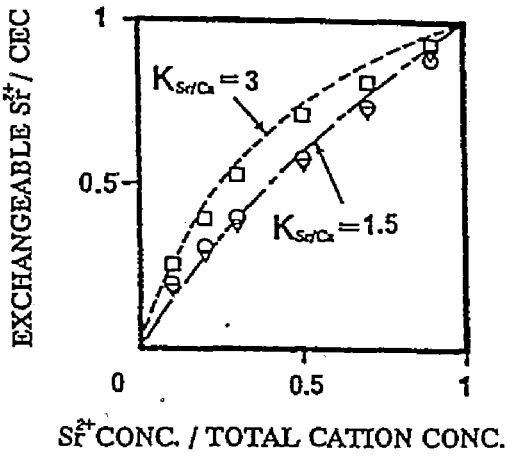

Fig. 7-6 Measured Sr^{2+}-Ca^{2+} exchange isotherms (□ pH 4.55, 100 $mol_c\ m^{-3}$; ○ pH 4.9, 10 $mol_c\ m^{-3}$; ▽ pH 5.5, 1 $mol_c\ m^{-3}$) and exchange isotherms calculated from Eq.(7.4) (curves).

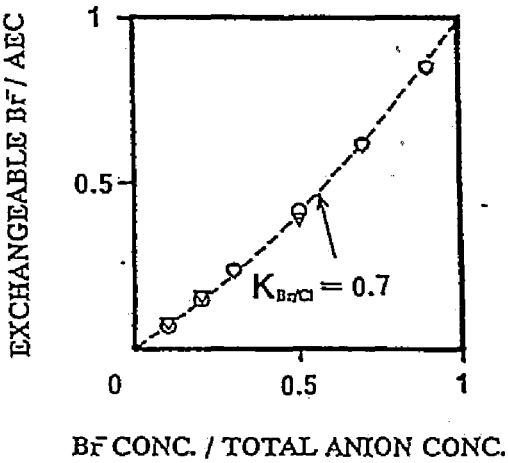

Fig. 7-7 Measured Br^--Cl^- exchange isotherms (○ pH 4.9, 10 $mol_c\ m^{-3}$; ▽ pH 5.5, 10 $mol_c\ m^{-3}$) and exchange isotherms calculated from Eq.(7.4) (dotted curve).

is slightly flatter than that for Run 2. The reason for this can be explained by the difference of D_d. Because D_d for Run 1 for Sr^{2+} is smaller than that for Run 2, the influence of the Sr^{2+}-Ca^{2+} exchange isotherm for Run 1 is less. Therefore, the Sr^{2+} BTC for Run 1 is slightly flatter than that for Run 2. A smaller value of D_d decreases the influence of the nonlinear exchange isotherm on the BTC. Due to the smaller values of D_d, the Sr^{2+} and the Br^- BTC's for Run 1 became closer to a BTC for a linear isotherm than those for Run 2.

7.6. CONCLUSIONS

Exchanging ionic-solute transport through soil columns is significantly affected by ion exchange reaction. The BTC for the input ion based on time or pore volume shifts to the right in the figure as the ion exchange capacity increases or the input ion concentration decreases. The shapes of the BTC's with different mean breakthrough times are easily compared in one figure when the BTC's are normalized by the mean breakthrough times. In this chapter, the influence of the distribution ratio, D_d, the ratio of the amount of ions adsorbed in the soil to that in the solution in unit volume of the soil, on normalized BTC's with nonlinear exchange isotherms was evaluated. The cases studied here involved ion exchange in a binary system at a constant total concentration under steady-state water-flux conditions. The BTC's were calculated and interpreted using a normalized, one-dimensional advective dispersive equation. It was determined that the effect of the nonlinear

isotherm on the BTC increases as D_θ increases. It was also shown that when D_θ is much greater than unity, an increase in D_θ has no effect on the BTC. These results were confirmed with experimental data on actual soil columns of Allophanic Andisol. When the BTC's have a similar nonlinear exchange isotherm and Péclet number, the deviations among them were easily interpreted by the D_θ values. When both the nonlinear exchange isotherm and the D_θ differ among BTC's, the deviations of the BTC's can be explained by comparing both the nonlinear exchange isotherm and the D_θ.

CHAPTER 8

CONCLUDING REMARKS

Significant effects of macropores on the movements of both non-sorbed and sorbed solutes in the hard pans of paddy fields were investigated. When the mean water velocity in the macropores was faster, solute discharged rapidly before diffusing well into the soil matrix. On the other hand, when the mean water velocity in the macropores was slower, solute discharged slowly while sufficiently diffusing into the soil matrix. Such phenomena are common in fields because their soils have diverse nonuniform structures which vary from place to place. Moreover, the structures change according to the water content, human activities, living organisms, etc. Macropores and complicated structures are decisive factors for solute transport in soils. However, evaluation of such spacially variable structures, which often change over time, remains one of the largest problems in soil science.

The effects of electric charges of the Allophanic Andisol on ion transport were investigated in the latter part. Because the Allophanic Andisol has variable charges, the solution concentration and the pH affected the AEC and the CEC of the soil significantly. The solution pH also affected the ion exchange isotherms. Therefore, the transport of the counterions in the soil was influenced strongly by such charge characteristics. The increase of the AEC or the CEC delayed the movement of

the counterions, and changes in the exchange isotherm altered the shape of the BTC. When the input concentration was lower, the counterion penetrated more slowly because the supplied amount of the counterion contained in the unit solution volume was smaller. The charge characteristics of the soil can be understood with reference to the microscopic structures of the soil. The phenomenon of the interaction between a soil particle and a solute, which occurs in the microscopic space, significantly affects solute transport in the macroscopic space such as a field or a basin. To understand solute transport in the field or the basin, further progress in research on interactions between soil particles and solutes is highly desirable.

The natural environment is extremely delicate. Once it is polluted, it is most difficult to remove those pollutants and restore the natural environment. Technology to preserve the environment requires further understanding of solute transport in soils.

REFERENCES

[A]

Adachi, K. 1988. Experimental studies of the effects of puddling on percolation control. -Studies on the water movement of rotational paddy fields. Trans. JSIDRE. 135:1-8 (in Japanese with English abstract)

Anderson, J. L., and J. Bouma. 1977a. Water movement through pedal soils : I. Saturated flow. Soil Sci. Soc. Am. J. 41:413-418

Anderson, J. L., and J. Bouma. 1977b. Water movement through pedal soils :II. Unsaturated flow. Soil Sci. Soc. Am. J. 41:419-423

Aris, R., and N.R. Amundson. 1973. Mathematical methods in chemical engineering. 2. First order partial differential equations. Prentice-Hall, Englewood Cliffs, NJ.

Atkins, P. W. 1982. Physical chemistry (second edition). Oxford University Press, Oxford, U.S.A. (Chihara, H. and Nakamura, N. translated into Japanese. Tokyo Kagaku Doujin, Tokyo, Japan. (1985) pp.1021)

[B]

Bear, J. 1969. Hydrodynamic dispersion. In Flow through porous media. De Wiest,R.J.M.(ed.). Academic Press, New York and London, pp.109-199.

Beven, K., and Germann, P. 1982. Macropores and water flow in soils. Water Resour. Res. 18:1311-1325

Biggar, J. W., and D. R. Nielsen. 1962. Miscible displacement: II. Behavior of tracers. Soil Sci. Soc. Am. Proc. 26:125-128

Biggar, J. W., and D. R. Nielsen. 1976. Spatial variability of the leaching characteristics of a field soil. Water Resour. Res., 12:78-84

Blake, G., E. Schlichting, and U. Zimmermann. 1973. Water recharge in a soil with shrinkage cracks. Soil Sci. Soc. Am. Proc. 37:669-672

Bolt, G. H. 1978. Transport and accumulation of soluble soil components. In Soil chemistry: A. Basic elements. G.H.Bolt and M.G.M.Bruggenwert (ed.). Elsevier, Amsterdam, The Netherlands, pp.126-140

Bolt, G. H. 1982. Movement of solutes in soil: principles of adsorption/ exchange chromatography. In soil chemistry: B. physico-chemical models. (G. H. Bolt ed.) Elsevier, Amsterdam, The Netherlands, pp.285-348

Bolt, G. H., M. G. M. Bruggenwert, and A. Kamphorst. 1978. Adsorption of cations by soil. In Soil chemistry: A. Basic elements. G.H.Bolt and M.G.M.Bruggenwert (ed.). Elsevier, Amsterdam, The Netherlands, pp.54-90

Bouma, J., and J. L. Anderson. 1977. Water and chloride movement through soil columns simulating pedal soils. Soil Sci. Soc. Am. J. 41:766-770

Bouma, J., and L. W. Dekker. 1978. A case study on infiltration into dry clay soil: I . Morphological observations. Geoderma, 20:27-40

Bouma, J., and J. H. M. Wosten. 1979. Flow patterns during extended saturated flow in two, undisturbed swelling clay soils with different macrostructures. Soil Sci. Soc. Am. J. 43:16-1979

Bouma, J. 1981. Soil morphology and preferential flow along macropores. Agr. Water Manage. 3:235-250

Brenner, H. 1962. The diffusion model of longitudinal mixing in beds of finite length. Numerical values. Chem. Engng. Sci., 17:229-243

Bresler, E., and G. Dagan. 1981. Convective and scale dispersive solute transport in ussaturated heterogenious field. Water Resour. Res. 17: 1683-1693

Bruggenwert, M. G. M., and A. Kamphorst. 1982. Survey of experimental information on cation exchange in soil systems. In Soil chemistry: B. Physico-chemical models. G. H. Bolt (ed.). Elsevier, Amsterdam, The Netherlands, pp.141-203

[C]

Chan, K.Y., B.G. Davey, and H.R. Geering. 1978. Interaction of treated sanitary landfill leachate with soil. J. Environ. Qual. 7:306-310

Chan, K.Y., H.R. Geering, and B.G. Davey. 1980a. Movement of chloride in a soil with variable charge properties: 1. Chloride systems. J. Environ. Qual. 9:579-582

Chan, K.Y., H.R. Geering, and B.G. Davey. 1980b. Movement of chloride in a soil with variable charge properties: 2. Sanitary landfill leachate. J. Environ. Qual. 9:583-586

Cho, C.M. 1985. Ionic transport in soil with ion-exchange reaction. Soil Sci. Soc. Am. J. 49:1379-1386

Coats, K. H., and B. D. Smith. 1964. Dead-end pore volume and dispersion in porous media. Soc. Pet. Eng. J. 4:73-84

[D]

Dagan, G., and E. Bresler. 1979. Solute dispersion in unsaturated

heterogenious soil at field scale: I. Theory. Soil Sci. Soc. Am. J. 43:461-472
Deans, H. A. 1963. A mathematical model for dispersion in the direction of flow in porous media. Soc. Pet. Eng. J. 3:49-52
De Smedt, F., and P. J. Wierenga. 1984. Solute transfer through columns of glass beads. Water Resour.Res. 20:225-232
DeVault, D. 1943. The theory of chromatography., J. Am. Chem. Soc., 65: 532-540
Dufey, J. E., T. H. Sheta, G. R. Gobran, and H. Laudelout. 1982. Dispersion of chloride, sodium,and calcium ions in soils as affected by exchangeable sodium. Soil Sci.Soc.Am.J. 46:47-50
Dyson, J. S., and R. E. White. 1989. The effect of irrigation rate on solute transport in soil during steady water flow. J. Hydrol. 107:19 -29

[E]

Elrick, D. E., and L. K. French. 1966. Miscible displacement patterns on disturbed and undisturbed soil cores. Soil Sci. Soc. Am. Proc., 30: 153-156

[F]

Fujioka, Y., and T. Maruyama. 1971. Studies on underdrainage of clayey paddy field (I) Drainage effect of cracks in plow-layers and backfilled trench. Trans. JSIDRE. 35:48-53 (in Japanese with English abstract)

[G]

Grisak, G. E., and J. F. Pickens. 1980. Solute transport through fractured media. 1. The effect of matrix diffusion. Water Resour. Res. 16:719-730

[H]

Hanai, T. 1978. Membranes and ions. Kagaku Doujin, Kyoto, Japan, pp.39-87 (in Japanese)
Hashimoto, I., K. B. Deshpande, and H. C. Thomas. 1964. Peclet numbers and retardation factors for ion exchange columns. Ind. Eng. Chem. Fund. 3:213-218
Hatano, R., T. Sakuma, and H. Okajima. 1983. The effect of the macropore system on solution movement in soil: 1. Observations on macropores stained by methyleneblue in a variety of fields soils. Jpn.J.Soil

Sci.Plant Nutr. 54:490-498 (in Japanese)
Hatano, R., T. Sakuma, and H. Okajima. 1985. The source-sinc effect of clayey soil peds on solute transport. Soil Sci. Plant Nutr. 31:199-213
Higgins, G.H. 1959. Evaluation of the ground-water contamination hazard from underground nuclear explosions. J. Geophys. Res.64:1509-1519
Hillel, D. 1980. Fundamentals of soil physics. Academic Press, New York, U.S.A. pp.233-238

[I]

Iimura, K. 1966: Acidic properties and cation exchange of allophane and volcanic ash soils. Bull. Natl. Inst. Agr. Sci., B17,101-157 (in Japanese with English abstract)
Inoue, H., S. Hasegawa, and T. Miyazaki. 1988. Lateral flow of water in an extremely cracked crop field. Trans. JSIDRE. 134:51-59 (in Japanese with English abstract)
Ishiguro, M. 1989. Seasonal changes in distributions of macropores of hard pan and subsoil in a paddy field.-Their observation in andosol paddy field using white vinyl water paint-. Trans. JSIDRE 142:107-108 (in Japanese)
Ishiguro, M. 1991. Solute transport through hard pans of paddy fields: 1. Effect of vertical tubular pores made by rice roots on solute transport. Soil Sci. 152:432-439
Ishiguro, M. 1992. Solute transport through hard pans of paddy fields: 2. Cation exchange processes. Soil Sci. 153:42-47
Ishiguro, M. 1992. Ion transport in soil with ion exchange reaction: Effect of distribution ratio. Soil Sci. Soc. Am. J. 56 (in press)
Ishiguro, M. and S. Iwata. 1988. Substance movement in soils: 4. Ion exchange and adsorption in soils. Jour.JSIDRE 56:1017-1024 (in Japanese)
Ishiguro, M, K. Song, and K. Yuita. 1992. Ion transport in an allophanic andisol under the influence of variable charge. Soil Sci. Soc. Am. J. 56 (in press)

[J]

Jpn. Soc. Chemistry. 1984. Handbook of chemistry (Third edition) FoundamentalsII. Maruzen, Tokyo, Japan, pp.66 (in Japanese)
Jury, W. A. 1982. Simulation of solute transport using a transfer function model. Water Resour.Res. 18:363-368
Jury, W. A., and L. H. Stolzy. 1982. A field test of the transfer

function model for predicting solute transport. Water Resour. Res. 18:369-375

Jury, W. A., and G. Sposito. 1986. A transfer function model of solute transport through soil. 1. Fundamental concepts. Water Resour. Res. 22:243-247

[K]

Kanchanasut, P., D. R. Scotter, and R. W. Tillman. 1978. Preferential solute movement through larger soil voids: II. Experiments with saturated soil. Aust. J. Soil Res. 16:269-276

Kanou, T., S. Nakagawa, H. Oonishi, T. Maruyama, and T. Furuki. 1961. Effect of drainage improvement on water requirement. Trans. AESJ. 28 :425-431 (in Japanese)

Kawata, S., M. Katano, and K. Yamazaki. 1980. The root system development of rice plants in the worked- and sub-soil of an actual paddy field. Japan. J. Crop Sci. 49:311-316 (in Japanese with English abstract)

Kissel, D. E., J. T. Ritchie, and E. Burnett. 1973. Chloride movement in undisturbed swelling clay soil. Soil Sci. Soc. Am. Proc. 37:21-24

Kitagawa, Y. 1977. Determination of allophane and amorphous inorganic matter in soils. Bull. Natl. Inst. Agric. Sci. B29:1-48 (in Japanese with English abstract)

Kodama, S., and T. Hishinuma. 1959. Puddling and hydraulic conductivity. In Study on puddling. (F. Yamazaki ed) Kinbara Pbl., Tokyo, Japan, pp.107-118 (in Japanese)

Kolenbrander, G. J. 1970. Calculation of parameters for the evaluation of the leaching of salts under field conditions, illustrated by nitrate. Plant and Soil 32:439-453

[L]

Lai, S.-H., and J. J. Jurinak. 1971. Numerical approximation of cation exchange in miscible displacement through soil columns. Soil Sci. Soc. Am. J. 35:894-899

Lai, S.-H., and J. J. Jurinak. 1972. Cation adsorption in one-dimensional flow through soils:a numerical solution. Water Resour. Res. 8:99-107

Lapidus, L., and N. R. Amundson. 1952. Mathematics of adsorption in beds : IV. The effect of longitudinal diffusion in ion exchange and chromato graphic columns. J.Phys.Chem. 56:984-988

Lawes, J. B., J. H. Gilbert, and R. Warington. 1882. On the amount and

composition of the rain and drainage waters collected at Rothamsted. William Clowers and Sons, London, U.K.

[M]

Mansell, R.S., S.A. Bloom, H.M. Selim, and R.D. Rhue. 1986. Multispecies cation leaching during continuous displacement of electrolyte solutions through soil columns. Geoderma 38:61-75

Maruyama, T. 1966a. The variation of soil permeability caused by underdrainage. The study of underdrainage (I). Trans. AESJ. 16:9-13 (in Japanese with English abstract)

Maruyama, T. 1966b. Hydraulic mechanism of underdrainage in paddy fields having underground aquifer. The study of underdrainage (II). Trans. AESJ. 16:14-19 (in Japanese with English abstract)

Maruyama, T., and M. Morikawa. 1966. The mechanism and the effect of underdrainage at Omino district (muck), Saitama Prefecture. The study of underdrainage (III). Trans. AESJ. 17:28-33 (in Japanese with English abstract)

Maruyama, T., and I. Kimata. 1973. The water flow resistance in the crack network. The study of underdrainage (IV). Trans. JSIDRE. 45:1-5 (in Japanese with English abstract)

Masujima, H. 1970. Anisotropy of water permeability in paddy fields. J. Sci.Soil and Manure,Jpn. 41:119-120 (in Japanese)

McMahon, M. A., and G. W. Thomas. 1974. Chloride and tritiated water flow in disturbed and undisturbed soil cores. Soil Sci. Soc. Am. Proc. 38:727-732

Mehra, O.P., and M.L. Jackson. 1959. Iron oxide removal from soils and clays by a dithionite-citrate system buffered with sodium bicarbonate. Clays Clay Miner. 7:317-327

Mitsuno, T. 1988. On the requirement for soil improvement. Soil Physic. Conditions Plant Growth, Jpn. 57:32-40 (in Japanese with English abstract)

Miyazaki, T. 1988. Water infiltration into layered soil slopes. Trans. JSIDRE. 133:1-9

[N]

Nagahama, K., S. Tejima, M. Tomita, and H. Taniguchi. 1968. On the study of cracks caused by underdrainage of paddy field in the reclaimed land from the sea. The substantial study on the mechanism of underdrainage (IV). Trans. JSIDRE. 26:23-28 (in Japanese with English abstract

Narioka, H. 1987. Study on the phyisical functions of soil macropores and the instrumentation for their measurement. Bull. NODAI Res. Inst. Tokyo Univ. Agr. 1:1-58 (in Japanese with English abstract)

Nati. Inst. Agric. Sciences. 1984. Outline of the test of soils and the major nutrients in the field of the National Institute of Agricultural Sciences. Materials No.3, Dep. Chemistry Natl. Inst. Agric. Sci. (in Japanese)

Nielsen, D. R., and J. W. Biggar. 1962. Miscible displacement:Ⅲ. Theoretical considerations. Soil Sci. Soc. Am. Proc. 26:216-221

Nielsen, D. R., M. Th. van Genuchten, and J. W. Biggar. 1986. Water flow and solute transport processes in the unsaturated zone. Water Resour. Res. 22:89S-108S

[O]

Okamura, Y., and K. Wada. 1983. Electric charge characteristics of horizons of Ando (B) and Red-Yellow B soils and weathered pumices. J. Soil Sci. 34:287-295

Okamura, Y., and K. Wada. 1984. Ammonium-calcium exchange equilibria in soils and weathered pumices that differ in cation-exchange materials. J. Soil Sci. 35:387-396

Omoti, U., and A. Wild. 1979. Use of fluorescent dyes to mark the pathways of solute movement through soils under leaching conditions: 2. Field experiments. Soil Sci. 128:98-104

Ooi, S. 1986. A theory of dispersion in a porous medium. World Congress Ⅲ of Chem. Eng. Vol.2. pp.495-498

Ooi, S. and S. Iwata. 1988. Substance movement in soils: 5. Movement of chemical substances in soils. Jour.JSIDRE 56:1115-1121 (in Japanese)

[P]

Parker, J. C., and A. J. Valocchi. 1986. Constraints on the validity of equilibrium and first-order kinetic transport models in structured soils. Water Resour. Res. 22:399-407

Passioura, J. B. 1971. Hydrodynamic dispersion in aggregated media: 1. Theory. Soil Sci. 111:339-351

Patankar, S. V. 1980. Numerical heat transfer and fluid flow. McGraw-Hill, New York, USA. (Mizutani,Y. and Katsuki,M. translated into Japanese. Morikita Publishing Corporation.(1985))

[Q]

Quisenberry, V. L., and R. E. Phillips. 1976. Percolation of surface-

applied water in the field. Soil Sci. Soc. Am. J. 40:484-489

[R]

Rahe, T. M., C. Hagedorn, E. L. Mccoy, and G. F. Kling. 1978. Transport of antibiotic-resistant Escherichia coli through western Oregon hillslope soils under conditions of saturated flow. J. Environ. Qual. 7:487-494

Rao, P. S. C., R. E. Jessup, D. E. Rolston, J. M. Davidson, and D. P. Kilcrease. 1980. Experimental and mathematical description of nonadsorbed solute transfer by diffusion in spherical aggregates. Soil Sci. Soc. Am. J. 44:684-688

Rao, P. S. C., D. E. Rolston, R. E. Jessup, and J. M. Davidson. 1980. Solute transport in aggregated porous media: Theoretical and experimental evaluation. Soil Sci. Soc. Am. J. 44:1139-1146

Rasmuson, A., and I. Neretnieks. 1980. Exact solution of a model for diffusion in particles and longitudinal dispersion in packed beds. AIChE J. 26:686-690

Ritchie, J. T., D. E. Kissel, and E. Burnett. 1972. Water movement in undisturbed swelling clay soil. Soil Sci. Soc. Am. Proc. 36:874-879

Roberts, P.V., P.L. McCarty, and M.R.J. Schreiner. 1980. Organic contaminant behavior during groundwater recharge. J. Water Pollut. Control Fed. 52:161-172

Rose, D. A., and J. B. Passioura. 1971. The analysis of experiments on hydrodynamic dispersion. Soil Sci., 111:252-257

Rubin, J., and R.V. James. 1973. Dispersion-affected transport of reacting solutes in saturated porous media: Galerkin method applied to equilibrium-controlled exchange in unidirectional steady water flow. Water Resour. Res. 9:1332-1356

[S]

Saffman, P. G. 1959. A theory of dispersion in a porous medium. J. Fluid Mech. 6:321-349

Sakuma, T., H. Oimatsu, F. Iizuka, and H. Okajima. 1979. The non-uniform character of solute transport in undisturbed soils. J. Sci. Soil and Manure, Jpn. 50:10-16 (in Japanese)

Sakuma, T., H. Oimatsu, F. Iizuka, and H. Okajima. 1979. Nitrate leaching in soil columns containing coarse aggregates. J.Sci.Soil and Manure, Jpn. 50:17-24 (in Japanese)

Schulin, R., H. Flühler, R.S. Mansell, and H.M. Selim. 1986. Miscible displacement of ions in aggregated soils. Geoderma 38:311-322

Schumacher, W. 1864. Die physik des Bodens. Berlin.
Schweich, D., and M. Sardin. 1981. Adsorption, partition, ion exchange and chemical reaction in batch reactors or in columns - A review. J. Hydrology 50:1-33
Scotter, D. R. 1978. Preferential solute movement through larger soil voids: I. Some computations using simple theory. Aust. J. Soil Res. 16:257-267
Selim, H.M., and R.S. Mansell. 1976. Analytical solution of the equation for transport of reactive solutes through soils. Water Resour. Res. 12:528-532
Selim, H. M., R. Schulin, and H. Flühler. 1987. Transport and ion exchange of calcium and magnesium in an aggregated soil. Soil Sci. Soc. Am. J. 51:876-884
Seyfried, M. S., and P. S. C. Rao. 1987. Solute transport in undisturbed columns of an aggregated tropical soil: Preferential flow effects. Soil Sci.Soc.Am.J. 51:1434-1444
Shaffer, K. A., D. D. Fritton, and D. E. Baker. 1979. Drainage water sampling in a wet, dual-pore soil system. J. Environ. Qual. 8:241-246
Smith, M. S., G. W. Thomas, R. E. White, and D. Ritonga. 1985. Transport of Escherichia coli through intact and disturbed soil columns. J. Environ. Qual. 14:57-91
Sudicky, E. A., and E. O. Frind. 1982. Contaminant transport in fractured porous media: Analytical solutions for a system of parallel fractures. Water Resour. Res. 18:1634-1642

[T]

Tabuchi, T. 1966. Studies on drainage in clayey paddy fields. (1) A hypothesis of drainage and the classification of drainage in clayey paddy fields. Trans. AESJ. 18:1-11 (in Japanese with English abstract)
Tabuchi, T., M. Nakano, and S. Suzuki. 1966a. Studies on drainage in clayey paddy fields. (2) Mid-summer drainage in large paddy fields having no underdrain. Trans. AESJ. 18:12-17 (in Japanese with English abstract)
Tabuchi, T., M. Nakano, and S. Suzuki. 1966b. Studies on drainage in clayey paddy fields. (3) Harvest time drainage in large paddy fields having no underdrain. Trans. AESJ. 18:18-24 (in Japanese with English abstract)
Tabuchi, T., M. Nakano, and S. Suzuki. 1966c. Studies on drainage in

clayey paddy fields. (4) Drainage in non-irrigated period in large paddy fields having no underdrain. Trans. AESJ. 18:25-30 (in Japanese with English abstract)

Tabuchi, T., M. Nakano, A. Sumita, and I. Maruta. 1966d. Studies on drainage in clayey paddy fields. (5) Mid-summer and harvest time drainage of small paddy fields having underdrains. Trans. AESJ. 18: 31-38 (in Japanese with English abstract)

Tabuchi, T., M. Nakano, A. Sumita, and I. Maruta. 1966e. Studies on drainage in clayey paddy fields. (6) Drainage of non-irrigated period in small paddy fields having underdrains. Trans. AESJ. 18:39 -47 (in Japanese with English abstract)

Takijima, Y., and H. Sakuma. 1969. Effect of soil strength as a function of soil compaction on the root development, upper growth and yield of the rice plants. Bull. Nat. Inst. Agr. Sci. B21:255-328 (in Japanese with English abstract)

Tang, D. H., E. O. Frind, and E. A. Sudicky. 1981. Contaminant transport in fractured porous media: Analytical solution for a single fracture. Water Resour. Res. 17:555-564

Taylor, G. I. 1953. Dispersion of soluble matter in solvent flowing slowly through a tube. Proc. Roy.Soc.London. A219:186-203

Thomas, G. W., R. L. Blevins, R. E. Phillips, and M. A. McMahon. 1973. Effect of a killed sod mulch on nitrate movement and corn yield. Agron. J. 65:736-739

Thomas, G. W., R. E. Phillips, and V. L. Quisenberry. 1978. Characterization of water displacement in soils using simple chromatgraphic theory. J. Soil Sci. 29:32-37

Tokunaga, K., H. Narioka, and T. Fukaya. 1984. Development of the heavy liquid infiltration method and consideration on the soil void images photographed by soft X-ray projection with the above method. Trans. JSIDRE. 114:61-68 (in Japanese, with English abstract)

Tokunaga, K., T. Sato, H. Kikuchi, and K. Kon. 1985. On the real state of coarse pores in clayey paddy field's soil and their permeability: Study on the soil and its void by X-ray radiograph (II). Soil Phys. Cond.and Plant Growth,Jpn. 51:49-62 (in Japanese, with English abstract)

Toride, N., and M. Nakano. 1991. Transport of exchanging Ca^{2+} and Na^{+} in clay systems. Soil Physic. Conditions Plant Growth, Jpn. 62:3-11 (in Japanese with English abstract)

Tyler, D. D., and G. W. Thomas. 1977. Lysimeter measurements of nitrate and chloride losses from soil under convectional and no-tillage

corn. J. Environ. Qual. 6:63-66
Tyler, D. D., and G. W. Thomas. 1981. Chloride movement in undisturbed soil columns. Soil Sci. Soc. Am. J. 45:459-461

[V]

Valocchi. A.J. 1980. Transport of ion-exchanging solutes during groundwater recharge. Ph.D. diss. Stanford Univ., Stanford.
Valocchi, A. J., R. L. Street, and P. V. Roberts. 1981. Transport of ion-exchanging solutes in groundwater: Chromatgraphic theory and field simulation. Water Resour. Res. 17:1517-1527
Van De Pol, R. M., P. J. Wierenga, and D. R. Nielsen. 1977. Solute movement in a field soil. Soil Sci. Soc. Am. J. 41:10-13
van Eijkeren, J. C. H., and J. P. G. Loch. 1984. Transport of cationic solutes in sorbing porous media. Water Resour. Res. 20:714-718
van Genuchten, M. Th., and P. J. Wierenga. 1976. Mass transfer studies in sorbing porous media: I. Analytical solutions. Soil Sci.Soc.Am.J. 40:473-480
van Genuchten, M.Th., and R.W. Cleary. 1982. Movement of solutes in soil : Computer-simulated and laboratory results. p.349-386. In G.H. Bolt (ed.) Soil chemistry: B. Physico-chemical models. Elsevier, Amsterdam, The Netherlands.
van Genuchten, M. Th., D. H. Tang, and R. Guennelon. 1984. Some exact solutions for solute transport through soils containing large cylindrical macropores. Water Resour. Res. 20:335-346
van Genuchten, M. Th., and F. N. Dalton. 1986. Models for simulating salt movement in aggregated field soils. Geoderma 38:165-183

[W]

Wada, K., and Y. Harada. 1971. Effects of temperature on the measured cation-exchange capacities of ando soils. J. Soil Sci. 22:109-117
Wada, K., and Y. Okamura. 1977. Measurements of exchange capacities and hydrolysis as means of characterizing cation and anion retentions by soils. Proc. Intl. Seminar on Soil Environ. and Fertility Management in Intensive Agriculture, Soc. Sci. Soil Manure, Jpn. pp. 811-815
Wada, K., and Y. Okamura. 1980. Electric charge characteristics of Ando A_1 and buried A_1 horizon soils. J. Soil Sci., 31:307-314
Wada, K. 1981. Ion exchange in clay soils. In adsorption in soils. Soc. Sci. Soil Manure, Jpn. (ed) Hakuyuushya, Tokyo, Japan, pp.5-57 (in Japanese)

White, R. E., G. W. Thomas, and M. S. Smith. 1984. Modelling water flow through undisturbed soil cores using a transfer function model derived from ^{3}HOH and Cl transport. J. Soil Sci. 35:159-168

White, R. E. 1985a. The transport of chloride and non-diffusible solutes through soil. Irrig. Sci. 6:3-10

White, R. E. 1985b. The influence of Macropores on the transport of dissolved and suspended matter through soil. Advances in Soil Sci. 3. pp.95-120. Springer-Verlag, New York, U.S.A.

Wild, A., and I. A. Babiker. 1976. The asymmetric leaching pattern of nitrate and chloride in a loamy sand under field conditions. J. Soil Sci. 27:460-466

[Y]

Yamazaki, F., T. Yawata, H. Takenaka, and T. Tabuchi. 1962. On the effect of cracks in sub-soil, upon draining of the heavy clay soil in Komukai, Hokkaido. Trans. AESJ. 8:427-434 (in Japanese with English abstract)

Yamazaki, F., H. Takenaka, T. Tabuchi, and A. Tada. 1964. On the effect of cracks in subsoil upon tile draining of clayey paddy field soil. Trans. AESJ. 32:151-159 (in Japanese with English abstract)

Yamazaki, F., H. Takenaka, T. Tabuchi, R. Yasutomi, and A. Tada. 1966. The role of cracks in subsoil on underdrainage in clayey reclaimed paddy fields. Trans. AESJ. 16:1-8 (in Japanese with English abstract)